MASTERARBEIT

zur Erlangung des akademischen Grades Master of Science

Moduli Spaces of Gluon Graphs

Lukas Harlan

Gutachter:

1. *Prof. Dr. Dirk Kreimer*
2. *Dr. Marko Berghoff*

Eingereicht am Institut für Physik der Humboldt-Universität zu Berlin am:
16.09.2019

Contents

Chapter 1
Introduction

The experimental predictions made by quantum field theories are astonishing. To push this success further, a generation of theoreticians has been working towards a deeper understanding of the scattering amplitudes. There are still many mysteries surrounding the structure of Feynman integrals. They persist a rich structure with connections to number theory and algebraic geometry, to name just two, which are not fully understood.

The interaction between maths and physics has been fruitful throughout the past. Both fields were able to provide new perspectives to the other. For example, studying Feynman amplitudes as complex-valued functions resulting from integration is also useful in mathematics. It serves as an example of a function that is defined through an integral. Improving the knowledge about these functions will help to learn more about the structure of high energy physics.

In recent work, it has been suggested that Feynman integrations are related to the Culler Vogtmann Outer space [1]. These spaces consist of degenerated metrics associated with graphs and were first defined in [2]. They are related to topological complexes and possess a rich combinatorial and geometrical structure. A convenient quotient of Outer space, the moduli space of graphs, can be related to Feynman amplitudes associated with a scattering process [3]. Restricting the set of graphs that built up these spaces to physical relevant cases is the task of ongoing research, and this thesis tries to contribute its part. One possibility is to look at graphs with colored edges, whose colors are place holders for masses and particle types. For example, the paper [4] evolves around this. This thesis focuses on vertices that are allowed by physics (especially QCD or Yang-Mills theories), i.e., only graphs with three or four valent vertices are admissible.

The chapters 4 and 5 contain the main results, which are the calculation of the f-vectors of different versions of the moduli spaces. They are achieved by considering matchings on three regular graphs, where a matched edge corresponds to a four valent vertex. Additionally, some statements about the Euler characteristic could be made. Chapter 2 serves as an introduction to the underlying mathematical concepts. It also contains some general results. For example, it is shown that the moduli spaces stay connected after restricting the valency of vertices to the physical case. The intermediate chapter 3 establishes a connection between the moduli space of graphs and the parametric form of Feynman integrals. Furthermore, it gives a brief, unusual perspective on the absence of 5-valent vertices in Yang-Mills theories.

Chapter 2

Mathematical Framework

The mathematical concepts that are used in this thesis will be defined in this Chapter. It starts with a small section about maybe the most general concept: Sets. Then increasingly more structure will be introduced, with sections about simplicial complexes, posets, graphs and the more advanced concept of metric graphs spaces.

2.1 Basic Definitions and Simplicial Complexes

2.1.1 Sets

Before simplicial complexes and posets are defined, some basic notation used throughout the thesis is introduced.
For a finite set A denote its cardinality or size, i.e., its number of elements, by $|A|$.

Definition 2.1. *Let $n \in \mathbb{N}$. Define the set $[n]$ by $[n] := \{i \in \mathbb{N} \mid 0 < i \leq n\}$. Denote the powerset, i.e., the set of all subsets of $[n]$, by $2^{[n]}$.*

Definition 2.2. *Define the complement of a set $X \subseteq [n]$ by $\overline{X} := [n] - X = \{x \in [n] \mid x \notin X\}$.*

Note that $\overline{(\overline{X})} = \{x \in [n] \mid x \notin \overline{X}\} = \{x \in [n] \mid x \in X\} = X$.

Property 2.3. $X \subseteq Y \Leftrightarrow \overline{Y} \subseteq \overline{X}$

Proof. From $x \in X \Rightarrow x \in Y$ follows $x \notin Y \Rightarrow x \notin X$ which translates to $x \in \overline{Y} \Rightarrow x \in \overline{X}$, i.e., $\overline{Y} \subseteq \overline{X}$. The converse follows by replacing X with $\overline{V}$ and Y with $\overline{W}$. □

Next, the disjoint union of sets is defined.

Definition 2.4. *The disjoint union of a family of sets A_i with $i \in I \subseteq \mathbb{N}$ is defined via*

$$\bigsqcup_{i \in I} A_i := \bigcup_{i \in I} \{(a, i) \mid a \in A_i\} \ .$$

Note that the intersection of the sets $\{(a,i) \mid a \in A_i\} \cap \{(a,j) \mid a \in A_j\} = \emptyset$ for $i \neq j$ even if $A_i = A_j$. Conversely if $A \cap B = \emptyset$ then their union equals $A \cup B = A \sqcup B$ and $|A \cup B| = |A \sqcup B| = |A| + |B|$.

2.1.2 Relative Simplicial Complexes

Definition 2.5. *A (combinatorial) simplicial complex consists of a vertex set $[n]$ and a set of sets $\Delta \subset 2^{[n]}$ such that:*

$$(i) \quad \forall v \in [n] : \{v\} \in \Delta$$
$$(ii) \quad \textit{if } \tau \subseteq \sigma \in \Delta \textit{ then } \tau \in \Delta$$

The dimension of a simplicial complex is $\dim \Delta := \max_{\tau \in \Delta} |\tau| - 1$ *.*

Remark. The empty set is considered as an element of a simplicial complex.
For $\sigma, \tau \in \Delta$ it follows by the second condition in the definition above, that $\sigma \cap \tau \in \Delta$.

Definition 2.6. *A geometrical simplex* $\sigma \subset \mathbb{R}^d$ *is defined by*

$$\sigma := \left\{ (e_1, e_2, \dots, e_{d+1}) \in [0,1]^{d+1} \;\middle|\; \sum_{i=1}^{d+1} e_i = 1 \right\}$$

A geometrical simplicial complex K *is a collection of geom. simplices, s.t.* $\emptyset \in K$*, if* $\sigma, \tau \in K$ *then* $\sigma \cap \tau \in K$ *and* $\partial\sigma \in K$*.*

Any element of a complex Δ is called a face. If a face $\sigma \in \Delta$ is not included in any other face of Δ, then σ is called a facet. Any complex can therefore also denoted by its set of facets, write $\Delta = \langle \sigma_1, \dots, \sigma_k \rangle := \cup_i^k 2^{\sigma_i}$, where σ_i denotes a facet of Δ.

Remark. Any combinatorial simplicial complex Δ possesses a geometrical realization, that is a geometrical complex K_Δ. It can be constructed by embedding all vertices into $\mathbb{R}^N$ linear independently and then identify each face $\sigma \in \Delta$ with the geometrical simplex spanned by the corresponding vertices.

Definition 2.7. *Define* $F_k[\Delta] \subseteq \Delta$ *to be the set of* k *dimensional faces of* Δ *and* $f_k := |F_k[\Delta]|$ *as well as* $f_{-1} := 1$*. The* f*-vector of a simplicial complex is then given by* $\boldsymbol{f}(\Delta) = (f_{-1}, f_0, \dots, f_{n-1})$*.*

Definition 2.8. *The Euler characteristic* $\mathcal{X}$ *of a (relative) simplicial complex* Δ *is defined via*

$$\mathcal{X}(\Delta) = \sum_{k=0}^{\dim \Delta} (-1)^k f_k(\Delta)$$

where f_k *is the* f*-vector of the complex.*

Originally the characteristic $\mathcal{X}$ was defined by Euler as the alternating sum over the number of vertices, edges, and faces of a triangulated surface. The definition above is a consequent generalization for higher dimensions. It follows a short remark on the algebraic concepts formalizing the idea of the Euler characteristic.

Remark. A further generalization relates $\mathcal{X}$ to the rank or dimension of the n-th homology group H_n via $\mathcal{X}(X) = \sum_n (-1)^n \dim H_n(X)$ for a topological space X. Here the dimension of a group counts its independent generators as a vector space [5].
There is a lot more going on here, but it is not necessary for this thesis.

For the central object of this thesis, it is needed to introduce language to describe missing faces in the complexes defined above. The following definition enables the description of such spaces.

Definition 2.9. *Let* Δ *and* Γ *be combinatorial complexes s.t.* $\Gamma \subset \Delta$*, a relative combinatorial complex* (Δ, Γ) *is defined via set subtraction* $(\Delta, \Gamma) := \Delta - \Gamma$*.*

The f-vector of a relative complex (Δ, Γ) is given by $f_i(\Delta, \Gamma) = f_i(\Delta) - f_i(\Gamma)$ for $i \leq \dim \Gamma$ and $f_i(\Delta, \Gamma) = f_i(\Delta)$ for $i > \dim \Gamma$. For $\Gamma = \emptyset$ the definition of usual complexes is restored. Note that although relative complexes are not uniquely defined by such a pair, their f-vector is.
The geometric realization of a relative complex is obtained by deleting the complex K_Γ from K_Δ, so $K_{(\Delta,\Gamma)} := K_\Gamma - K_\Delta$. As a consequence, the complex $K_{(\Delta,\Gamma)}$ has missing boundaries.

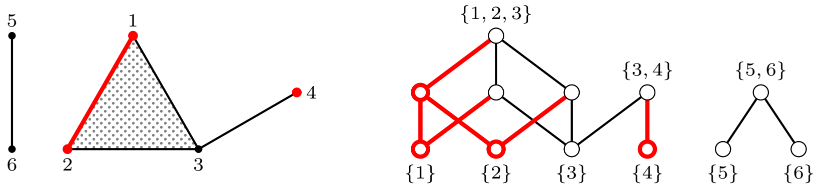

FIGURE 2.1: The relative combinatorial complex (Δ, Γ) with Γ in red from Example 2.11 on the left and its face poset $P[\Delta, \Gamma]$ on the right.

Definition 2.10. *A (rel.) simplicial complex* (Δ, Γ) *is disconnected if* $\exists \sigma, \tau \subseteq (\Delta, \Gamma)$*, s.t.* $\sigma \sqcup \tau = (\Delta, \Gamma)$*.*

A relative simplicial complex (Δ, Γ) has the structure of a partially ordered set or in short a poset. A poset is a set equipped with a relation $<$, that relates two elements of the set, such that $<$ is reflexive (an element is related to itself), antisymmetric (two distinct elements can only be related in one direction) and transitive (if $a < b$ and $b < c$ then $a < c$). For a complex (Δ, Γ) this relation is given by set inclusion. The corresponding poset is denoted by $P[(\Delta, \Gamma)]$ or two simplify the notation remove the brackets and denote it as $P[\Delta, \Gamma]$. Clearly any complex can be equipped with that relation, such that the poset $P[\cdot]$ is not limited to combinatorial complexes.

Now the previous definitions are applied to an example.

Example 2.11. Let (Δ, Γ) be a rel. simplicial complex given by
$\Delta = \{\{1, 2, 3\}, \{1, 2\}, \{1, 3\}, \{3, 2\}, \{3, 4\}, \{5, 6\}, \{1\}, \{2\}, \{3\}, \{4\}, \{5\}, \{6\}, \emptyset\}$
and $\Gamma = \{\{1, 2\}, \{1\}, \{2\}, \{4\}, \emptyset\}$ (cf. Figure 2.1).
The f-vectors are given by

$$\boldsymbol{f}(\Delta) = (1, 6, 5, 1)\,, \ \boldsymbol{f}(\Gamma) = (1, 3, 1) \ \text{ and } \ \boldsymbol{f}(\Delta, \Gamma) = (0, 3, 4, 1)\,.$$

Calculating the Euler characteristic results in

$$\begin{aligned} \mathcal{X}(\Delta) &= -1 + 6 - 5 + 1 = 1, \\ \mathcal{X}(\Gamma) &= -1 + 3 - 1 = 1 \text{ and} \\ \mathcal{X}(\Delta, \Gamma) &= -0 + 3 - 4 + 1 = 0. \end{aligned}$$

Clearly (Δ, Γ) is disconnected, since

$$\begin{aligned} (\Delta, \Gamma) &= \{\{1, 2, 3\}, \{1, 3\}, \{3, 2\}, \{3, 4\}, \{3\}, \{4\}, \emptyset\} \sqcup \{\{5, 6\}, \{5\}, \{6\}, \emptyset\} \\ &=: (\Delta_1, \Gamma_1) \sqcup (\Delta_2, \Gamma_2), \end{aligned}$$

where each (Δ_i, Γ_i) is a rel. simplicial complex by its own.

2.2 Elementary Group Theory

2.2.1 General Introduction

A group G is a set together with a bilinear map $\star : G \times G \to G$, the group operation, under which the group G is closed. Additionally, there must be an element $e \in G$ such that $e \star g = g \star e = g$ for all group elements $g \in G$. Lastly, a group is closed under inversion, i.e., $\exists g^{-1} \in G$ such that $g \star g^{-1} = g^{-1} \star g = e$ for all $g \in G$. For the n-fold product write

$$\underbrace{g \star g \star \cdots \star g}_{n\text{-times}} =: \begin{cases} g^n & \text{in multiplicative notation} \\ ng & \text{in additive notation} \end{cases} .$$

The external direct product of groups is a simple way to define a new group from already existing ones. It is defined as follows.

Definition 2.12. *The external direct product of a finite collection of groups $G_1, G_2, \dots, G_n$ is defined as*

$$G_1 \oplus G_2 \oplus \cdots \oplus G_n := \left\{ (g_1, g_2, \dots, g_n) \;\middle|\; g_i \in G_i \right\}$$

with the group operation taken componentwise from its constituents. If $G_1 = G_2 = \cdots = G_n = G$ write $G_1 \oplus G_2 \oplus \cdots \oplus G_n = G^n$.

To check that $G_1 \oplus G_2 \oplus \cdots \oplus G_n$ is indeed a group observe that it just carries on the group structure from each G_i. It might be worth noting that the unit $e \in G_1 \oplus G_2 \oplus \cdots \oplus G_n$ is given by $e = (e_1, e_2, \dots, e_n)$, where of course every $e_i \in G_i$ is the unit of G_i. Moreover, the size of the external direct product is given by the product of the sizes of each group G_i: $|G_1 \oplus G_2 \oplus \cdots \oplus G_n| = |G_1||G_2| \cdots |G_n|$.

Example 2.13. One particularly important and also fundamental group is the set of integers modulo n, denoted by $\mathbb{Z}_n$. It is a group with respect to modular arithmetic and its elements are the congruence classes. The set takes the form

$$\mathbb{Z}_n := \{0, 1, \dots, n-1\}$$

and for $a, b \in \mathbb{Z}_n$ the group operation is given by, in quite impure notation,

$$a + b = (a + b) \bmod n \,,$$

where a, b are viewed as elements in $\mathbb{Z}$ (the set of all integers) on the right hand side.

2.2.2 The Symmetric Group S_n

Definition 2.14. *The group of all bijective maps $\sigma : [n] \to [n]$ on a finite set $[n]$ (the group operation is given by function composition) is called symmetric group S_n. Elements of S_n are given explicitly as lists of the images of each element in $[n]$ under σ:*

$$\sigma = \begin{pmatrix} 1 & 2 & \dots & n \\ \sigma(1) & \sigma(2) & \dots & \sigma(n) \end{pmatrix} .$$

Denote the unit by $(1) \in S_n$ and the inverse of an element $\sigma \in S_n$ by σ^{-1}.

Definition 2.15. *A transposition or a swap is a bijection $\sigma \in S_n$ such that*

$$\sigma = \begin{pmatrix} 1 & \dots & i-1 & i & j & j+1 & \dots & n \\ 1 & \dots & i-1 & j & i & j+1 & \dots & n \end{pmatrix}$$

for $i \neq j$ and $i, j \in [n]$. A transposition will be denoted as (i, j).

Any $\sigma \in S_n$ can be written as a composition of transpositions, although this is not unique. In the literature and in more general group-theoretic terms, a transposition is called a 2-cycle. There is one more fact worth observing, every 2-cycle is its own inverse. Generally, a k-cycle in the symmetric group is defined as follows. Let $k \in \mathbb{N}$ and $k > 1$. A k-cycle is an element $\sigma \in S_n$ for which $\sigma^k(x) = x$ for all $x \in X \subset [n]$ and $\sigma(x) = x$ for $x \in [n] \setminus X$. Clearly $|X| = k$ follows.

2.2.3 Group Actions

Definition 2.16. *Let X be a set and G a group, then a group action φ is a map $\varphi : X \times G \to X : (x, g) \mapsto \varphi_g(x)$ satisfying the following two conditions $\forall g, h \in G$ and $\forall x \in X$:*

$$\begin{aligned} &(i) \quad \varphi_e(x) = x \\ &(ii) \quad \varphi_{gh}(x) = \varphi_g(\varphi_h(x)) \end{aligned}$$

The group action φ defines an equivalence relation on the set X, via $x \sim y \Leftrightarrow \exists g \in G \colon \varphi_g(x) = y$. The two conditions above are precisely making sure that the equivalence relation is well defined:
Reflexiveness follows immediately from (i). To show symmetry and transitivity use the closeness of G under inversion and the group operation.
The resulting equivalence classes are called orbits and defined as follows.

Definition 2.17. *Let φ be a group action of a group G on a set X. The orbit of an element $x \in X$ is a set $\mathrm{Orb}_x^\varphi \subseteq X$ defined as*

$$\mathrm{Orb}_x^\varphi := \{\varphi_g(x) \mid g \in G\} \; .$$

X/φ or X/G denotes the partition of X into orbits of an action of G via φ.

Definition 2.18. *Let φ be a group action of a group G on a set X. The stabilizer of an element $x \in X$ is a set $\mathrm{Stab}_x^\varphi \subseteq G$ defined as*

$$\mathrm{Stab}_x^\varphi := \{g \in G \mid \varphi_g(x) = x\} \; .$$

Stab_x^φ is a subgroup of G, which can be checked easily by the definition of group actions.

Theorem 2.19. *The Orbit Stabilizer Theorem. Let φ be a group action of a group G on a set X and $x \in X$. Then*

$$|\,\mathrm{Orb}_x^\varphi\,| = \frac{|G|}{|\,\mathrm{Stab}_x^\varphi\,|} \; .$$

Proof. This result is well known. A proof can be found in any standard textbook, for example in [6]. $\square$

2.3 Graphs

This section will define graphs and some basic operations on them. Including the definition of the central graph in Chapter 4, and an analyzation of its symmetries.
In order to allow for graphs with multiple edges, a slight generalization of sets is needed: A multiset is a set where repetitions of the same element are allowed.
A lot of the upcoming definitions and notations are taken from [7].

Definition 2.20. *A graph G is a triple $\langle H_G, E_G, V_G\rangle$, where H_G is a finite set of half-edges, E_G a finite multiset of edges $e = \{h_1, h_2\}$ and V_G a finite set of vertices $v = \{h_1, h_2, h_3, \dots\}$ with $h_i \in H_G$. Furthermore, the following conditions must hold*

(i) *Either* $e_i \cap e_j = \emptyset$ *or* $e_i = e_j \;\; \forall e_i, e_j \in E_G$

(ii) *Either* $v_i \cap v_j = \emptyset$ *or* $v_i = v_j \;\; \forall v_i, v_j \in V_G$

(iii) $\bigcup\limits_{v \in V_G} v = H_G$.

Note that the definition above allows for several edges between two vertices, these edges are referred to as *multi-edges*. These graphs are often referred to as multigraphs in the mathematical literature, but throughout this thesis, this distinction will not be made. Further notation and language useful to describe the graphs in this thesis will be introduced in the following.
Not all half-edges $h \in H_G$ have to be part of an edge, therefore define the set $H_G^{ext} := H_G \setminus \bigcup_{e \in E_G} e$. Elements of H_G^{ext} are the *external half-edges* (sometimes also called external legs) of the graph G. Similarly, define the a subset of vertices V_G^{ext} that contains all $v \in V_G$ for which holds $\exists h \in v$ such that $h \in H_G^{ext}$. The *internal half-edges* are defined as $H_G^{int} := H_G \setminus H_G^{ext}$.
Two distinct vertices $v_1, v_2 \in V_G$ *share an edge* if there is an edge $e \in E_G$ such that $e \cap v_1 \neq \emptyset \neq e \cap v_2$. The vertices are said to be connected via e.
The *valency of a vertex* $v \in V_G$, denoted by $|v|$, is the number of half-edges in v. So it is just the cardinality of the set v. Pictorially speaking the valency of a vertex is the number of half-edges connected to it.
A graph G is called *n-regular* if all vertices in G have the same valency n, i.e. $\forall v \in V_G : |v| = n$.
A *subgraph* g of G is a graph and $E_g \cup V_g \subset E_G \cup V_G$. Their relation is denoted by $g \subset G$.
A graph G is *connected* if it does not have two subgraphs g_1 and g_2 such that $g_1 \cup g_2 = G$ and $g_1 \cap g_2 = \emptyset$.
The *loopnumber* or *rank* of a graph G, denoted by $|G|$ is given by its first Betti number $h_1(G) = \dim H_1(G)$ and counts the number of independent loops in a graph. It is also the number of edges in the graph obtained from G by contracting a subset of edges and all vertices to one point along a homotopy equivalence.
In quantum field theories, it is often useful to require additional conditions on the graphs under considerations. These are combined in the following definition.

Definition 2.21. *A graph G is called admissible if*

(i) *G is 1PI, i.e. G is still connected after the removal of one edge $e \in E_G$*

(ii) *G is not a tadpole, i.e. $\nexists v \in V_G$ such that one connected component of $G - v$ has no external legs.*

(iii) $\forall v \in V_G : |v| \geq 3$

Definition 2.22. *Denote the set of all admissible graphs with n external legs and a maximal valency of v by $\mathcal{G}_n^v$. The subset $\mathcal{G}_{l,n}^v \subset \mathcal{G}_n^v$ is given by all rank l graphs in $\mathcal{G}_n^v$.*

An important operation on graphs is the contraction of a subgraph. It is defined as follows.

Definition 2.23. *Let G be an admissible graph and $\gamma \subset G$ a connected subgraph. The contracted graph G/γ is defined by*

$$G/\gamma := \langle H_G \setminus H_\gamma^{int}, E_G \setminus E_\gamma, (V_G \setminus V_\gamma) \cup H_\gamma^{ext} \rangle.$$

For disconnected subgraphs, the contracted graph is defined componentwise.

So G/γ is the graph where the subgraph γ is replaced by a vertex $v = H_\gamma^{ext}$. Pictorially spoken the graph γ shrinks to a point in G as shown in the upcoming example.

Example 2.24. Let G be given as

$G =$ 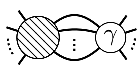

.

Where the internal structure of the subgraph $\gamma \subset G$ is depicted as a blob, but its external legs are shown explicitly. Then the contracted graph takes the form

$G/\gamma =$ 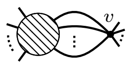

.

The vertex v contains the external legs of γ. Note that the edges connecting v to the remaining blob are not altered by the contraction. In order to generate a admissible graph G/γ the subgraph needs at least three external legs $|H_\gamma^{ext}| \geq 3$. Thereby it is ensured that no two valent vertices are generated.

Remark. Later on, the contraction of graphs will be mainly used to shrink edges of 3-regular graphs. Let $G \in \mathcal{G}_n^3$ and $e = \{h_1, h_2\} \in E_G$. To contract an edge consider the subgraph

$$\varepsilon = \langle e \cup \mathrm{Adj}_e, e, \{\{h_1, a_1, a_2\}, \{h_2, a_3, a_4\}\} \rangle,$$

where $\mathrm{Adj}_e := \{a_1, a_2, a_3, a_4\}$ is the set of half-edges of the vertices connected by e that are not part of e itself. The graph G with e contracted is then G/ε. In an abuse of notation write also G/e for the contracted graph and also extend this notation to disjoint unions of edges (later defined as a matching).

2.3.1 Symmetry and Isomorphisms of Graphs

In order to define the symmetries of the graphs under consideration, define isomorphic graphs.

Definition 2.25. *Let G and G' be graphs. They are called isomorphic if there exists a bijection $i : H_G \to H_{G'}$ such that whenever two vertices share an edge in G, they get mapped to vertices that also share an edge in G'.*
Call such a map i an isomorphism between the graphs G and G'.

At this level, graph isomorphisms rename the half-edges that built the graph. This divides the set of graphs into equivalence classes, which are called isomorphism classes. The subset of maps that leaves an isomorphy class invariant is loosely called symmetry group[1]. In the next section, the symmetry group of three regular one-loop graphs will be derived.

[1]If this set indeed forms a group is not important here. However, for the case considered in the next section, the set forms a group.

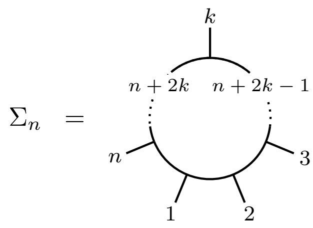

FIGURE 2.2: The n-sun Σ_n with n external legs. The half-edges of the vertex containing k are labeled explicitly.

In the context of Feynman graphs, define the symmetry factor of a graph. Therefore note that the symmetry group contains a special subgroup given by automorphisms.

Definition 2.26. *Let G be a graph. An automorphism of G is an isomorphism $i : H_G \to H_G$ that maps G onto itself. All automorphisms of G form a group* $\mathrm{Aut}(G)$ *and the symmetry factor of G is defined by* $\mathrm{Sym}(G) := |\mathrm{Aut}(G)|$.

In this thesis, the isomorphisms (and therefore the automorphisms) of Feynman graphs are restricted to the internal half-edges. This means the external legs are fixed. The physical explanation comes from the interpretation of external legs as incoming or outgoing particles in a scattering amplitude. Note that the symmetry factor of a graph without fixed legs is always related to a sum of symmetry factors where the external legs are fixed.
Furthermore, in this thesis, graphs that differ by rotation or reflection of the external legs are considered to be the same graph. This is motivated by Yang-Mills theory, where the particles are massless bosons that cannot be distinguished. Rotating is a symmetry since there are no masses and reflections because the edges are not directed.
As a last remark note that the following considerations will not depend on the choice of a graph inside an isomorphism class. Therefore it will not be distinguished between graphs and their isomorphism class for the most part. Graphs are understood as their isomorphism classes. However, the automorphisms of a graph will play a crucial role at several points.

The Symmetry Group of n-Suns

There is only one topology for a one-loop graph with n external legs, namely the circle with attached legs, see Figure 2.2. This graph is now defined explicitly.

Definition 2.27. *The n-sun Σ_n is the 3-regular, one loop graph with n external legs, given by the sets below. For a picture see Figure 2.2.*

$$\begin{aligned}
H_{\Sigma_n} &:= [3n] \\
V_{\Sigma_n} &:= \{\{1, n+1, n+2\}, \dots, \{k, n+2k-1, n+2k\}, \dots, \{n, 3n-1, 3n\}\} \\
E_{\Sigma_n} &:= \{\{n+2, n+3\}, \dots, \{n+2k, n+2k+1\}, \dots, \{3n, n+1\}\} \\
H^{ext}_{\Sigma_n} &:= [3n] \setminus \{n+1, \dots, 3n\} = [n]
\end{aligned}$$

Remark. The isomorphisms of the n-sun can be represented by a permutation on its external legs. Furthermore, note that there are no non trivial automorphisms for $n > 2$: $|\mathrm{Aut}(\Sigma_n)| = 1$.

To properly treat the symmetries, it is useful to define a group action that acts on the n-suns. In order to do that some additional notation is needed. First, define a set that contains all graphs that can be generated by an arbitrary permutation of the external legs of Σ_n. After that, an action on this set is defined, which renders all isomorphic graphs into one orbit. The following definition also gives an explicit description of how the symmetric group S_n acts on the external legs of a graph $G \in \mathcal{G}^3_{l,n}$.

Definition 2.28. *Let $\gamma \in \mathcal{G}^3_{l,n}$. The action of $\sigma \in S_n : H^{ext}_\gamma \to H^{ext}_\gamma$ is given by $\sigma\gamma := \langle H_\gamma, E_\gamma, \sigma V_\gamma \rangle$. The elements of σV_γ, denoted by $\sigma.v$, are defined by the following. Let $v \in V^{ext}_\gamma$ and $k \in v$ be the unique element in v such that $k \in H^{ext}_\gamma$, then*

$$\sigma.v = \sigma.\{k, v_1, v_2\} := \{\sigma(k), v_1, v_2\}\,.$$

For $v \notin V^{ext}_\gamma$ define $\sigma.v := v$.

Definition 2.29. *For $l = 1$ define the set $\mathcal{S}_n$ of all permuted n-suns by*

$$\mathcal{S}_n := \{\sigma\Sigma_n \mid \sigma \in S_n\} / \sim\,,$$

where two n-suns are equivalent if they are isomorphic with fixed external legs.

Now a subgroup of S_n will be defined that represents the symmetries of a n-sun. It will characterize the equivalence relation in the definition above via a group action. Start with defining the cyclic group $\mathrm{Cyc}_n \subset S_n$ and the reflective group $R_n \subset S_n$. They represent the symmetries under rotations and reflections of the graph Σ_n.

Definition 2.30. *Let $c_+ \in S_n$ be defined as*

$$c_+ := \begin{pmatrix} 1 & 2 & 3 & \dots & n-1 & n \\ n & 1 & 2 & \dots & n-2 & n-1 \end{pmatrix}.$$

Note that $c_+^n = (1)$. Define $\mathrm{Cyc}_n \subset S_n$ by $\mathrm{Cyc}_n := \left\{ c_+^k \;\middle|\; k \in [n] \right\}$.

One easily observes that Cyc_n indeed forms a subgroup of the symmetric group S_n and furthermore that $\mathrm{Cyc}_n \cong \mathbb{Z}_n$. This can be made intuitive by the composition law of Cyc_n: $c_+^k \circ c_+^l = c_+^{l+k}$, while all exponents are taken modulo n due to the cyclic nature of Cyc_n.

Definition 2.31. *The reflective group $R_n \subset S_n$ is defined by*

$$R_n := \left\{ (1), (1, n-1)(2, n-2) \dots \left(\left\lfloor \frac{n-1}{2} \right\rfloor, \left\lceil \frac{n+1}{2} \right\rceil \right) \right\} =: \{(1), r_n\}\ .$$

R_n is indeed a subgroup of S_n since $r_n \circ r_n = (1)$, which holds because r_n consists only of commuting 2-cycles. Analogously to Cyc_n one gets $R_n \cong \mathbb{Z}_2$.
An isomorphism of a n-sun can either be a rotation, reflection or both. Therefore, the internal direct product of the two groups represents the symmetries:

$$R\mathrm{Cyc}_n := \left\{ rc \;\middle|\; r \in R_n \text{ and } c \in \mathrm{Cyc}_n \right\}.$$

It is worth noting that this is a semidirect product $R\mathrm{Cyc}_n = R_n \ltimes \mathrm{Cyc}_n$. Thus, note that $R_n \cap \mathrm{Cyc}_n = (1)$ and

$$\begin{aligned} r_n c_+ r_n &= c_+^{n-1} \\ r_n c_+^k r_n &= (r_n c_+ r_n)^k = c_+^{k(n-1)} = c_+^{n-k} \in \mathrm{Cyc}_n\ . \end{aligned}$$

The first line follows by direct computation and in the second line the identities $r_n^2 = (1)$ and $c_+^{kn} = c_+^n$ were used.
For future results the order of $R_n \ltimes \mathrm{Cyc}_n$ will be needed. Since the two groups only intersect at (1), conclude that $|R_n \ltimes \mathrm{Cyc}_n| = 2n$.

Definition 2.32. *Define a group action* $\phi : R_n \ltimes \mathrm{Cyc}_n \times \{\sigma\Sigma_n \mid \sigma \in S_n\} \to \{\sigma\Sigma_n \mid \sigma \in S_n\}$ *via* $\phi_s(\sigma\Sigma_n) := (s \circ \sigma)\Sigma_n$.

Then the set of all permuted n-suns $\mathcal{S}_n$ is given as a partition by ϕ

$$\mathcal{S}_n := \{\sigma\Sigma_n \mid \sigma \in S_n\}/\phi.$$

Lemma 2.33. *Let* $\sigma \in S_n$ *then* $\mathrm{Stab}^{\phi}_{\sigma\Sigma_n}$ *is trivial.*

Proof. Let $s \in R_n \ltimes \mathrm{Cyc}_n$. $\phi_s(\sigma\Sigma_n) = \sigma\Sigma_n \Leftrightarrow s \circ \sigma = \sigma$ then $\mathrm{Stab}^{\phi}_{\sigma\Sigma_n} = \{(1)\}$ by the uniqueness of the identity in groups. □

Corollary 2.34. *Let* $\sigma \in S_n$ *then* $|\mathrm{Orb}^{\phi}_{\sigma\Sigma_n}| = 2n$ *and* $|\mathcal{S}_n| = (n-1)!/2$.

Proof. $|\mathrm{Orb}^{\phi}_{\sigma\Sigma_n}| = |R_n \ltimes \mathrm{Cyc}_n|$ is obtained by the orbit stabilizer Theorem 2.19 and Lemma 2.33. Furthermore this is true for any $\sigma \in S_n$, so every partition in $\mathcal{S}_n$ has the same size and therefore

$$|\mathcal{S}_n| = \frac{|S_n|}{|R_n \ltimes \mathrm{Cyc}_n|} = \frac{n!}{n/2} = \frac{(n-1)!}{2}\,.$$ □

2.4 Moduli Spaces of Graphs

This section begins with a definition of the moduli spaces of graphs $MG_{l,n}$ for graphs with l loops and n external legs. It is then restricted to graphs of Yang-Mills theories. Furthermore, the colored versions $MCG_{l,n,C}$ and $MRG_{l,n}$ are defined. The last part treats the particular case of one-loop graphs, which is the central object of this thesis.
First, the points of which the spaces $MG_{l,n}$ are made of, namely metric graphs, need to be defined.

Definition 2.35. *A metric graph is a tuple (λ, G), where G is a graph and $\lambda : E_G \to \mathbb{R}_{\geq 0}$ a map called the metric, which assigns to every edge $e \in E_G$ a length $\lambda(e) \geq 0$.*
The volume $\operatorname{vol}(\lambda, G)$ *of a metric graph is defined by* $\operatorname{vol}(\lambda, G) := \sum_{e \in E_G} \lambda(e)$.

Metric graphs that have a vanishing metric on a subset of their edges should be identified with the graph where these edges are contracted. To implement this define the subset $Z_\lambda \subset E_G$ of edges with length zero of a metric graph (λ, G) by

$$Z_\lambda := \left\{ e \in E_G \;\middle|\; \lambda(e) = 0 \right\}.$$

The metric of the contracted graph G/Z_λ[2] is given by the restriction of λ to the edges that have non zero length $\lambda|_{E_G \setminus Z_\lambda}$. Denote a contracted metric graph by

$$(\lambda, G)/Z_\lambda := (\lambda|_{E_G \setminus Z_\lambda}, G/Z_\lambda).$$

Definition 2.36. *The moduli spaces of graphs $MG^v_{l,n}$ are defined by*

$$MG^v_{l,n} := \left\{ (\lambda, G) \;\middle|\; G \in \mathcal{G}^v_{l,n},\ \operatorname{vol}(\lambda, G) = 1 \right\} / \sim$$

with the equivalence relation $(\lambda, G)/Z_\lambda \sim (\lambda', G')/Z_{\lambda'}$ if there is a external leg preserving isomorphism $i : G/Z_\lambda \to G'/Z_{\lambda'}$ s.t. $\lambda' \circ i = \lambda$.

When there is no restriction to the valency of the graphs in $MG^v_{l,n}$, write $MG_{l,n} := MG^\infty_{l,n}$. The restriction to metrics with volume one is useful since it eliminates scaling of the graphs in MG. Graphs in a equivalence class of $MG^v_{l,n}$ whose metric does not vanish anywhere are isometric as metric spaces.
Notice that in the definition above two metric graphs with non zero metrics still might describe the same point in the moduli space. This origins in automorphisms of the graph under consideration. An example of two equivalent graphs is shown below, where the isomorphism that swaps the edges satisfies the condition from the Definition 2.36. The qualitative value of the metric is shown as the length of the drawn lines.

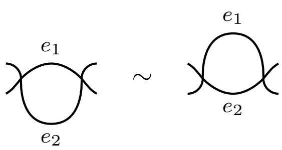

An identification of metric graphs that have a partially vanishing metric is given in the next example. In the picture, the metric on solid edges is one half and it vanishes on the dashed ones.

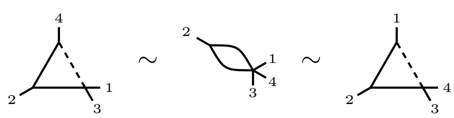

[2]Here Z_λ denotes the tree subgraph of G whose edges have zero length by λ.

Also notice how graphs with different permutation on the external legs might get identified, when the metric vanishes on a subset of their edges.
To understand the topological structure of $MG_{l,n}^v$ it is useful to neglect the equivalence relation for graphs that have non zero metrics and implement it later. The equivalence of graphs with partially vanishing metrics with contracted graphs guarantees that there are face relations.
Due to the condition $\mathrm{vol}(\lambda, G) = 1$, the length of the edges in a graph can not vary independently. Considering only one metric graph (λ, G), the space spanned by the allowed metrics might be written as the cell

$$\delta_G = \left\{ (e_1, e_2 \ldots e_N) \mid e_i \in [0,1], \sum_{i=1}^{N} e_i = 1 \right\} ,$$

where $N = |E_G|$ is the number of internal edges of G. It is important to notice, that δ_G is equivalent to the geometrical simplex of dimension $N - 1$, see Definition 2.6. The boundary of a simplex corresponds therefore to a graph where at least one edge e has length zero, i.e., $\lambda(e) = 0$. Due to the equivalence relation for contracted metric graphs, these boundaries are therefore generated by the contracted graph.
Conclude that any simplex on the boundary of δ_G therefore is given by $\delta_{G/F}$, where F is a forest. A forest $F \subset G$ is a disjoint union of tree subgraphs and all of its edges can be assigned zero length simultaneously, since a forest has no loops and therefore $|G| = |G/F|$. Conclude that it is not allowed to contract with graphs γ that have at least one loop $|\gamma| > 0$.

Remark. The graphs in $\mathcal{G}_{l,n}^v$ can be partially ordered by $G \leq G' \Leftrightarrow F \subset G' : G'/F = G$. This poset is the same as $P[MG_{n,l}^v]$.

In the moduli space of graphs, not all edges can be given a zero length simultaneously since this might alter the rank of the graph or the degree of a new vertex in G/F is too high. This restricts the allowed forests by their number of external legs, which is summarized by the next property. In conclusion, the cell δ_G misses some faces and has thus the structure of a relative simplex.

Definition 2.37. *A relative simplex associated with the graph G is denoted by $\langle G \rangle$.*

Property 2.38. *Let $G \in \mathcal{G}_{l,n}^v$ and $F \subset G$ be a forest with $\max_{T \in F} |H_T^{ext}| \leq v$ and assume that G/F is not a tadpole, then*

$$\begin{aligned} &(i) \quad G/F \in \mathcal{G}_{l,n}^v \text{ or equivalently} \\ &(ii) \quad \delta_{G/F} \text{ is a face of } \langle G \rangle. \end{aligned}$$

The restriction that has to be made, such that G/F is not a tadpole is investigated in the next section.
Adding more graphs to the picture results in more simplices that can share faces, so it gives a relative simplicial complex structure. In Figure 2.3 a subspace of $MG_{1,4}$ is shown. Here any of the three internal edges of the graph can be shrunken to zero length. The results are shown on the edges of the 2-dimensional simplex. The graphs on the 1-dimensional edges always result in the same graph if one of their edges has zero length, namely the 1-loop graph with four external legs and one vertex. Therefore the vertices of the shown simplicial complex all describe the same point in MG. The neighboring face on the right consists of the same graph with permuted external legs.
The 3-regular graphs of MG form the facets of the simplicial complex, since they contain the maximal number of edges for a given loop number and external leg structure. Combinatorially all faces of MG can be constructed from the facets, by investigating the possible

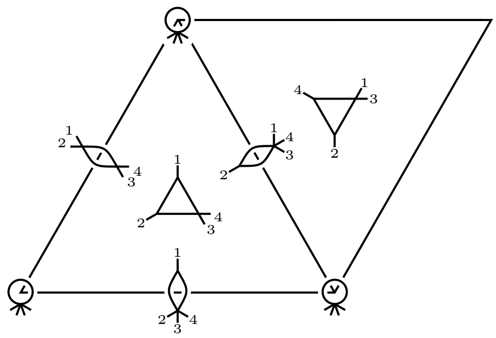

FIGURE 2.3: A simplex in $MG_{1,4}$ and one of its neighbors

forests of the 3-regular graphs.
By implementing the equivalence relation of MG on the metric graphs, the space loses the structure of a simplicial complex. In the example of Figure 2.3 all edges fold on themselves. Looking only at the left cell, it becomes a 2-sphere under the equivalence relation. In this thesis, the structure of one-loop Yang-Mills theories is investigated, and it will turn out that the problems caused by the equivalence relation do not affect the studied cases for the most part.

Sometimes it is useful to define a further map $c : E_G \to [C]$, called the coloring of a graph G. $C \in \mathbb{N}$ denotes the number of colors. This extension can be used to restrict the isometries between the metric graphs. From a physical perspective, these colors act as placeholders for additional information on the edges, such as mass or spin.

Definition 2.39. *The colored moduli spaces of graphs $MCG^v_{l,n,C}$ are defined by*

$$MCG^v_{l,n,C} := \left\{ (c, \lambda, G) \;\middle|\; G \in \mathcal{G}^v_{l,n},\ \mathrm{vol}(\lambda, G) = 1 \right\} / \sim$$

with the same equivalence relation as in definition 2.36, where the isomorphisms need to respect the coloring as well, i.e. $c' \circ i = c$.
Graphs whose coloring is injective are called rainbow-colored and their moduli spaces are denoted by $MRG^v_{l,n}$.

Remark. The uncolored moduli spaces can be recovered by a group action of S_n, that changes the colors such that $MG^v_{l,n} = MRG^v_{l,n}/S_n$.

Outer Space

These types of moduli spaces for graphs without external legs were first defined by Culler and Vogtmann [2]. They used them to investigate the automorphisms of free groups. Points of the Culler Vogtmann Outerspace CV_l are given by metric graphs together with a marking. A marking of the graph Γ is a homotopy equivalence from the rose graph R_l (the unique graph with l loops and one vertex), where each edge is labeled by a generator of the free group F_l together with a direction, to the graph. In practice to mark a graph, choose a spanning tree, and label the remaining edges with elements of F_l that form a basis. Two marked metric graphs $(g, \Gamma) \sim (g', \Gamma')$ are equivalent if there exists an isometry $i : \Gamma \to \Gamma'$ between them, such that $g' \circ i$ is homotopic to g.
The automorphisms of F_l then act naturally on marked graphs by changing the marking. It turns out that the inner automorphisms act trivially. Let $\phi \in \mathrm{Out}(F_l)$ then it acts on the

right by

$$(g, \Gamma)\phi = (g \circ f, \Gamma)$$

where $f : R_l \to R_l$ is a representative of ϕ on the rose graph. The orbit space $CV_l/\mathrm{Out}(F_l) = MG_l$ forgets the marking and is therefore identical to the moduli space of graphs.
Analog to the definitions above one can allow external legs on the graphs (also called basepoints). In that case, equivalent graphs are given by isometries that additionally preserve these points. One can still define natural actions of certain groups on these spaces, such that the orbit spaces are again equal to $MG_{l,n}$ [3, 8].

2.4.1 Moduli Spaces of Yang-Mills Theory $MG^4_{l,n}$

In Yang-Mills theories, there are cubic and quartic interactions, this means on a graphical level, that the only two types of vertices have valency three or four. Therefore, the corresponding moduli space is $MG^4_{l,n}$.

Matchings on 3-regular Graphs

Given a 3-regular metric graph $(\lambda, G) \in MG^4_{l,n}$, the forests $F \subset G$ that form a set of edges that can have zero length simultaneously take a particular form called matchings. The following definition introduces matched graphs, and the identification of matched 3-regular graphs with graphs in $\mathcal{G}^4_n$ is specified.

Definition 2.40. *A forest $M \subseteq G$ of a graph G is called a matching if all its connected components $T \in M$ have exactly one edge, i.e. $|E_T| = 1\ \forall T \in M$. Matchings on 3-regular graphs are also denoted as subsets of their edges.*
A matching is called maximal if there is no edge $e \in E(G)$ such that $\{e\} \cup M$ is a matching. A maximal matching that is a vertex cover is called perfect.

Given any matching M of a 3-regular graph $G \in \mathcal{G}^3_n$, all edges in that matching can be contracted simultaneously. A further restriction, whose motivation comes from physics, is made to ensure that the graph G/M is tadpole free and is therefore in the set of admissible graphs $\mathcal{G}^4_n$ and generates a cell in $MG^4_{l,n}$.

Definition 2.41. *Let $G \in \mathcal{G}^3_n$ and M a matching of G. M is called valid if $\nexists e \in M$ s.t. G/e is a tadpole, cf. Definition 2.21. Graphically they take the form*

$G/e =$ 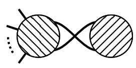 .

Note that the deletion of the four valent vertex would lead to a connected component without external legs.

Definition 2.42. *The set of all valid matchings M on a graph G with $|M| = m$ is denoted by $\mathfrak{M}_m G$.*

It is intuitively clear that a matching M of a 3-regular graph corresponds to a graph in $\mathcal{G}^4_n$, by collapsing the matched edges to 4-valent vertices. In the next definitions and the upcoming Lemma, this correspondence is investigated. First, extend $\mathcal{G}^v_n$ to a set that carries information about possible matchings.

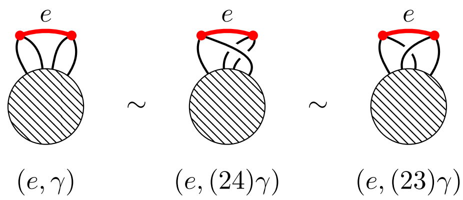

FIGURE 2.4: Equivalent graphs in $\mathfrak{M}_1\mathcal{G}_n^3/\,\mathrm{STU}$

Definition 2.43. *Define the set of all matched graphs in $\mathcal{G}_n^v$ via*

$$\mathfrak{M}\mathcal{G}_n^v := \bigsqcup_{m\in\mathbb{N}} \mathfrak{M}_m\mathcal{G}_n^v$$

where $\mathfrak{M}_m\mathcal{G}_n^v := \big\{(M,\gamma)\bigm| \gamma \in \mathcal{G}_n^v, M \in \mathfrak{M}_m\gamma\big\}$.

The symbol $\sqcup$ denotes disjoint union, i.e. here $\mathfrak{M}_i\mathcal{G}_n^v \cap \mathfrak{M}_j\mathcal{G}_n^v = \emptyset$ for $i \neq j$. It is evident that the set $\mathcal{G}_n^4$ splits into a disjoint union:

$$\mathcal{G}_n^4 = \bigsqcup_{m\in\mathbb{N}} \mathcal{G}_n^{4,m}$$

where m is the number of 4-valent vertices of the graphs in $\mathcal{G}_n^{4,m}$. The aim is to show some relation of the kind "$\mathfrak{M}\mathcal{G}_n^3 \cong \mathcal{G}_n^4$". Due to the structure of the two sets it is enough to show that there is a bijection of the kind "$\rho_m : \mathfrak{M}_m\mathcal{G}_n^3 \to \mathcal{G}_n^{4,m}$". Define $\rho_m(M,\gamma) := \gamma/M$, an example of this mapping is:

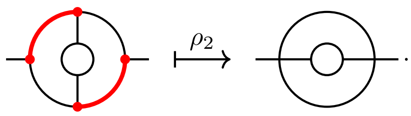

Note that if an edge of the multi-edge were part of the matching, the multi-edge would map to a tadpole.
The map $\rho_m : \mathfrak{M}_m\mathcal{G}_n^3 \to \mathcal{G}_n^{4,m}$ is not a bijection yet, because any of the graphs illustrated in Figure 2.4 gets mapped to the same graph in $\mathcal{G}_n^4$ by ρ_1. This is fixed by an equivalence relation on $\mathfrak{M}_m\mathcal{G}_n^3$, which sets the graphs of Figure 2.4 equivalent.

Definition 2.44. *The set Adj_e is defined to be the set of half-edges given by the two vertices connected by e with the half-edges of e removed.*
Let $(e,\gamma) \in \mathfrak{M}_1\mathcal{G}_n^3$ and $\sigma : H_\gamma \to H_\gamma$ be a bijection s.t. $\sigma|_{H_\gamma\setminus\mathrm{Adj}_e} = (1)$ and $\sigma|_{\mathrm{Adj}_e} \in R_4 \ltimes \mathrm{Cyc}_4 =: \mathrm{STU}$. [3]
Define a group action $\Phi : \mathfrak{M}_1\mathcal{G}_n^3 \times \mathrm{STU} \to \mathfrak{M}_1\mathcal{G}_n^3$ by $\Phi_\sigma(e,\gamma) := (e,\sigma\gamma)$, where $\sigma\gamma := \langle H_\gamma, E_\gamma, \sigma V_\gamma\rangle$. The vertices $\sigma.v \in \sigma V_\gamma$ are given by $\sigma.v := \{\sigma(v_1),\sigma(v_2),\sigma(v_3)\}$. See also Figure 2.4.

This group action easily extends to $\mathfrak{M}_m\mathcal{G}_n^3$ and therefore to the whole space of all matched 3-regular graphs. An important observation is that the size of the equivalence classes (or orbits of Φ_σ) of graphs in $\mathfrak{M}_m\mathcal{G}_n^3$ can be different, since the action of STU might be a symmetry of the graph or the permuted graph is no longer part of $\mathcal{G}_n^3$. One still can give an upper bound. Let $[(M,\gamma)] \in \mathfrak{M}_m\mathcal{G}_n^3/\,\mathrm{STU}^m$ then $|[(M,\gamma)]| \leq |R_4 \ltimes \mathrm{Cyc}_4|^m = 3^m$.

[3] The notation is inspired by the s, t, and u channels known in physics.

Lemma 2.45. *Let $\rho_m : \mathfrak{M}_m\mathcal{G}_n^3/\operatorname{STU}^m \to \mathcal{G}_n^{4,m}$ be defined as above, then ρ_m is a bijection.*

Proof. It is enough to show that $\rho_1 : \mathfrak{M}_1\mathcal{G}_n^3/\operatorname{STU} \to \mathcal{G}_n^{4,1}$ is bijective because ρ_m can be constructed from m copies of ρ_1 (one for each matched edge) since they all commute with each other.
ρ_1 is surjective: Let $\Gamma \in \mathcal{G}_n^{4,1}$, take the 4 valent vertex and replace it by the following rule

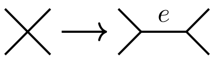

then the resulting graph γ is 3-regular, e is clearly a matching and $\rho_1(e,\gamma) = \Gamma$. ρ_1 is also injective. Let $[(e,\gamma)], [(e',\gamma')] \in \mathfrak{M}_1\mathcal{G}_n^3/\operatorname{STU}$ and $[(e,\gamma)] \neq [(e',\gamma')]$ and therefore their representatives differ by more than a permutation of Figure 2.4. But then $\rho_1((e,\gamma)) \neq \rho_1((e',\gamma'))$. ☐

Corollary 2.46. $\bigsqcup_{m\in\mathbb{N}} \mathfrak{M}_m\mathcal{G}_n^v/\operatorname{STU}^m =: \mathfrak{M}\mathcal{G}_n^3/\!\sim\ \cong \mathcal{G}_n^4$

Proof. By the decomposition of both sets as direct sums and Lemma 2.45 ☐

This result is quite central for this thesis, because later on the f-vector of the moduli space of graphs $MG_{1,n}^4$ is constructed by counting the number of possible matchings on 3-regular graphs. Furthermore, note that the number of graphs with m four valent vertices equals the number of cells dimension $n-m-1$ in the moduli spaces of graphs, as long as the isometries are neglected.

Compactification

As already mentioned, the cells of the moduli space MG contain open faces. It is useful to study the compactification or bordification of MG (originally this was done for the Outer space), which systematically replaces these faces with new ones to obtain a compact space. For example, the work [9] describes this procedure. The presented construction is taken from there. However, several details are skipped over in this section, since this is only meant to be a brief introduction.
Regard the moduli space of Yang-Mills graphs $MG_{l,n}^4$ and consider the set of all matchings $\mathfrak{M}_mG$ on a graph G. Let $\overline{\mathfrak{M}}_mG$ denote its complement with respect to 2^G, the set of all subgraphs of G. (To construct the compactification for general moduli spaces this set is altered accordingly). For every $\gamma \in \overline{\mathfrak{M}}_mG$ define a coordinate restriction map $r_\gamma : \langle G\rangle \to \langle\gamma\rangle$ which restricts the given metric on G to γ and rescales it accordingly. Then construct the product map as

$$\prod_{\gamma\in\overline{\mathfrak{M}}_mG} r_\gamma : \langle G\rangle \to \prod_{\gamma\in\overline{\mathfrak{M}}_mG} \langle\gamma\rangle$$

and define the compactified cell $\widehat{\langle G\rangle}$ as the closure of $\operatorname{im}\prod r_\gamma$. This image is the cartesian product of the image of each map r_γ.
The compactification of the moduli space $\widehat{MG}$ is defined for each cell and identifying the faces of the compactified cells via the face relations of the cells in MG.

Remark. In contrast to the usual construction for Outer space, the set $\overline{\mathfrak{M}}_mG$ contains non 1PI subgraphs of G, in the form of tree or loop subgraphs.

Example 2.47. Consider the one loop graph Σ_3 and neglect any isometries, then the relative simplex is $\langle\Sigma_3\rangle = (2^{[3]}, \{\{1\},\{2\},\{3\}\})$, which is a 2-cell with removed vertices. The set $\overline{\mathfrak{M}}_m\Sigma_3$ is given by the three spanning trees of Σ_3, denoted by T_i and the graph

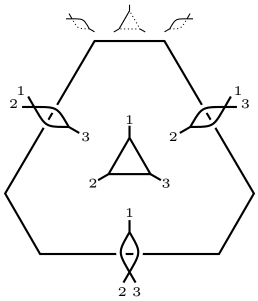

FIGURE 2.5: The compactified cell $\langle\hat{\Sigma}_3\rangle \subset MG^4_{1,3}$

itself. The compactification described above maps this to the hexagon and is shown in Figure 2.5. Where edges with non-zero length with respect to the metric on Σ_3 are drawn solid and those with non-zero length on T_i are drawn dotted. This representation is also used in [9].

The graphs $\gamma_i \in \overline{\mathfrak{M}}_m G$ can be arranged in flags, which is a collection of graphs such that $\gamma_n \subset \gamma_{n-1} \subset \cdots \subset \gamma_0$. Such a flag describes a missing face in $\langle G\rangle$.
There is an identical construction of the compactified cell by considering blow-ups along subspaces of the projective implementation of a simplex. Their equivalence is shown in [3]. The theory of blow-ups, a concept arising in algebraic geometry, is used to regularize the poles of the Feynman integrand derived below. The compactification of the moduli space is therefore tied to the renormalization procedure. Section 3.2 contains a brief passage with additional comments on that linkage.

Connectedness of $MG^4_{l,n}$

The following considerations are made to prove the connectedness of the moduli space $MG^4_{l,n}$ eventually. The proof relies on an induction over the loop number l, for which it useful to look at sets that are generated from graphs of a lower loop number by inserting an edge. They are defined by deleting edges of graphs with higher loops. Deleting an edge e from a graph G would technically leave two 2-valent vertices in $G \setminus e$. To render the graph $G \setminus e$ admissible delete the 2-valent vertices and connect the open ends accordingly. This is done implicitly in the following definition and henceforth.

Definition 2.48. *Let $g \in \mathcal{G}^3_{l-1,0}$ then define the set of l-loop graphs generated from g via*

$$\{g\}_e := \{\alpha \in \mathcal{G}^3_{l,0} \mid \alpha \setminus e = g\}.$$

Property 2.49. *Let $l > 1$ then*

$$\mathcal{G}^3_{l,0} = \bigcup_{g\in\mathcal{G}^3_{l-1,0}} \{g\}_e \ .$$

Proof. The inclusion $\mathcal{G}^3_{l,0} \supseteq \bigcup_g \{g\}_e$ is satisfied by definition. To show $\mathcal{G}^3_{l,0} \subseteq \bigcup_g \{g\}_e$ let $\gamma \in \mathcal{G}^3_{l,0}$ and $e \in E_\gamma$, then $\gamma \setminus e$ is clearly 3-regular and has no external legs. Furthermore, γ is 1PI and therefore by definition $|\gamma \setminus e| = l - 1$.[4]
If $\gamma \setminus e$ is not 1PI the graph γ must take the form

$\gamma =$ 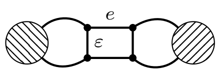

[4] Since γ is 1PI there is a spanning tree t of γ such that $e \notin t$.

for $l > 2$. However in that case $\gamma \setminus \varepsilon$ is 1PI. (For $l = 2$ $\gamma \setminus e$ is the 0-sun and thus 1PI). Eventually conclude that $\forall \gamma \in \mathcal{G}^3_{l,0}$ $\exists e \in E_\gamma$ such that $\gamma \setminus e \in \mathcal{G}^3_{l-1,0}$. □

The next definition formalizes the process of shrinking an edge e in a graph γ and expanding it. Note that the resulting graph γ' might be different from the originating one, but the graphs satisfy the equation $\gamma/e = \gamma'/e'$.

Definition 2.50. *Recall the group action Φ_σ given in Definition 2.44. Define for $(e, \gamma) \in \mathfrak{M}_1\mathcal{G}^3_n$ a similar group action $\tilde{\Phi}_{\varepsilon,\sigma}(e, \gamma) := \Phi_\sigma(\varepsilon(e), \gamma)$, where $\varepsilon : E_\gamma \to E_\gamma \in S_{|E_\gamma|}$.*
For the k-fold composition write $\tilde{\Phi}_{\varepsilon_k,\sigma_k} \circ \cdots \circ \tilde{\Phi}_{\varepsilon_1,\sigma_1} =: \Omega^x$, where
$x = (\varepsilon_k, \ldots, \varepsilon_1, \sigma_k, \ldots, \sigma_1) \in S^k_{|E_\gamma|} \times \mathrm{STU}^k$.

The map ε_1 selects an edge to be matched. Therefore, the domain of Ω^x can equivalently be given by the unmatched graphs $\mathcal{G}^3_n$. Together with a projection $(e, \gamma) \overset{\pi}{\mapsto} \gamma$, that forgets the marked edge, the following map arises $\pi \circ \Omega^x : \mathcal{G}^3_n \to \mathcal{G}^3_n$. Essentially this gives a slightly different perspective, where $\pi \circ \Omega^x$ is an operation on unmatched graphs and its image graph is unmatched as well. In the following the maps $\pi \circ \Omega^x$ and Ω^x are not distinguished notationally.
For each graph γ there is a subset $X_\gamma \subseteq \cup_k S^k_{|E_\gamma|} \times \mathrm{STU}^k$, such that any graph appearing in the composition $\Omega^x\gamma$ is admissible and the matching is valid for all $x \in X_\gamma$. If $x \in X_\gamma$ it is called *valid*.

Example 2.51. Consider an example to clarify the action of Ω^x. Let $\gamma \in \mathcal{G}^3_{3,0}$ be given by

$\gamma =$ 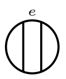 ,

where one edge is labeled with e and the half-edges in $\mathrm{Adj}_e = \{1, 2, 3, 4\}$ are counter clockwise starting from the left most half-edge in the picture above. Now let $x = (e, (23))$, then the graph γ maps to

$\Omega^x\gamma =$ 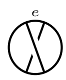 ,

where

$(\Omega^x\gamma)/e = \gamma/e =$ 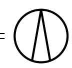 .

This mapping can be pictured by first shrinking the edge e of γ and then expanding it again. Replacing the 4-valent vertex with an edge can be done in three ways. Here one is specified by the permutation (23) in x.
Note that there are $x, y \in X_\gamma$ such that $\Omega^x\gamma = \Omega^y\gamma$, therefore observe that the stabilizer of Ω is clearly not trivial.

Property 2.52. *Let $\gamma \in \mathcal{G}^3_{l,n}$. The relative simplex $\langle\gamma\rangle$ is connected.*

Proof. Any element in the face poset $P[\langle\gamma\rangle]$ is connected to the vertex of $\langle\gamma\rangle$ since it is achieved by γ/M where M is a matching on γ. □

Lemma 2.53. *$MG^4_{l,0}$ is connected.*

Proof. Note that with the help of Property 2.49 the moduli space can be written as

$$MG^4_{l,0} = \bigcup_{\gamma \in \mathcal{G}^3_{l,0}} \langle\gamma\rangle = \bigcup_{g \in \mathcal{G}^3_{l-1,0}} \bigcup_{\alpha \in \{g\}_e} \langle\alpha\rangle .$$

Together with Property 2.52 it is then evident that $MG^4_{l,0}$ is connected if

$$\forall \gamma, \delta \in \mathcal{G}^3_{l,0} \quad \exists x \in X_\gamma, \text{ s.t. } \Omega^x \gamma = \delta. \tag{2.1}$$

This will be shown in two steps. First show that the condition (2.1) holds for $\alpha, \beta \in \{g\}_e$ for any $g \in \mathcal{G}^3_{l-1,0}$. The second step uses induction over the loop number l by assuming the connectivity of $MG^4_{l-1,0}$ to eventually proof that (2.1) indeed holds.
Let $\alpha \in \{g\}_e$ and $l > 2$, since α is admissible it is defined by g and two edges $e_1, e_2 \in E_g$, between whose the new edge e is formed. This allows the notation $\alpha = [g, e_1, e_2]$. Now consider matchings on α, where one of the adjacent vertices of e is matched to any vertex $v \in V_g$:

$(\epsilon, \alpha) =$ 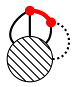 , (2.2)

where e is from now on depicted as a dotted line. Note that ϵ cannot be part of a multi-edge, since then g would not be 1PI. The graph α is also 1PI and therefore ϵ can not be a bridge of α. Conclude that the matching ϵ is valid.
Now investigate the action of Φ on (ϵ, α), the orbit is given by

$\mathrm{Orb}^\Phi_{(\epsilon,\alpha)} = \Big\{$ 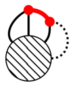 , 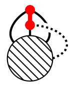 , 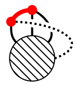 $\Big\}$.

Therefore observe that the action of Φ on graphs (ϵ, α), where the matching is of the type (2.2) can be written as

$$\Phi_\sigma(\epsilon, \alpha) = \Phi_\sigma[g, e_1, e_2] = [g, e_1, f_\sigma(e_2)],$$

where f_σ is a appropriate permutation on the edges of g. The matching on the graphs in $\mathrm{Orb}^\Phi_{(\epsilon,\alpha)}$ is also valid, because if it were not, $[g, e_1, f_\sigma(e_2)]$ would take the form

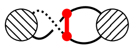 or 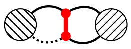 ,

but in both cases g would not be 1PI. Therefore all graphs in $\mathrm{Orb}^\Phi_{(\epsilon,\alpha)}$ corresponds to a face of $MG^4_{l,0}$.
Conclude that the map Ω^x, where $x \in X_\alpha$ is chosen such that it only contains matchings of the type (2.2), can be written as $\Omega^x \alpha = [g, \sigma(e_1), \tau(e_2)]$, where σ and τ are permutations on the edge set E_g. Furthermore, $(\Omega^x \alpha) \setminus e = g$ for any x. Therefore conclude, that the condition (2.1) holds for graphs $\alpha, \beta \in \{g\}_e$.

Now assume that (2.1) holds for $l-1$. Then any two sets $\{g\}_e$ and $\{h\}_e$ with $g, h \in \mathcal{G}^3_{l-1,0}$ posses a sequence of shrinking and expanding edges, represented by a mapping Ω^y, such that $\{g\}_e = \{\Omega^y h\}_e$. Now it is described how this map extends on elements of $\{h\}_e$. Therefore pick a graph $\alpha' = [h, a, a] =$  $\in \{h\}_e$. Note that any graph $[h, e_1, e_2]$ can be mapped to a graph of the form $[h, a, a]$ by the above. Recall the definition of the mapping $\Omega^y h$ in terms of the action $\tilde{\Phi}$

$$\Omega^y h = \big(\tilde{\Phi}_{\varepsilon_k, \sigma_k} \circ \cdots \circ \tilde{\Phi}_{\varepsilon_1, \sigma_1}\big) h,$$

this is well defined as a map on α' as long as $\varepsilon_i \neq (\sigma_{i-1} \circ \cdots \circ \sigma_1) a =: \rho_{i-1} a$, so that the edge a is never matched. Further note that Ω^y is constant on the half-edges $e \cup \mathrm{Adj}_e$. Denote the composition of the first j maps $\tilde{\Phi}_{\varepsilon_i, \sigma_i}$, that are well defined on α' as Ω^{y_j}. So it remains to construct the map $\tilde{\Phi}_{\rho_{j-1} a, \sigma_j}$ on $(\Omega^{y_{j-1}} \alpha')$, that realizes the permutation σ_j in through a valid edge shrinking and expanding. Therefore look at the following sequence, which illustrates the permutation (24) (the other ones are similar) on $\rho_{i-1}a$:

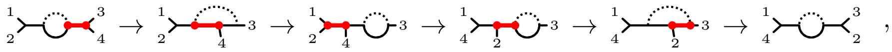

where at each step, the highlighted edge is shrunken and expanded to get to the next graph. Note that any matching containing a vertex of the edge e is valid as shown above. The matching on the third graph is also valid, since it is still a matching after the removal of e and $y \in X_h$ by assumption. Conclude that the sequence above defines a map $\Omega^{\tilde{y}_j}$ and by replacing the map $\tilde{\Phi}_{\rho_j a, \sigma_j}$ with $\Omega^{\tilde{y}_j}$, one obtains a valid action on α'. Repeatedly applying this replacement the map Ω^y on h can be extended to α' and is written as $\Omega^Y \alpha'$ with $Y \in X_{\alpha'}$. Consequently for any $\alpha \in \{h\}_e$ and $\beta \in \{g\}_e$ one finds a edge shrinking and expanding as follows

$$(\Omega^{x_2} \circ \Omega^Y \circ \Omega^{x_1})\alpha = (\Omega^{x_2} \circ \Omega^Y)[h, a, a] = \Omega^{x_2}[g, Ya, Ya] = \beta,$$

where Ya denotes the edge to which e is attached, which is the image of a under Ω^Y. The map $\Omega^{x_1} : \{h\}_e \to \{h\}_e$ is such that it only contains matchings given in (2.2), so does the map Ω^{x_2}.
For $l = 1, 2$ there is only one graph in $\mathcal{G}^3_{l,0}$, which completes the induction. ☐

Remark. The proof above constructs a path along the spine of $MG^4_{l,0}$ The spine is the geometric realization of the face poset $P[MG^4_{l,0}]$.
Furthermore, notice that only 1-matchings were used. This means, that the moduli spaces are already connected when only one four valent vertex is allowed.

Corollary 2.54. *$MG^4_{l,n}$ is connected.*

Proof. Let $(e, g) \in \mathfrak{M}_1\mathcal{G}^3_{l,n}$ and $h \in H^{ext}_g \cap \mathrm{Adj}_e$. These can take two general forms:

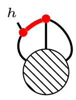

or
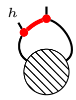

,

where the edges going into the blob are internal edges of g. In the latter one, the two external edges can be transposed by an edge shrinking and expanding. In the first one, the external edge h can be attached to any of the three internal edges. As a conclusion for a fixed graph $g_0 \in \mathcal{G}^3_{l,0}$ all graphs arising by attaching n external legs to g_0 are connected in $MG^4_{l,n}$.
Furthermore, the edge shrinking and expanding that relates g_0 to any other graph $h_0 \in \mathcal{G}^3_{l,0}$ can be extended to $\mathcal{G}^3_{l,n}$, since whenever a matched edge of g_0 contains external half-edges, the permutation can still be realized, by first shifting the external half-edges to an adjacent edge. ☐

In the next section, the properties of one loop moduli spaces of graphs are investigated.

2.4.2 One Loop Moduli Spaces $MG_{1,n}$

Understanding the moduli spaces requires to investigate the isometries between the metric graphs. Isometries are isomorphisms between two graphs that respect the metric. Here isomorphic contracted metric graphs are explicitly excluded. In the case of one-loop graphs, the following observation is crucial for the results of this thesis.

Property 2.55. *Let $g \in MG_{1,n}$, then $\exists h \in MG_{1,n}$ which is isometric to g iff g has a multi-edge.*

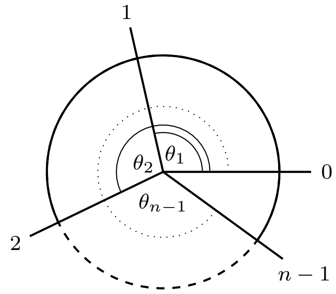

FIGURE 2.6: $MG_{1,n} \cong \mathbb{T}^{n-1}/\mathbb{Z}_2$

Proof. First, recall that tadpoles are excluded. Further note that there are no external leg fixing isomorphisms between one-loop graphs unless the graph possesses a multi-edge. □

For the moduli space with restricted vertex valencies, this can be further specified by the number of external legs.

Property 2.56. *Let $g \in MG^v_{1,n}$, then $\exists h \in MG^v_{1,n}$ which is isometric to g iff $n \leq 2v - 4$.*

Proof. Fix $v > 2$. A one-loop graph with a multi-edge must have two vertices. This graph can have at most $n = 2v - 4$ external legs. Adding a further one implies that a new vertex is needed and thus the multi-edge is destroyed. □

Now a slightly different perspective on the one-loop moduli space is presented. It is only used in this section to illustrate some examples for small n.
A one-loop graph with n external legs in the moduli space of graphs can be thought of as a circle divided in n segments. The length of each segment represents the length of an internal edge and is parametrized by an angle θ. Since one angle can be set to zero, there are $n-1$ independent angles describing a graph in $MG_{1,n}$, this is shown in Figure 2.6. Let $\boldsymbol{\theta} \in \mathbb{T}^{n-1}$ denote this tuple of angles, where $\mathbb{T}^n$ is the n dimensional torus. The two points $\boldsymbol{\theta}$ and $-\boldsymbol{\theta}$ describe the same point in $MG_{1,n}$. This induces a group action $\rho : \mathbb{T}^{n-1} \times \mathbb{Z}_2 \to \mathbb{T}^{n-1}$ and $MG_{1,n}$ can be described as the quotient space $\mathbb{T}^{n-1}/\mathbb{Z}_2$.
This group action also takes care of the possible isometries between two one-loop graphs. The corresponding isomorphisms switch the edges of a multi-edge, which is precisely the action of ρ.
A list of the spaces $MG_{1,n}$ for small n is given below. There $\{\text{pt}\}$ denotes the space consisting of only one point, I an interval and $\mathbb{S}^2$ the 2-sphere.

$$\begin{aligned} MG_{1,1} &\cong \mathbb{T}^0/\mathbb{Z}_2 \cong \{\text{pt}\} \\ MG_{1,2} &\cong \mathbb{T}^1/\mathbb{Z}_2 \cong I \\ MG_{1,3} &\cong \mathbb{T}^2/\mathbb{Z}_2 \cong \mathbb{S}^2 \end{aligned}$$

Derivation of $\mathbb{T}^2/\mathbb{Z}_2 \cong \mathbb{S}^2$

Figure 2.7 shows how one can construct that $\mathbb{T}^2/\mathbb{Z}_2 \cong \mathbb{S}^2$. The first picture shows the torus as a square with identified opposite sites, indicated by the color of the arrows and the vertical, dashed line. The action of $\mathbb{Z}_2$ establishes an additional equivalence relation, indicated by the dashed line going through the point in the middle. A point x on such a line is identified with a different point $-x$, the unique point on the line which has the same distance from the middle. This causes a second equivalence on the boundary of the square:

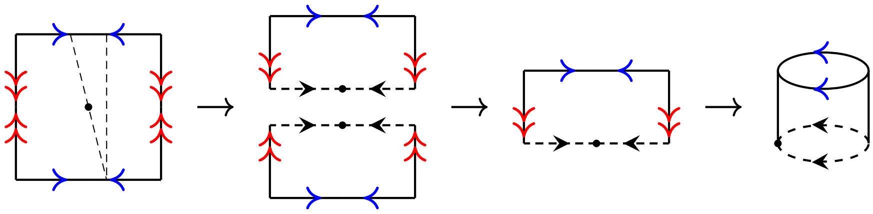

FIGURE 2.7: Construction of $\mathbb{T}^2/\mathbb{Z}_2 \cong \mathbb{S}^2$

a folding, indicated by the inwards pointing arrows.
The action of $\mathbb{Z}_2$ can be realized by cutting the square in half, rotating one half by 180 degrees about the middle point and gluing the halves on top of each other. The second picture shows the cut along a line through the middle. On this line, there are also two equivalences, one to reverse the cut and the other is the action of $\mathbb{Z}_2$.
The third picture shows $\mathbb{T}^2/\mathbb{Z}_2$ after the two halves are glued together. The remaining identifications come from the representation of the torus and the cut. The line marked in blue still needs to be folded, since at this stage only one of the two equivalences is satisfied. The same applies to the edges marked in red. Here the remaining identification is coming from the representation of the torus. The cut (marked as a dashed line in the figure) also still needs a folding, because this is just redoing the cut after the rotation.
Carrying out the equivalence on the line marked with red arrows leads to a cylinder, with the each of the boundaries glued together, which is just the sphere, see also the last picture in Figure 2.7.

Examples of $MG^4_{1,n}$

Shrinking edges of a graph in $MG_{1,n}$ corresponds to setting two angles equal. Allowing only vertex valencies of 3 or 4 corresponds to remove a subspace $\Gamma_n \subset MG_{1,n}$ from the whole moduli space $MG_{1,n}$. So in this notation $MG^4_{1,n} = MG_{1,n} - \Gamma_n$.
Γ_n contains the points $\boldsymbol{\theta}$ where at least three angles coincide. For this discussion, the angle of the external leg marked with 0 in Figure 2.6 is treated as the nth angle fixed at 0. It follows immediately that $\dim \Gamma_n = n - 3$. This result is later reproduced combinatorially.
The upcoming examples look at $MG^4_{1,n}$ for some values of n.

Example 2.57. $n = 3$.
Since Γ_3 contains of all points in $MG_{1,3}$ where at least 3 angles are fixed, the only point in Γ_3 is $\boldsymbol{\theta} = 0$, i.e. $\theta_1 = \theta_2 = 0$. Therefore $MG^4_{1,3} = \mathbb{S}^2 - \{\text{pt}\} \cong \mathbb{R}^2$.

Example 2.58. $n = 4$.
Γ_4 contains of one point $\boldsymbol{\theta} = 0$ and 4 intervals all connected to that point. Pictorally,

$\Gamma_4 =$ 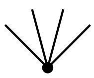 $\underset{\text{h.e.}}{\cong} \{\text{pt}\}.$

Example 2.59. $n = 5$.
Γ_5 contains the point $\boldsymbol{\theta} = 0$, five intervals I connected to that point and $\binom{5}{3} = 10$ copies of $\mathbb{S}^2$ all of which contain two distinct intervals. The only points that are shared by two spheres must lie on one of the intervals. As for $n = 4$ these intervals are contractible and so it remains a wedge sum of spheres, glued together at the point $\boldsymbol{\theta} = 0$. This leads to the conclusion

$$\Gamma_5 \cong \left(\mathbb{S}^2\right)^{\wedge 10}.$$

Chapter 3
Connection to Physics

This chapter carries out the connection between the physical viewpoint, coming from a perturbative quantum field theory approach to the central object of this thesis, the moduli space of gluon graphs. First, a summary of Yang-Mills theory and an argument why in non-abelian gauge theories five valent vertices do not appear. A second section introduces parametric Feynman integrals, and subsequently, the appearance of moduli spaces of graphs in scattering amplitudes is made clear.

3.1 The Absence of 5-Valent Vertices in Yang-Mills Theories

In this section, an argument is presented why there is no need for a 5-valent gauge boson vertex in non-abelian gauge theories. It relies on the underlying Lie algebra structure and is performed via a recap of the gauge invariance of YM theory and therefore the corresponding Ward identities, which are also called Slavnov-Taylor identities. The considerations at hand are based on argumentations presented in [10].

3.1.1 Recap of Non-Abelian Gauge Theories

A crucial concept of quantum field theories is gauge invariance. Proceeding from a Lagrangian $\mathcal{L}$ that permits a certain local symmetry, one demands that the quantized theory still owns that symmetry. In the case of Yang-Mills theories, the classical Lagrangian $\mathcal{L}^c_{YM}$ is invariant under the action of $SU(n)$. The generators of the corresponding Lie algebra $\mathfrak{su}(n)$ are denoted by t^a, where $a = 1, 2, \ldots, n^2 - 1$. They satisfy the commutation relation

$$[t^a, t^b] = i f^{abc} t^c \ .$$

By implementing the normalization $\mathrm{Tr}(t^a t^b) = \delta_{ab}/2$ the structure constant f^{abc} is totally antisymmetric. The generators t^a satisfy the so called Jacobi identity given by

$$\begin{aligned} 0 &= \big[[t^a, t^b], t^c\big] + \big[[t^c, t^a], t^b\big] + \big[[t^b, t^c], t^a\big] \\ &= -\left(f^{dec} f^{eab} + f^{deb} f^{eca} + f^{dea} f^{ebc}\right) t^d \ , \end{aligned} \tag{3.1}$$

where in the second line the expression in the brackets has to vanish, which imposes a identity on the structure constants. In the following both identities are referred to as the Jacobi identity.

Throughout this chapter color indices are given by roman letters and spacetime indices by greek ones. Using the Einstein sum convention the Lagrangian takes the form

$$\mathcal{L}^c_{YM} = -\frac{1}{4} F^a_{\mu\nu} F^{a\mu\nu},$$

where $F^a_{\mu\nu}$ are the components of the field strength tensor, which is defined in terms of the gluon field $A_\mu = t^a A^a_\mu$:

$$F^a_{\mu\nu} := \partial_\mu A^a_\nu - \partial_\nu A^a_\mu - ig[A_\mu, A_\nu]^a \ .$$

The Lagrangian $\mathcal{L}^c_{YM}$ persists a global symmetry, it stays invariant under the action of $U \in SU(n)$ on the fields A_μ given by

$$A_\mu \to U A_\mu U^{-1}$$

The corresponding Noether current is $j^\nu_a = f^{abc} F^{c\mu\nu} A^b_\mu$ and the equation of motion reads $\partial_\mu F^{\mu\nu} = j^\nu$. The Lagrangian is invariant under the following the field transformation:

$$A_\mu \to U A_\mu U^{-1} + (\partial_\mu U) U^{-1} \ .$$

Where U is now taken to be a $SU(n)$ valued function of spacetime. This invariance is called local gauge invariance and forbids a mass term for the field A_μ. Conclude that gluons are massless. This symmetry might be viewed as an artifact of the theory. It is not a symmetry of nature. Gauge fields that are related by a local gauge transformation are physically equivalent, which means they do not describe different states in nature.
To consistently quantize Yang-Mills Theory, this symmetry needs to be taken into account by breaking it at the classical level via gauge fixing. This reduces the degrees of freedom of the gauge field to physical relevant ones. During quantization, one needs to ensure that these constraints remain true, such that the unphysical degrees of freedom do not appear in measurable results. This procedure is described in many QFT textbooks, for example, in [11]. Famously, new non-observable particles, hence often called ghosts, which cancel the unphysical degrees need to be introduced.
The gauge fixing is done by an additional constraint on the gauge fields A_μ. In the presented approach the Lorentz condition

$$\partial^\mu A^a_\mu = 0 \tag{3.2}$$

is chosen.
A further ingredient of a quantum field theory is an unitary representation of the Lorentz group of the fields under consideration. For massless vector particles (e.g. A_μ) this imposes the transversality condition on the polarization vectors $e^\mu(k,\sigma)$ [12]:

$$k_\mu e^\mu(k,\sigma) = 0 \ , \tag{3.3}$$

where k_μ describes the momentum and $\sigma = \pm 1$ the spin of the particle. Since A_μ is massless note that the condition (3.3) is unaffected by the following transformation of the polarization vector

$$e^\mu(k,\sigma) \to e^\mu(k,\sigma) + k^\mu \omega(k,\sigma), \tag{3.4}$$

where $\omega(k,\sigma)$ is a arbitrary function. Further observe that the gauge condition (3.2) is equivalent to transversality. Therefore deduce that the polarization vectors still possess a gauge symmetry that needs to be preserved in the quantum theory. In the sense that such a transformation does not alter the measurable results, which means that $\omega(k,\sigma)$ does not add a physical degree of freedom.

Perturbative quantum field theories best describe scattering events. The probability that an incoming state evolves to a certain outgoing state of particles is described by the S-matrix. It is a central quantity of the theory that is directly related to experimental results. In perturbation theory, its elements are calculated using Feynman diagrams. The S-matrix of pure Yang-Mills theory is given by the LSZ Formula which schematically takes the form

$$S_{ab} \propto \left(\prod_{j}^{n} e_{\rho_j}(k_j, \sigma_j) \right) \mathcal{M}^{\rho_1 \cdots \rho_n}(k_1, \ldots, k_n) \,, \tag{3.5}$$

where k_j are the external momenta. Furthermore the vectors $e_{\rho_j}(k_j, \sigma_j)$ are the polarization of the external gluons. The matrix element $\mathcal{M}^{\rho_1 \cdots \rho_n}$ describes the interaction and is given by the graphs under consideration and the Feynman rules of the theory. For this thesis the precise structure of the S-matrix is not needed, since in the following a invariance already arising from this general form is studied.
The gauge freedom of the polarization vector (3.4) should still be valid in the quantum theory. Therefore the S-matrix needs to be invariant under this transformation. This would be the case if

$$k_{i\rho_i} \mathcal{M}^{\rho_1 \cdots \rho_i \cdots \rho_n}(\boldsymbol{k}) = 0. \tag{3.6}$$

In the following, it is motivated how this equation can be proven and how it is related to the allowed interactions of a gauge theory. To analyze the structure of the matrix element use Feynman diagrams and rules which are introduced next.

Feynman Rules of Yang-Mills Theory

The Feynman rules of Yang-Mills theory are given below, using the same conventions as in [11], and they are presented as a map $\mathcal{F}$. The rules are given in Feynman gauge. The wiggly lines denote gluons, and the dotted ones are ghosts. Furthermore, all momenta are taken to flow inwards. The external particles are always numbered clockwise, and the structure constant f^{abc} is read off clockwise as well (although this will only become important later).

$$\xmapsto{\mathcal{F}} \quad \frac{\eta_{\mu_1\mu_2}\delta_{a_1a_2}}{k^2 + i\epsilon}$$

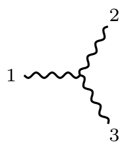

$$\xmapsto{\mathcal{F}} \quad -igf^{a_1a_2a_3}\big(\eta^{\mu_1\mu_2}(k_2 - k_1)^{\mu_3} + \eta^{\mu_1\mu_3}(k_1 - k_3)^{\mu_2} + \eta^{\mu_3\mu_2}(k_3 - k_2)^{\mu_1}\big)$$

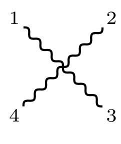

$$\xmapsto{\mathcal{F}} \quad g^2\big(f^{ea_1a_2}f^{ea_3a_4}(\eta^{\mu_1\mu_4}\eta^{\mu_2\mu_3} - \eta^{\mu_1\mu_3}\eta^{\mu_2\mu_4}) + f^{ea_1a_3}f^{ea_4a_2}(\eta^{\mu_1\mu_2}\eta^{\mu_3\mu_4} - \eta^{\mu_1\mu_4}\eta^{\mu_2\mu_3}) + f^{ea_1a_4}f^{ea_2a_3}(\eta^{\mu_1\mu_3}\eta^{\mu_2\mu_4} - \eta^{\mu_1\mu_2}\eta^{\mu_3\mu_4})\big)$$

$$\xmapsto{\mathcal{F}} \quad \frac{\delta_{a_1a_2}}{k^2 + i\epsilon}$$

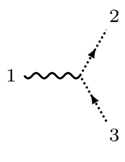

$$\xmapsto{\mathcal{F}} \quad igf^{a_1a_2a_3}k_2^{\mu_1}$$

It is useful to note that the color structure of the four valent vertex allows rewriting its Feynman rule as

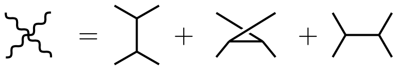

(3.7)

where $\mathcal{F}$ () $= g^2 f^{ea_1a_4} f^{ea_2a_3}(\eta^{\mu_1\mu_3}\eta^{\mu_2\mu_4} - \eta^{\mu_1\mu_2}\eta^{\mu_3\mu_4})$. The above equation does not distinguish between graphs and their images under $\mathcal{F}$. This abuse of notation is used as long as it does not leads to confusion.

Definition 3.1. *Let G be a connected Feynman graph with l_g closed ghost loops, then define the Feynman integral by*

$$I_G := (-1)^{l_g}\left[\prod_{e\in E_G}\int dk_e \mathcal{F}(e)\right]\prod_{v\in V_G}\mathcal{F}(v)\delta(k_v).$$

Where $\delta(k_v)$ ensures momentum conservation at the vertex v. If $G = G_1 \sqcup G_2$ define $I_G := I_{G_1} I_{G_2}$.

Note that for the upcoming discussion the precise structure of the Feynman rules for non tree graphs is not important. The definition above will be made accurate in the next section where the Feynman integral is related to the structure of moduli spaces of graphs.
Finally define the matrix element $\mathcal{M}$ for a process with n external gluons, also called n-point functions in terms of Feynman diagrams by

$$\mathcal{M}^{\rho_1\cdots\rho_n} = \sum_{|E_G^{ext}|=n} I_G, \tag{3.8}$$

where the sum is over all possible graphs. The indices on the right hand side in equation (3.8) are given implicitly, they label the external edges of G. If the sum of the definition in (3.8) is restricted to a certain loop number l of the graphs G, the corresponding matrix element is denoted by $\mathcal{M}_l$.

3.1.2 Invariance of the 4-Gluon Vertex

Multiplying the three valent vertex with the momenta k_1^α leads to the bare three point Ward identity by using momentum conservation as follows:

$$\begin{aligned} &k_{1\alpha}(-igf^{abc})\left(\eta^{\alpha\beta}(k_2-k_1)^\gamma + \eta^{\alpha\gamma}(k_1-k_3)^\beta + \eta^{\gamma\beta}(k_3-k_2)^\alpha\right) = \\ &= -igf^{abc}\left(k_1^\beta k_2^\gamma - k_1^\gamma k_3^\beta + \eta^{\gamma\beta}(k_1\cdot k_3 - k_1\cdot k_2)\right) = \\ &= igf^{abc}\left(k_2^\beta k_2^\gamma - k_3^\beta k_3^\gamma + \eta^{\gamma\beta}(k_3^2 - k_2^2)\right) \end{aligned}$$

Together with the diagrammatic rules

 $:= k_e^{\mu_e}$ and (3.9)

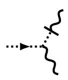 $:= igf^{abc}\eta^{\beta\gamma}k_2^2$ (3.10)

the three point Ward identity can be written diagrammatically as

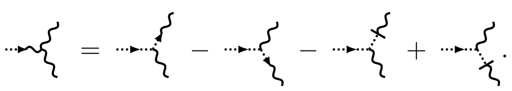

(3.11)

The four vertex satisfies the following Ward identity

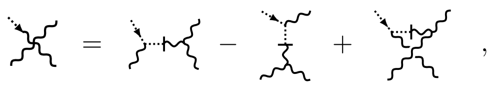

(3.12)

which is proven by direct computation. Starting with the first graph on the right hand side of equation (3.12) one obtains

$$\begin{aligned} & g^2 f^{dec} f^{eab} \left[\eta^{\gamma\alpha}(2k_1+k_2)^\beta + \eta^{\gamma\beta}(-2k_2-k_1)^\alpha + \eta^{\beta\alpha}(k_2-k_1)^\gamma\right] \\ &= \; g^2 f^{dec} f^{eab} \left[\eta^{\gamma\alpha}(k_1-k_3)^\beta + \eta^{\gamma\beta}(k_3-k_2)^\alpha + \eta^{\beta\alpha}(k_2-k_1)^\gamma\right] \\ &\quad + g^2 f^{dec} f^{eab} \left[\eta^{\gamma\alpha}(k_1+k_2+k_3)^\beta - \eta^{\gamma\beta}(k_1+k_2+k_3)^\alpha\right]. \end{aligned}$$

Where only the momentum conservation was used. Note that the last two diagrams on the r.h.s. of equation (3.12) are cyclic permutations of the external gluon edges of the first one. The minus sign of the second graph in (3.12) is caused by the antisymmetric structure constant f^{abc}, since the vertex defined in equation (3.10) is antisymmetric. Adding up the three diagrams of equation (3.12) the second term in the square brackets leads to the desired term and the first one vanishes due to the Jacobi identity (3.1):

$$\begin{aligned} & g^2 \left(f^{dec} f^{eab} + f^{dea} f^{ebc} + f^{deb} f^{eca}\right) \\ & \times \left[\eta^{\gamma\alpha}(k_1-k_3)^\beta + \eta^{\gamma\beta}(k_3-k_2)^\alpha + \eta^{\beta\alpha}(k_2-k_1)^\gamma\right] = 0\,. \end{aligned}$$

This expression is obtained by noting that the term in the square brackets is the same for every diagram on the right hand side of equation (3.12).
The tree level Ward identities (3.11) and (3.12) have a nice consequence for the on-shell[1] tree level matrix element $\mathcal{M}_0$ of the four point interaction, namely

$$k_{1\alpha}\mathcal{M}_0^{\alpha\beta\gamma\delta} := \delta\mathcal{M}_0 =$$

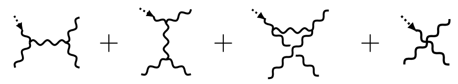

(3.13)

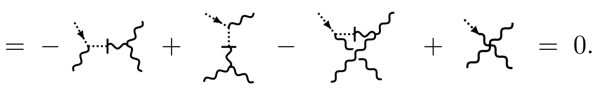

(3.14)

In a purely diagrammatic approach to QCD one might even define the 4-vertex via this relation.
To maintain $\delta\mathcal{M} = 0$ for higher loop orders one needs to introduce ghosts (already apearing in the three point bare Ward identity (3.11)). By momentum conservation the ghost vertex obeys the bare ghost Ward identity:

$$igf^{abc}k_2 \cdot k_1 - igf^{abc}k_2 \cdot k_3 = igf^{abc}(k_3^2 - k_1^2)$$

Which can be translated into a diagrammatic equation as

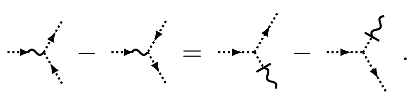

(3.15)

Where the diagrams on the right hand side are defined similar to (3.10), but without the metric.
To be able to proof that $\delta\mathcal{M} = 0$ to all loop orders one final identity is needed. It relates the four point interaction with a five legged diagram. It can be understood in the terms of

[1] On-shell refers to the external momenta squaring to zero, $k_e^2 = 0$ for $e \in E_G^{ext}$.

the four point Ward identity (3.12).

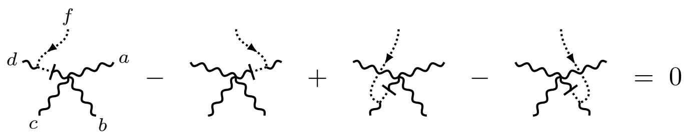

(3.16)

To prove (3.16) show that it holds for each term in (3.7) individually. Then each term of (3.16) has the same Minkowski structure and the equation reduces to the following statement involving the structure constants.

$$\begin{aligned}
&f^{fed}f^{gab}f^{gce} - f^{fae}f^{geb}f^{gcd} + f^{fec}f^{gab}f^{ged} - f^{fbe}f^{gae}f^{gcd} = \\
&\quad = f^{gab}\left(f^{fed}f^{gce} + f^{fec}f^{ged}\right) + f^{gcd}\left(f^{fea}f^{geb} + f^{feb}f^{gae}\right) \\
&\quad = f^{gab}\left(-f^{feg}f^{ecd}\right) + f^{gcd}\left(-f^{feg}f^{eab}\right) \\
&\quad = -\left(f^{gab}f^{feg}f^{ecd} + f^{gcd}f^{feg}f^{eab}\right) = 0
\end{aligned}$$

Were in the second line the antisymmetry of the structure constant and in the third line the Jacobi identity were used.

The structure of the invariance equation of the 4-vertex (3.16) is similar to the Ward identity of the 4-vertex. So one might interpret this equation as a 5 point Ward identity and the fact that it vanishes as a indicator that a 5-vertex in Yang-Mills Theories would also vanish. In different words, the theory does not need a 5-point interaction to be gauge invariant, which can be proven by using the tree level Ward Identities derived in this chapter [10, 13]. Reversing this argument, a potential five gluon vertex would need this color structure to be gauge invariant, and since (3.16) vanishes purely due to the color algebra, its Feynman rule would vanish. In that sense there is no need for higher gluon interaction terms to render gluons transversal in the quantized theory.

3.2 Outer Space and Feynman Integrals

3.2.1 Introduction

The renormalized Feynman integral $I_G^R(\boldsymbol{p},\mu)$[2], which regularises the Feynman integral I_G schematically, is a (analytic continued) complex-valued function of the external momenta, the masses of the particles appearing in the diagram G (combined in the variable $\boldsymbol{p}$) and the renormalization point μ.
In the paper [1] $I_G^R(\boldsymbol{p},\mu)$ is investigated as a multi-valued function and its relation to Outer space. A cell of Outer space is given by a metric graph together with a marking. Equivalent markings then correspond to different equivalent representations of I_G^R as an iterated integral by the Fubini Theorem and vice versa. An iterated integration is given by choosing a spanning tree together with an ordering of its edges. All these orders are equivalent due to the Fubini Theorem. Note that a choice of a spanning tree and a basis of the fundamental group of G gives an inverse marking. In [1] it is further suggested that different markings on the same graph correspond to different sheets of the multi-valued $I_G^R(\boldsymbol{p},\mu)$.

In the previous section, the S-matrix was introduced. In a scattering process with n external particles at a given loop order l it is given by the amplitude $\mathcal{A}_{l,n}(p,m)$ as a function of the external momenta and masses.

$$\mathcal{A}_{l,n}(p,m) := \sum_{G\in\mathcal{G}^4_{l,n}} I_G\,,$$

where I_G is the Feynman integral defined above and $\mathcal{G}^4_{l,n}$ is the set of rank l graphs with n external legs and bounded vertex valency at four. Amplitudes of Yang-Mills theories fall into this type. The following consideration aims for a better understanding of these amplitudes and the corresponding integrations. It will turn out, that the combined integration domain of the amplitude is equivalent to the moduli space of graphs $MG^4_{l,n}$ [3].

3.2.2 Derivation of Parametric Feynman Integrals

In the previous section, Feynman rules and integrals were introduced. The next step is to manipulate the Feynman integrals such that a connection to the moduli space can be made. Here only scalar integrals were with no k dependency in the nominator are considered. This restriction will be justified later. The derivation presented is taken from [14] with slight deviations. Write the integral under consideration as

$$I_G = \left[\prod_{e\in E_G}\int_{\mathbb{M}^D}\frac{\mathrm{d}^D k_e}{i\pi^{D/2}}\left(k_e^2+m_e^2\right)^{-1}\right]\prod_{v\in V_G\setminus v_0}\pi^{D/2}\delta^D(k_v)\,. \tag{3.17}$$

where k_e is the momentum assigned to edge e and the factor $\delta^D(k_v)$ establishes momentum conservation at each vertex, with

$$k_v := p(v) + \sum_{e\in E_G}\mathcal{E}_{e,v}k_e\,.$$

The momentum $p(v)$ is the external momentum flowing into v, if v has no external edge attached to it, set $p(v)=0$. The matrix elements $\mathcal{E}_{e,v}$ are 1 if k_e flows into v and -1 if the momentum points in the other direction.
In the following considerations it is useful to omit one arbitrary vertex $v_0\in V_G$ from the

[2] Rigorous definitions can be found in any QFT textbook and the actual renormalization prescription is not important here.

momentum conservation. This discards a factor $\delta^D(\sum_{v\in V_G} p(v))$, the conservation of the external momenta, from the final result. It is well known that I_G diverges and therefore needs regularization. In this thesis is not focused on this procedure, so for the derivation of the parametric form of I_G it is simply assumed that the integral is well defined.
Preceding from (3.17) use the Schwinger trick

$$\frac{1}{P} = \int_0^\infty e^{-\alpha P} \mathrm{d}\alpha \quad \text{for } P > 0$$

and $(2\pi)^D \delta^D(k) = \int e^{ixk} \mathrm{d}^D x$ to arrive at

$$\begin{aligned} I_G = &\left[\prod_{e\in E_G} \int_0^\infty \mathrm{d}\alpha_e\right] \left[\prod_{v\in V_G\setminus v_0} \int_{\mathbb{R}^D} \frac{\mathrm{d}^D x_v}{(4\pi)^{D/2}}\right] \left[\prod_{e\in E_G} \int_{\mathbb{M}^D} \frac{\mathrm{d}^D k_e}{i\pi^{D/2}}\right] \\ &\times \exp\left[-\sum_{e\in E_G} \alpha_e\big(k_e^2 + m_e^2\big) + i \sum_{v\in V_G\setminus v_0} x_v \Big(p(v) + \sum_{e\in E_G} \mathcal{E}_{e,v} k_e\Big)\right]. \end{aligned} \tag{3.18}$$

Now introduce two matrices with its help the argument of the exponential function can be rearranged.

Definition 3.2. *The Laplace matrix $\mathcal{L}_G$ and its dual $\hat{\mathcal{L}}_G$ are $|V_G| \times |V_G|$ matrices defined as*

$$\mathcal{L}_G := \mathcal{E}^T \Lambda \mathcal{E} \quad \textit{and} \quad \hat{\mathcal{L}}_G := \mathcal{E}^T \Lambda^{-1} \mathcal{E}$$

with $\Lambda := \mathrm{diag}\big(\alpha_1, \ldots, \alpha_{|E_G|}\big)$.

For a matrix A and I, J being subsets of the rows or respectively columns, denote by $A[I, J]$ the matrix with rows and columns I, J removed. If $I = J$ write $A[I]$. Moreover collect all internal momenta k_e into the vector $\boldsymbol{k} \in \mathbb{R}^{D|E|}$ and all external momenta $p(v)$ and positions x_v into the vectors $\boldsymbol{x}, \boldsymbol{p} \in \mathbb{R}^{D(|V|-1)}$ whose elements are 4-vectors. Then the argument of the exponential in (3.18) can be written as

$$-\boldsymbol{k}^T(\Lambda \otimes \eta_D)\boldsymbol{k} + i\left(\boldsymbol{x}^T \cdot \boldsymbol{p} + \boldsymbol{x}^T(\mathcal{E}^T[\emptyset, v_0] \otimes \eta_D)\boldsymbol{k}\right) - \sum_{e\in E_G} \alpha_e m_e^2\,,$$

where the tensor product with the Minkowski metric η_D arises since the scalar products are calculated with that signature. Likewise the dot product $\boldsymbol{x}^T \cdot \boldsymbol{p}$ is understood as $\boldsymbol{x}^T(1_{|V|-1} \otimes \eta_D)\boldsymbol{p}$, where 1_D is the D-dimensional unit matrix.
Complete the square, omit the notation of the tensor product, and the removal of the v_0 column, then the expression takes the form

$$\begin{aligned} &-\left(\boldsymbol{k} - \frac{i}{2}\Lambda^{-1}\mathcal{E}\boldsymbol{x}\right)^T \Lambda \left(\boldsymbol{k} - \frac{i}{2}\Lambda^{-1}\mathcal{E}\boldsymbol{x}\right) - \left(\frac{\boldsymbol{x}}{2} - i\hat{\mathcal{L}}^{-1}\boldsymbol{p}\right)^T \hat{\mathcal{L}}\left(\frac{\boldsymbol{x}}{2} - i\hat{\mathcal{L}}^{-1}\boldsymbol{p}\right) \\ &- \boldsymbol{p}^T \hat{\mathcal{L}}^{-1}\boldsymbol{p} - \sum_{e\in E_G} \alpha_e m_e^2\,. \end{aligned}$$

Now the integration over $\boldsymbol{k}$ and $\boldsymbol{x}$ may be performed. Use translation invariance and the integral over $\boldsymbol{k}$ becomes

$$\begin{aligned} \left[\prod_{e\in E_G} \int_{\mathbb{M}^D} \frac{\mathrm{d}^D k_e}{i\pi^{D/2}}\right] \exp\left[-\boldsymbol{k}^T(\Lambda \otimes \eta_D)\boldsymbol{k}\right] &= \left[\prod_{e\in E_G} \int_{\mathbb{R}^D} \frac{\mathrm{d}^D k_e}{\pi^{D/2}}\right] \exp\left[-\boldsymbol{k}^T(\Lambda \otimes 1_D)\boldsymbol{k}\right] \\ &= \frac{1}{\pi^{|E_G|D/2}} \frac{(2\pi)^{|E_G|D/2}}{\sqrt{\det 2\,(\Lambda \otimes 1_D)}} = \frac{1}{(\det\Lambda)^{D/2}}. \end{aligned}$$

For the first equal sign perform the usual Wick rotation to transform the integration domain from Minkowski signature to euclidean. The last step is the typical Gauss integration for matrices. The integration over $\boldsymbol{x}$ is computed analogously and this leads to the parametric representation of I_G

$$I_G = \left[\prod_{e \in E_G} \int_{\mathbb{R}_+} \mathrm{d}\alpha_e \right] \frac{e^{\Xi_G/\psi_G}}{\psi_G^{D/2}} , \tag{3.19}$$

where ψ_G and Ξ_G are polynomials defined by

$$\psi_G := \det\Lambda \det\hat{\mathcal{L}}_G[v_0] \;\text{ and }\; \Xi_G := \psi_G \left(\sum_{e \in E_G} \alpha_e m_e^2 + \boldsymbol{p}^T \big(\hat{\mathcal{L}}_G^{-1}[v_0] \otimes \eta_D \big) \boldsymbol{p} \right).$$

The polynomial ψ_G is the first Symanzik polynomial and $\Xi_G = \psi_G \sum \alpha_e m_e^2 + \varphi_G$, where φ_G denotes the second Symanzik polynomial. Properties of these polynomials are investigated in the next section.

Tensor Integrals

Integrands with loop momenta in the nominator (also called tensor integrals) can be reduced to the studied case by different approaches. Any of them uses a slightly more general integrand in (3.17), where one allows for an arbitrary negative exponent of the propagator $-a_e$. The generalized Schwinger trick introduces a factor $\alpha_e^{a_e - 1}/\Gamma(a_e)$ for each edge in the nominator of the final result [14].
The first one uses the fact, that the shift of the integration variables $\boldsymbol{k} \to \boldsymbol{k} - i/2\Lambda^{-1}\mathcal{E}\boldsymbol{x}$ introduces parameters α in the nominator. (Note that in the derivation presented above, it is not clear how to perform the integration over $\boldsymbol{x}$ after the shift.) These can be treated by allowing higher powers of the propagator term in (3.17). Furthermore, the terms involving loop momenta in the nominator are related to scalar integrals in a shifted dimension by Lorentz invariance [15].
A different approach uses a differential operator. Therefore one introduces auxiliary momenta ξ_e and replaces $k_e \to k_e + \xi_e$ in the generalized integrand. Note that a momentum k_e^μ in the numerator of this integrand can be produced by the differential operator $\hat{\xi}_{e,\mu} := -\frac{1}{2\alpha_e}\frac{\partial}{\partial \xi_e^\mu}$

$$\hat{\xi}_{e,\mu} \frac{1}{((k_e + \xi_e)^2 + m_e^2)^{a_e}} = \frac{a_e}{\alpha_e} \frac{k_e^\mu + \xi_e^\mu}{((k_e + \xi_e)^2 + m_e^2)^{a_e + 1}}$$

Applying the Schwinger trick one sees that the factor $a_e/\alpha_e \times \alpha_e^{a_e}/\Gamma(a_e + 1)$ on the right hand side equals the factor $\alpha_e^{a_e - 1}/\Gamma(a_e)$ on the left hand side. Therefore momenta appearing in the numerator of a tensor integral can be replaced by the given operator. It remains to study its action on the scalar integrand derived above. For more details see [14, 16]. An application to Yang-Mills theory can be found in [17].

3.2.3 Graph Polynomials

With the help of the upcoming theorem the polynomials ψ_G and φ_G can be derived from the topology of the graph G. Before the theorem can be stated some further notation is needed. Denote by $\mathcal{T}_k^{I,J}$ the set of spanning k-forests[3] of a given graph where each tree contains exactly one vertex of I and J. If $F \in \mathcal{T}_k^{I,J}$ write $F = (T_{i_1}, \ldots, T_{i_k})$, where $I = \{i_1, \ldots, i_k\}$ and $i \in T_i$, then $\pi_F : I \to J$ is the bijection such that $j \in T_{\pi_F(i)}$ for $j \in J$ and $i \in I$.

[3] A spanning k-forest is a subgraph $F \subseteq G$ with k connected components each of which is a tree graph and $V_F = V_G$.

Theorem 3.3. (All Minors Matrix-Tree Theorem). *Let $\mathcal{L}_G$ be the Laplacian of a graph G, $I, J \subseteq [|V_G|]$, with $|I| = |J| = k$ and let $\mathcal{L}_G[I, J]$ denote the minor obtained by deleting the rows I and columns J. Then*

$$\det \mathcal{L}_G[I, J] = \epsilon(I, J) \sum_{F \in \mathcal{T}_k^{I,J}} \operatorname{sgn}(\pi_F) \prod_{e \in F} \alpha_e$$

with $\epsilon(I, J) := (-1)^{\sum_{i \in I} i + \sum_{j \in J} j}$.

Proof. A proof can be found, for example in [18, 19]. ☐

Remark. Note that $\det \hat{\mathcal{L}}_G[I, J] = \epsilon(I, J) \sum_{F \in \mathcal{T}_k^{I,J}} \operatorname{sgn}(\pi_F) \prod_{e \in F} 1/\alpha_e$ since the transformation $\alpha_e \to 1/\alpha_e$ converts $\mathcal{L}_G$ into its dual $\hat{\mathcal{L}}_G$.

Then it follows immediately for the first Symanzik polynomial ψ_G that

$$\psi_G = \det\Lambda \det\hat{\mathcal{L}}_G[v_0] = \prod_{e \in E_G} \alpha_e \sum_T \prod_{e \in T} \frac{1}{\alpha_e} = \sum_T \prod_{e \notin T} \alpha_e \,, \tag{3.20}$$

where the sum is over all spanning trees T in G.

To calculate the second Symanzik polynomial φ_G express the elements of $(\hat{\mathcal{L}}_G^{-1})_{v,w}$ with elements of its adjugate matrix and then apply the All Minors Matrix-Tree Theorem. Let $I = \{v_0, w\}$ and $J = \{v_0, v\}$ and conclude

$$\begin{aligned}(\hat{\mathcal{L}}_G^{-1}[v_0])_{v,w} &= (-1)^{v+w} \det \hat{\mathcal{L}}_G\big[I, J\big] \det \hat{\mathcal{L}}_G^{-1}[v_0] \\ &= \sum_{F \in \mathcal{T}_2^{I,J}} \prod_{e \in F} \alpha_e^{-1} \det \hat{\mathcal{L}}_G^{-1}[v_0] \,.\end{aligned}$$

Where $\epsilon\left(\{v_0, w\}, \{v_0, v\}\right) = (-1)^{v+w}$ was used and furthermore note that necessarily $w \in T_v$ and therefore $\pi_F = (1)$ and $\operatorname{sgn}(\pi_F) = 1 \; \forall F \in \mathcal{T}_2^{I,J}$. Denote the tree which contains v_0 by T_0 and note that the sum over the set $\mathcal{T}_2^{I,J}$ is equivalent to summing over $\mathcal{T}_2$, it follows

$$\begin{aligned}\varphi_G &= \sum_{v_1, v_2 \in V_G \setminus v_0} p(v_1)p(v_2) \sum_{F \in \mathcal{T}_2^{I,J}} \prod_{e \notin F} \alpha_e \\ &= \sum_{(T_0, T) \in \mathcal{T}_2} p(T_0)^2 \prod_{e \notin (T_0, T)} \alpha_e\end{aligned}$$

with $\sum_{v_1, v_2 \notin T_0} p(v_1)p(v_2) = p(T_0)^2$. To achieve the equality observe that the summation sets are isomorphic

$$\Big\{v, w \in V_G \setminus v_0\Big\} \cong \Big\{v, w \notin T_0 \;\Big|\; (T_0, T) \in \mathcal{T}_2(G)\Big\} \,.$$

Finally, write the second polynomial appearing in the Feynamn integrand Ξ_G as

$$\Xi_G = \psi_G \sum_{e \in E_G} \alpha_e m_e^2 + \sum_{(T_0, T) \in \mathcal{T}_2} p(T_0)^2 \prod_{e \notin (T_0, T)} \alpha_e \,. \tag{3.21}$$

Observe that $p(T_0)^2$ is the squared sum of all momenta flowing into T_0, therefore $p(T_0)^2 = p(T)^2$ by momentum conservation and hence the choice of v_0 does not change the polynomial Ξ_G.

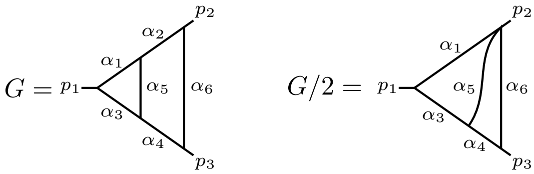

FIGURE 3.1: The graph G with three external momenta and the graph $G/2$ where edge 2 is shrunk

Example 3.4. Consider the graph G given in Figure 3.1 then its Symanzik polynomials are given by

$$\begin{aligned}\psi_G = &\alpha_1\alpha_2 + \alpha_1\alpha_4 + \alpha_1\alpha_5 + \alpha_1\alpha_6 + \alpha_2\alpha_3 + \alpha_2\alpha_5 \\ &+ \alpha_3\alpha_4 + \alpha_3\alpha_5 + \alpha_3\alpha_6 + \alpha_4\alpha_5 + \alpha_5\alpha_6\end{aligned}$$

and for $m_e = 0 \ \forall e \in E_G$

$$\begin{aligned}\Xi_G = \varphi_G = &p_2^2(\alpha_1\alpha_2\alpha_6 + \alpha_1\alpha_5\alpha_6 + \alpha_2\alpha_3\alpha_6 + \alpha_2\alpha_5\alpha_6) \\ &+ p_3^2(\alpha_1\alpha_4\alpha_6 + \alpha_3\alpha_4\alpha_6 + \alpha_3\alpha_5\alpha_6 + \alpha_4\alpha_5\alpha_6) \\ &+ (p_2+p_3)^2(\alpha_1\alpha_2\alpha_3 + \alpha_1\alpha_2\alpha_4 + \alpha_1\alpha_3\alpha_4 + \alpha_1\alpha_3\alpha_5 \\ &\quad + \alpha_1\alpha_3\alpha_6 + \alpha_1\alpha_4\alpha_5 + \alpha_2\alpha_3\alpha_4 + \alpha_2\alpha_3\alpha_5 + \alpha_2\alpha_4\alpha_5)\,.\end{aligned}$$

Note that for the graph $G/2$ where the edge labeled with α_2 is collapsed one gets $\psi_{G/2} = \psi_G|_{\alpha_2=0}$ and $\varphi_{G/2} = \varphi_G|_{\alpha_2=0}$ (which also holds for non zero masses).

The last observation in the example above can be generalized. The resulting straightforward property is essential to make a connection to moduli spaces of graphs.

Property 3.5. *Let ψ_G and Ξ_G be the graph polynomials defined above, then*

$$\begin{aligned}(i) &\quad \psi_{G/e} = \psi_G\Big|_{\alpha_e=0} \ \textit{and} \ \Xi_{G/e} = \Xi_G\Big|_{\alpha_e=0} \\ (ii) &\quad \psi_G \textit{ and } \Xi_G \textit{ are homogeneous functions of} \\ &\quad \deg(\psi) = |G| \textit{ and } \deg(\Xi) = |G|+1\end{aligned}$$

Proof. (i) Let $F \subset G$ be a spanning forest and $e \in F$ then $F/e \subset G/e$ is still a spanning forest. Conversely let F' be a spanning forest of G/e, then $F' \cup \{e\}$ is a spanning forest of G. This induces a bijection of the set of spanning forests in G/e and those of G that contain e. The monomials corresponding to forests without e are set to zero on the right hand side. (ii) follows directly from the equations (3.20) and (3.21). □

Denote the graph polynomials whose edge variables corresponding to a subgraph $\gamma \subset G$ are set to zero by $\psi_G|_\gamma$ and $\Xi_G|_\gamma$.

Property 3.6. *Let $\gamma \subseteq G$ then $\psi_G|_\gamma = 0$ iff $|\gamma| > 0$.*

Proof. Let $T \subset G$ be a tree subgraph, then $\psi_G|_\gamma = 0 \Leftrightarrow \nexists T$ with $\gamma \subseteq T \Leftrightarrow |\gamma| > 0$. □

In the next property it is assumed that $p(T)^2 > 0$, which is clearly true for euclidean momenta, and therefore it is referred to as the region of euclidean momenta.

Property 3.7. *Let $\gamma \subseteq G$ and assume $p(T)^2 > 0 \ \forall T \subset G$ then $\Xi_G|_\gamma = 0$ if either $|\gamma| > 0$ or γ is a spanning tree which satisfies $m_e = 0 \ \forall e \in E_{G\setminus\gamma}$.*

Proof. Let $|\gamma| > 0$ then $\psi_G|_\gamma = 0$ by Property 3.6 and likewise follow $\varphi_G|_\gamma = 0$, therefore conclude $\Xi_G|_\gamma = 0$. Let γ be a spanning tree of G, then $\varphi_G|_\gamma = 0$, since $\nexists(T_0, T) \subset G$ with

$\gamma \subset (T_0, T)$. Furthermore the sum involving the masses reduces to $\sum_{e \in G \setminus \gamma} \alpha_e m_e^2$ which is only zero if $m_e = 0 \; \forall e \in E_{G \setminus \gamma}$. $\square$

The properties above relate the zero sets of these polynomials to topological properties of the graph under consideration. The zero sets are important to characterize the divergent parts of the integral I_G and to eventually regularise the integration.

Massless Graphs

Consider massless graphs, which means that $m_e = 0 \; \forall e \in E_G$. Studying this case is useful, since gluon edges do not carry a mass.
The requirement that $p(T)^2 > 0$ in Property 3.7 can now be omitted and the zeros of $\Xi_G = \varphi_G$ are described by spanning trees $T \subset G$.
For gluon graphs there is no higher vertex valancy then 4 allowed. As shown in the previous chapter, a face in $MG^4_{l,n}$ corresponds to a matching M on the 3-regular graph G by G/M. A matching on G can only be a spanning tree, when G has 2 vertices, which is only the case for the graphs 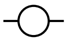 and , but matching these two vertices is forbidden since it leads to tadpoles, cf. definition 2.41. Therefore $\Xi_G \neq 0$ on the domain $\langle G \rangle$. Conclude that the poles of the integrand are given by the zero set of Ψ_G, which still holds if the integration takes the form (3.22) derived in the next section.

3.2.4 Feynman Integrals and the Moduli Spaces of Graphs

With a convenient choice of coordinates one integration of the parametric form of I_G in equation (3.19) can be performed. Define a hyperplane $H(\boldsymbol{\alpha}) := \sum_e H_e \alpha_e$, with $H_e \geq 0$ and not all H_e zero. Insert $1 = \int_0^\infty \mathrm{d}\lambda \delta(\lambda - H(\boldsymbol{\alpha}))$ into (3.19) and after substituting α_e for $\lambda \alpha_e$ the integral takes the form

$$\begin{aligned} I_G &= \int_0^\infty \mathrm{d}\lambda \left[\prod_{e \in E_G} \int_{\mathbb{R}_+} \mathrm{d}\alpha_e \lambda \right] \frac{e^{\lambda \Xi_G / \psi_G}}{\lambda^{|G|D/2} \psi_G^{D/2}} \frac{\delta(1 - H(\boldsymbol{\alpha}))}{\lambda} \\ &= \left[\prod_{e \in E_G} \int_{\mathbb{R}_+} \mathrm{d}\alpha_e \right] \frac{\delta(1 - H(\boldsymbol{\alpha}))}{\psi_G^{D/2}} \int_0^\infty \mathrm{d}\lambda \lambda^{\omega - 1} e^{\lambda \Xi_G / \psi_G} \\ &= \Gamma(\omega) \left[\prod_{e \in E_G} \int_{\mathbb{R}_+} \mathrm{d}\alpha_e \right] \frac{\delta(1 - H(\boldsymbol{\alpha}))}{\psi_G^{D/2}} \left(\frac{\psi_G}{\Xi_G} \right)^\omega \\ &= \Gamma(\omega) \int \Omega \, \frac{1}{\psi_G^{D/2}} \left(\frac{\psi_G}{\Xi_G} \right)^\omega =: \Gamma(\omega) \int \Omega f_G(\boldsymbol{\alpha}) \, . \end{aligned} \tag{3.22}$$

In the first line the homogeneity of the Symanzik polynomials were used. For the next step define the superficial degree of divergence of a graph $\omega(G)$ by

$$\omega(G) := |E_G| - |G| \frac{D}{2} \, ,$$

then the definition of the Γ function was applied. Finally define

$$\int \Omega := \left[\prod_{e \in E_G} \int_{\mathbb{R}_{\geq 0}} \mathrm{d}\alpha_e \right] \delta(1 - H(\boldsymbol{\alpha})) \, ,$$

to arrive at equation (3.22). The integration appearing there is independent of the choice of $H(\boldsymbol{\alpha})$. To establish a connection to the moduli space of graphs it is peculiar useful to choose $H_e = 1 \ \forall e \in E_G$. Then the δ-distribution constrains the integration domain to the set

$$\overline{\sigma}_G = \left\{ \boldsymbol{\alpha} \in [0,1]^{|E_G|} \;\middle|\; \sum \alpha_e = 1 \right\} ,$$

which is a simplex with $\dim \overline{\sigma}_G = |E_G| - 1$, c.f the definitions at the beginning of Chapter 2.

Remark. The connection between the two integration domains can be made mathematically more precise, by noting that $H(\boldsymbol{\alpha})$ induces an isomorphism. This is for example shown in [14].

The superficial degree of divergence $\omega(G)$ characterizes the type of divergence of the graph G. For $\omega = 0, -1, -2, \ldots$ the Gamma function in the expression (3.22) diverges. These graphs are called *logarithmic*, *quadratic*, ... divergent. Notice that the integration itself in equation (3.22) might still be ill defined, due to divergent subgraphs of G.

Modifications on the Integration Domain

The integral I_G is ill defined since there are faces of $\overline{\sigma}_G$ where the integrand f_G is singular. These faces can be described as a set of vanishing edge variables α_e such that the denominator of f_G is zero. Clearly this can only happen at faces of $\overline{\sigma}_G$. These sets are described by the properties 3.6 and 3.7. Excluding these faces will yield a relative simplex.
The aim is to construct a simplex that corresponds to the relative cell $\langle G \rangle$, therefore additionally delete the faces which correspond to graphs G/γ with $\gamma \notin \mathfrak{M}G$, i.e. γ is not a valid matching on G[4]. This clearly includes the zero sets of the graph polynomials. By this modification the relative simplex $\langle G \rangle$ is recovered. The removed faces of $\overline{\sigma}_G$ are null sets with respect to the integration, therefore for regular f_G deduce, while neglecting the possible isometries,

$$\int_{\overline{\sigma}_G} f_G = \int_{\langle G \rangle} f_G \,. \tag{3.23}$$

Remark. As the notation might imply $\overline{\sigma}_G$ is indeed the closure of $\langle G \rangle$.

To incorporate the equivalence of isometric graphs in the moduli spaces investigate the symmetries of the integrand $f_G(\boldsymbol{\alpha})$. First notice that $\boldsymbol{\alpha}$ can be seen as a map from G to $[0,1]^{|E_G|}$, which is a metric on G. Introducing this into the notation denote the integrand by $f_{(\boldsymbol{\alpha},G)}$.
For any automorphism $i \in \mathrm{Aut}(G)$ the integrand has the same value on exactly two points in the open cell $\langle \mathring{G} \rangle$

$$f_{(\boldsymbol{\alpha},G)} = f_{(\boldsymbol{\alpha} \circ \boldsymbol{i},G)} \,. \tag{3.24}$$

The equivalence relation of the moduli spaces exactly relates this points. The integration over the open cell is then related to the integral over the quotient $\langle \mathring{G} \rangle/\sim$ by the symmetry factor of G. Without a detailed proof observe that the integration can be written as

$$\int_{\langle \mathring{G} \rangle} f_{(\boldsymbol{\alpha},G)} = \sum_{i \in \mathrm{Aut}(G)} \int_{[\langle \mathring{G} \rangle]_i} f_{(\boldsymbol{\alpha},G)} \,,$$

where each $[\langle \mathring{G} \rangle]_i$ denotes a subspace of the open cell, such that all isometries are fixed. Now use equation (3.24) and a coordinate transformation that relates $[\langle \mathring{G} \rangle]_i$ with $\langle \mathring{G} \rangle/\sim$ in

[4] The graphs G/γ correspond to tadpoles or graphs with at least one vertex with a valency bigger then four.

each summand such that

$$\int_{\langle \mathring{G} \rangle} f_{(\boldsymbol{\alpha},G)} = \sum_{i \in \mathrm{Aut}(G)} \int_{\langle \mathring{G} \rangle / \sim} f_{(\boldsymbol{\alpha},G)} = \mathrm{Sym}(G) \int_{\langle \mathring{G} \rangle / \sim} f_{(\boldsymbol{\alpha},G)} \,. \tag{3.25}$$

The idea behind the equations above is best show in an simple example.

Example 3.8. Consider the graph $G = -\!\bigcirc\!-$ and denote its edge variables by α and β. Its Feynman integral can then be written as

$$\begin{aligned} I_G &= \int_{\alpha<\beta} f_G(\alpha,\beta) + \int_{\beta<\alpha} f_G(\alpha,\beta) \\ &= \int_{\alpha<\beta} f_G(\alpha,\beta) + \int_{\alpha<\beta} f_G(\beta,\alpha) \\ &= 2 \int_{\langle G \rangle / \sim} f_G(\alpha,\beta) \,. \end{aligned}$$

Where $\int_{\alpha<\beta}$ denotes the integration over the subspace of $\langle G \rangle$ for which $\alpha < \beta$. In the second line the coordinates swapped names in the second summand. To get the third line use equation (3.24) and note that $\int_{\alpha<\beta} = \int_{\langle G \rangle / \sim}$. The resulting factor coincides with the symmetry factor of G: $|\,\mathrm{Aut}(-\!\bigcirc\!-)| = 2$.

For a expression for the cell with boundary $\langle G \rangle$ all graphs that arise by shrinking valid matchings, which corresponds to setting a subset of the parameters to zero, need to be taken into account aswell. The resulting symmetry factor is certainly more complicated since on the boundary new isometries might arise. Assume that one can still write an equation of the form of equation (3.25) with some symmetry factor $S(G)$. Then deduce that

$$I_G = S(G) \int_{\langle G \rangle / \sim} f_G \,.$$

To manifest the connection to the moduli space of graphs it is necessary to check if derived form of the Feynman integral is well defined on the faces of $\langle G \rangle$. Due to Property 3.5 such a face corresponds to a graph G/M, where M is a valid matching in G. Furthermore the superficial degree of divergence $\omega(G)$ must also respect face relations. First note that $\omega(G/M) = |E_G| - |M| + |G|D/2$. Additionally rewrite ω in terms of the Heavyside distribution $\theta(x)$ as $\omega(G) = \sum_{e \in E_G} \theta(\alpha_e) - |G|D/2$, then conclude $\omega(G/M) = \omega(G)\big|_M$, where $\theta(x) = 0$ for $x \leq 0$ and $\theta(x) = 1$ else. Concluding

$$I_G\Big|_M := \int_{\langle G \rangle} \prod_{e \in M} \delta(\alpha_e) f_G = \int_{\langle G/M \rangle} f_{G/M} = I_{G/M} \,. \tag{3.26}$$

Finally write the unrenormalized Feynman amplitude $\mathcal{A}_{l,n}(p,m)$ as

$$\mathcal{A}_{l,n}(p,m) \; = \sum_{G \in \mathcal{G}^4_{l,n}} S(G) \int_{\langle G \rangle / \sim} f_G \,, \tag{3.27}$$

which establishes the moduli space of graphs as the integration domain of Feynman integrals involved in the calculation of the amplitude of a process. The dependence on the cinematic parameters p and m is hidden in the integrand f_G. If one considers colored graphs, with a color map s.t. there are no isometries, the factor $S(G)$ is always one, and the result given in [3] is recovered.

Comments on Renormalization

As already mentioned, the integral I_G might be divergent, due to poles arising from zeros of the graph polynomials in the integrand f_G. These can typically be characterized by topological properties of the graph under consideration, for example, seen in the properties 3.6 and 3.7. A more general treatment investigates the scaling behavior of the integrand f_G, for example, done in [14]. The upshot is that the integrations that need regularisation are given by the superficial degree of divergence of its subgraphs. For the case of only ultraviolet divergencies and euclidean momenta, this reduces to the following property, first formulated by Weinberg in [12].

Property 3.9. *The integral I_G is convergent if and only if for all subgraphs $\gamma \subset G$ it holds that $\omega(\gamma) > 0$.*

One way of regularizing the Feynman integral is to alter the integrand f_G. Denote the altered integrand by $f_{G,F}$ (its exact form is not required here), where F is a forest of divergent subgraphs of G. These are a collection of divergent subgraphs such that for any $\gamma, \gamma' \in F$ either $\gamma' \subset \gamma$, $\gamma \subset \gamma'$ or $\gamma \cap \gamma' = \emptyset$. To render the Feynman integral finite the divergences arising from these subgraphs need to be subtracted and to take overlapping divergences into account this subtraction is given by the forest formula, first given by Zimmermann [20]:

$$I_G^R = \sum_{F \subset G} (-1)^{|F|} \int_{\langle G \rangle} f_{G,F}. \tag{3.28}$$

The sum runs over all forest in G and $|F|$ denotes the number of elements in the forest. A proof that I_G^R is indeed finite and the form of the integrand $f_{G,F}$ for the parametric representation is given in [21].
For this work, only the effects on the structure of the integration domain are presented. For general theories with arbitrary vertex valencies, it was examined in [3]. One of the main results there is that the renormalized Feynman amplitude for a given process $\mathcal{A}_{l,n}^R(p)$ can be formulated as an integration over the compactified moduli space. Remarkably the combinatorial structure of compactification, i.e., the characterization of the new faces via flags corresponds to the combinatorics of forests that are used in the forest formula.
A further connection between compactification and renormalization arises in the equivalence between the compactification and blow-ups of certain subspaces of MG [3]. A blow-up is a concept from algebraic geometry. It is a transformation used to resolute singularities of zero sets of functions. In the case of Feynman integrals, this function is f_G. A good introduction is given in [22].

Now look a bit more closely to the compactified integration domain of the moduli space of gluon graphs and give a formula for the renormalized amplitude $\mathcal{A}_{l,n}^R(p, m)$ analog to equation (3.27). Previously the compactification of $\langle G \rangle$ was defined using subgraphs of G that are not a matching, c.f. Section 2.4. The result of [3], which uses a different compactification, should still be valid, since the faces that are additionally removed for $MG_{l,n}^4$ correspond to forests of tree graphs, f_G is regularly supported on these faces, and hence they do not contribute to I_G. Conclude that the renormalized amplitude for rainbow-colored graphs[5] is given by

$$\mathcal{A}_{l,n}^R(p, m) := \sum_{G \in \mathcal{G}_{l,n}^4} I_G^R = \sum_{G \in \mathcal{G}_{l,n}^4} \sum_{F \subset G} (-1)^{|F|} \int_{\langle \hat{G} \rangle} f_{G,F} \,. \tag{3.29}$$

[5]For the more general case one presumably needs to include a symmetry factor as in (3.27).

Notice that the combined integration domain of this physical amplitude is given by the compactified moduli space of gluon graphs. The procedure of regularisation therefore does not interfere to much with structure of the moduli space. As a conclusion the upcoming chapters are about the non compact version of the moduli spaces.

Remark. The preceding considerations are only made to sketch the given ideas. Rigorous definitions can be found in [3].

Chapter 4

One Loop Moduli Space: $MG^4_{1,n}$

In this chapter, the f-vectors of the one-loop moduli spaces $MG^4_{1,n}$ are derived. These vectors are denoted by $\boldsymbol{F_n}$. The f-vector of a simplex $\langle \sigma\Sigma_n \rangle$ in the complex $MG^4_{1,n} = \langle \sigma_1\Sigma_n, \sigma_2\Sigma_n, \dots, \sigma_{|\mathcal{S}_n|}\Sigma_n \rangle$ is notated as $\boldsymbol{f_n}$. Recall that a facet of the moduli space is generated by the non-degenerate metric on a n-sun $\sigma\Sigma_n \in \mathcal{S}_n$, where $\mathcal{S}_n$ is the set of permuted n-suns.
The first part of this chapter calculates $\boldsymbol{f_n}$. This result can then be used to derive the f-vector for the whole space. As a consequence, a statement about the Euler characteristic of $MG^4_{1,n}$ is made. In the third section, an alternative way to derive $\boldsymbol{F_n}$ using complete graphs is presented. In the last section, the result is generalized to a colored version of $MG^4_{1,n}$, and the entire space of QCD graphs is examined.

Observe that, due to the topology of the n-suns $\sigma\Sigma_n \in \mathcal{S}_n$ there is a bijection between the external legs and the vertices. Furthermore, there is another bijection between the vertices and the internal edges. This fact will be used throughout this chapter to simplify the notation for matchings in a one-loop graph.
Assume in the following that there are no isometries between non-degenerate metric graphs. Due to Property 2.56 this amounts into the requirement $n > 4$. Notice that the cases $n = 3, 2$ are already covered in Chapter 2.

4.1 The Simplices of $MG^4_{1,n}$: $\langle \sigma\Sigma_n \rangle$

As already mentioned, any graph in the set of permuted n-suns $\mathcal{S}_n$ generates a facet of $MG^4_{1,n}$. The relative simplex associated with a n-sun is denoted by $\langle \sigma\Sigma_n \rangle$. Below the set $\langle \sigma\Sigma_n \rangle \subseteq MG^4_{1,n}$ will be defined in terms of finite sets, such that $\langle \sigma\Sigma_n \rangle$ is a combinatorial simplex. For now observe, that any graph $\sigma\Sigma_n \in \mathcal{S}_n$ contains the same combinatorial structure since they all have the same topology and only differ by a permutation of the external edges. Therefore without loss of generality choose $\sigma = (1)$.
Shrinking an edge of Σ_n to zero length corresponds to matching the two vertices that are connected to the edge. Since one can assign to every edge of Σ_n a unique number given by Figure 4.1, a matching in Σ_n will be denoted by the edges it contains. In this notation, a valid matching of Σ_n does not contain two cyclic consecutive numbers in $[n]$[1].
Remember that such a matching has a correspondence to a graph with 4 valent vertices, see Lemma 2.45. Since only one graph is considered the equivalence relation in the mentioned lemma can be ignored. It will be implemented later when the full space $MG^4_{1,n}$ is investigated. Furthermore, collapsing a matching in $\sigma\Sigma_n$ will never lead to a tadpole graph.

[1] This means $1, n \in [n]$ are considered to be consecutive.

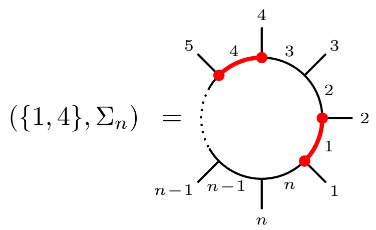

FIGURE 4.1: The graph Σ_n with a matching $M = \{1,4\}$ in red

Recall that a bar denotes the complement of a set, and define $\langle\Sigma_n\rangle$ as a combinatorial relative simplex.

Definition 4.1. *Define the combinatorial simplex associated with Σ_n by*

$$\langle\Sigma_n\rangle := \left\{\bar{x} \;\middle|\; x \subseteq [n], x \textit{ has no cyclic consecutive elements}\right\}.$$

Here $\emptyset$ is an element of $[n]$.

This definition has a convenient interpretation. The set x without any consecutive numbers is an unordered list of edges that might be shrunk simultaneously or equivalently x is a valid matching of Σ_n. The matched graph, denoted by (x, Σ_n), corresponds to a graph in $\mathcal{G}^4_n$ which can be uniquely denoted by its edges $\bar{x}$. In the example in Figure 4.1, the set of edges is $\{2,3,5,6,\dots,n\}$. Conclude that the discrete relative simplex $\langle\Sigma_n\rangle$ captures the combinatorial structure of the simplices of the moduli spaces of graphs $MG^4_{1,n}$.
To check that $\langle\Sigma_n\rangle$ is indeed a relative simplex, first note that $[n] \in \langle\Sigma_n\rangle$ since $\overline{\emptyset} = [n]$. Immediately follow that $\dim\langle\Sigma_n\rangle = n-1$. $\langle\Sigma_n\rangle$ is closed under taking subsets: Let $y \in \langle\Sigma_n\rangle$ and $y \neq [n]$, then for any $s \in [n] - y$ the set $\overline{y \cup \{s\}}$ has no consecutive elements, hence $y \cup \{s\} \in \langle\Sigma_n\rangle$. It is clear that $\langle\Sigma_n\rangle$ has missing faces, corresponding to sets $x \subseteq [n]$ with cyclic consecutive elements. In the following, it is written as $\langle\Sigma_n\rangle = (2^{[n]}, \Gamma)$.
An example can be seen in Figure 4.2, where the Hasse diagram of the poset associated with the relative simplex $\langle\Sigma_5\rangle$ is shown. There, the elements of $\langle\Sigma_5\rangle$ are represented by their complements, so the given sets are matched edges in Σ_5. The matched graph of Figure 4.1 for $n = 5$ corresponds to the second vertex from the left of the lowest row.

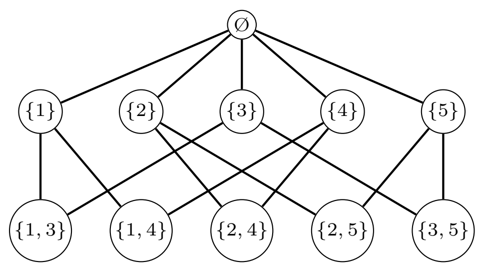

FIGURE 4.2: The Hasse diagram of $\langle\Sigma_5\rangle = (2^{[5]}, \Gamma)$

4.1.1 Some Elementary Properties of $\langle\Sigma_n\rangle$

In this section, some basic facts about the relative simplex $\langle\Sigma_n\rangle = (2^{[n]}, \Gamma)$ are worked out.

Property 4.2. *At most* $\lfloor n/2 \rfloor$ *edges of* Σ_n *can be shrunk.*

Proof. Let n be even. A perfect matching M on Σ_n allows collapsing a maximal number of edges. Therefore $n/2$ edges must be part of that matching.
Now consider Σ_{n+1} then M is still a matching and it is maximal since the only unmatched vertex is the newly added one. ☐

The last property is equivalent to the following. The longest chain in the poset of $\langle\Sigma_n\rangle$ has length $\lfloor n/2 \rfloor$ or the lowest dimensional face in $\langle\Sigma_n\rangle$ is $\lfloor n/2 \rfloor$-dimensional.
There need to be at least two elements in a set asspciated with a face of Γ. Otherwise, no consecutive numbers can occur. Hence deduce $\dim \Gamma = n - 3$, reproducing the result from the previous Chapter 2.

Property 4.3. Γ *is pure, i.e., all its facets have the same dimension.*

Proof. Denote the sets of two cyclic consecutive numbers by $\bar{a}_i \subset [n]$. Then any $x \in \Gamma$ is a subset of at least one a_i since $\bar{x}$ contains at least two consecutive numbers. Conclude $\Gamma = \langle a_1, a_2, \ldots, a_n \rangle$. ☐

Remark. The proof of Property 4.3 generalizes to relative simplices generated by arbitrary 3-regular graphs.

Property 4.4. Γ *is connected for* $n > 3$*.*

Proof. Let $x,\ y \in \Gamma$, then there are two chains $x, \sigma_1, \ldots, a_i$ and $y, \tau_1, \ldots, a_j$. For $n > 3$ consider the sequence $\overline{a_i} = \{i, i+1\} \subset \{i, i+1, i+2\} \supset \{i+1, i+2\} = \overline{a_{i+1}}$ (for $n = 3$ this contains $\emptyset$). By repeating this pattern, one can construct a sequence between any two $\overline{a_i}$ and therefore between any two a_i. Together with the chains above such a sequence represents a path from x to y in the Hasse diagram of Γ. ☐

4.1.2 The f-Vector of $\langle\Sigma_n\rangle$

In this section, the f-vector $\boldsymbol{f_n}$ of $\langle\Sigma_n\rangle$ is calculated. As already mentioned, the f-vector counts the number of faces of each dimension, so $f_k^{(n)} = |F_k[\langle\Sigma_n\rangle]|$. Where $F_k[\langle\Sigma_n\rangle]$ is the set of the k dimensional faces of $\langle\Sigma_n\rangle$. Here it can be written as

$$F_k[\langle\Sigma_n\rangle] = \left\{\bar{x} \;\middle|\; x \subseteq [n], x \text{ has no cyclic consecutive elements}, |x| = n-k-1\right\} =: F_{n,k}.$$

To compute the cardinality of $F_{n,k}$ it is useful to define an isomorphic set, whose elements have a slightly more convenient property since they are not described via complements.

$$\overline{F}_{n,k} := \left\{x \;\middle|\; x \subseteq [n], x \text{ has no cyclic consecutive elements}, |x| = n-k-1\right\}$$

Complementing a set is an invertible operation, hence the sets $F_{n,k}$ and $\overline{F}_{n,n-k-1}$ are -isomorphic.
From these definitions, one readily finds that

$$|\overline{F}_{n,m}| = |F_{n,n-m-1}| =: f^{(n)}_{n-m-1}\,. \tag{4.1}$$

In the majority of the following considerations, n is fixed and the superscript of the f-vector is then neglected.

Remark. The set $\overline{F}_{n,m}$ is isomorph to the set of all m-matchings on Σ_n, denoted by $\mathfrak{M}_m\Sigma_n$, since valid matchings of Σ_n cannot contain edges which are cyclic neighbors.

The upcoming lemma about the cardinality of $\overline{F}_{n,m}$ relates thus to the f-vector of the simplices of $MG^4_{1,n}$.

Lemma 4.5. *The cardinality of $\overline{F}_{n,m}$ for $0 \leq m \leq \lfloor n/2 \rfloor$ is given by*

$$|\overline{F}_{n,m}| = \binom{n-m}{m} \frac{n}{n-m}$$

and for $m > \lfloor n/2 \rfloor$ by $|\overline{F}_{n,m}| = 0$.

Proof. Let $m > \lfloor n/2 \rfloor$ the statement follows by Property 4.2.
To proof the statement for $0 \leq m \leq \lfloor n/2 \rfloor$, the method of stars and bars will be used. First place $n-m$ bars in a cycle, they represent the not chosen numbers. This leaves $n-m$ gaps between the bars to place m stars, which represent the chosen non-consecutive numbers.
Denote the set of all possible stars and bars diagrams by $D_{n,m}$. An example of such a set of diagrams is given in Figure 4.3. Counting the diagrams in $D_{n,m}$ and the possibilities to label their objects distinctly gives $|\overline{F}_{n,m}|$. The set $D_{n,m}$ consists of two symmetries, which eventually lead to overcounting when the diagrams are labeled. First observe, that rotating every diagram in $D_{n,m}$ leaves the set invariant. This can be fixed by choosing one bar, where the labeling begins. Secondly, a reflection of the diagrams will not change the set $D_{n,m}$ either, therefore choose a direction in which the objects will be labeled.
There are $\binom{n-m}{m}$ diagrams to label. Labeling the first bar with 1 yields one labeling. A second one is gained by labeling the first bar with 2. With these two ways to number the objects, every possibility is realized, since there are only 2 different objects to label.
These two labels may still result in the same labels on the stars, see Figure 4.4. This exactly happens when the first gap (the gap clockwise to the first bar) is not filled with a star, then the next bar is labeled 2, which will result in the second labeling for some other diagram in $D_{n,m}$. If there is more than one gap after the first bar, this still results in a duplicate label, alternating between the first and second labeling for every gap without a star.
Now calculate the number of diagrams where this happens. Since the first and empty gap is fixed, this is just the number of diagrams with one gap less. Conclude that the number of diagrams where the first gap is empty is given by

$$\binom{n-m-1}{m} = \frac{n-2m}{n-m}\binom{n-m}{m}.$$

Subtracting this from the total number of possible numerations gives

$$|\overline{F}_{n,m}| = 2\binom{n-m}{m} - \frac{n-2m}{n-m}\binom{n-m}{m} = \frac{n}{n-m}\binom{n-m}{m}. \qquad \square$$

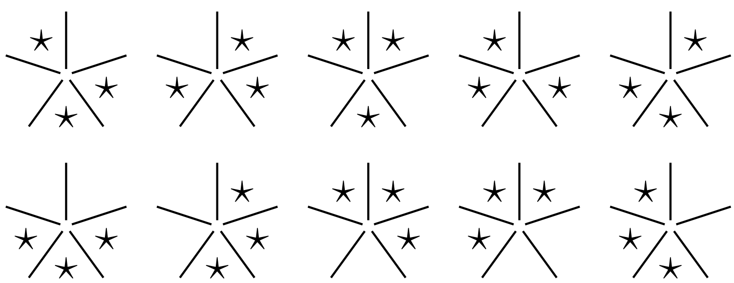

FIGURE 4.3: The elements of the set $D_{8,3}$

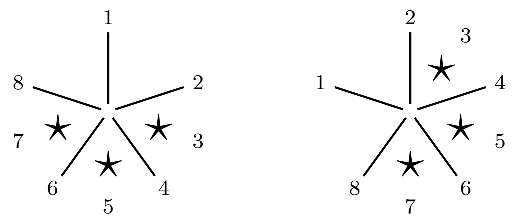

FIGURE 4.4: An example of two numerations of two distinct stars and bars diagrams of $D_{8,3}$ which result in the same numbers on the stars

Corollary 4.6. *The f-vector $\boldsymbol{f_n} = (f_{-1}, f_0, ..., f_{n-1})$ of $\langle \Sigma_n \rangle$ for $n > 4$ is given by*

$$f_k = \binom{k+1}{n-k-1} \frac{n}{k+1}.$$

Proof. By Equation (4.1). Furthermore, for $n > 4$ there are no possible isomorphisms between any graphs in $\langle \Sigma_n \rangle$ since the lowest number of internal edges is $n - \lfloor \frac{n}{2} \rfloor > 2$ for $n > 4$ (cf. Property 2.56). $\square$

Definition 4.7. *Define the Chebyshev-Polynomials of the first kind to be*

$$T_n(x) := \sum_{k=0}^{\lfloor n/2 \rfloor} c_k^{(n)} x^{n-2k}$$

$$\textit{with} \quad c_k^{(n)} = (-1)^k 2^{n-2k-1} \frac{n}{n-k} \binom{n-k}{k}.$$

This is one of many representations of the Chebyshev-Polynomials. A more geometrically representation is given by

$$T_n(x) := \cos(n \arccos(x)).$$

The equivalence of these representations is for example shown in [23].

Corollary 4.8. *The Euler characteristic $\mathcal{X}$ of $\langle \Sigma_n \rangle$ for $n > 4$ is given by*

$$\mathcal{X}(\langle \Sigma_n \rangle) = (-1)^{n+1} 2 \cos\left(n \frac{\pi}{3}\right) = \begin{cases} -2 & \textit{for } n = 6, 9, 12, ... \\ 1 & \textit{else} \end{cases}.$$

Proof.

$$\begin{aligned}
\mathcal{X}(\langle \Sigma_n \rangle) &= \sum_{k=n-\lfloor n/2 \rfloor}^{n} (-1)^{k-1} f_{k-1} = \sum_{k=0}^{\lfloor n/2 \rfloor} (-1)^{n-k-1} f_{n-k-1} \\
&= \sum_{k=0}^{\lfloor n/2 \rfloor} (-1)^{n-k-1} |S_{n,k}| = (-1)^{n+1} \sum_{k=0}^{\lfloor n/2 \rfloor} (-1)^k \binom{n-k}{k} \frac{n}{n-k} \\
&= (-1)^{n+1} 2 T_n(1/2) = (-1)^{n+1} 2 \cos\left(n \frac{\pi}{3}\right)
\end{aligned}$$

$\square$

The f-Vector and the (2,1)-Pascal Triangle

The f-vectors of Corollary 4.6 can be found in the (2,1)-Pascal triangle. Denote the elements of $\boldsymbol{f_n}$ by $f_k^{(n)}$ and arrange them in a grid by filling the $(j+2)$th row with $f_j^{(n)}$ for $n \geq j+1$, starting with $f_j^{(j+1)}$ in the first column. Furthermore set the first element in the first row to 2,

$$
\begin{array}{cccccc}
2 & f_{-1}^{(1)} & f_{-1}^{(2)} & \cdots & & \\
f_0^{(1)} & f_0^{(2)} & f_0^{(3)} & f_0^{(4)} & \cdots & \\
f_1^{(2)} & f_1^{(3)} & f_1^{(4)} & f_1^{(5)} & \cdots & \\
f_2^{(3)} & f_2^{(4)} & f_2^{(5)} & f_2^{(6)} & f_2^{(7)} & \cdots \\
f_3^{(4)} & f_3^{(5)} & f_3^{(6)} & f_3^{(7)} & f_3^{(8)} & \cdots \\
\vdots & \vdots & \vdots & \vdots & \vdots & \ddots
\end{array}
=
\begin{array}{cccccc}
2 & 0 & \cdots & & & \\
1 & 2 & 0 & \cdots & & \\
1 & 3 & 2 & 0 & \cdots & \\
1 & 4 & 5 & 2 & 0 & \cdots \\
1 & 5 & 9 & 7 & 2 & 0 \\
\vdots & & & & & \ddots
\end{array}
$$

FIGURE 4.5: The f-vector of a single cell lies in the (2,1)-Pascal triangle

see also Figure 4.5. A Pascal triangle, arranged in such a grid, has the defining property that the sum of two consecutive elements in a row equals the entry below the second summand. That the arrangement of the f-vectors of $\langle\Sigma_n\rangle$ is indeed a Pascal triangle can be proven by direct computation and is summarized in the following lemma.

Lemma 4.9. *The arrangement of the numbers $f_k^{(n)}$ described above forms a (2,1)-Pascal triangle.*

Proof.

$$
\begin{aligned}
f_{k-1}^{(n-1)} + f_{k-1}^{(n-2)} &= \\
&= \frac{1}{k}\left((n-1)\binom{k}{n-1-k} + (n-2)\binom{k}{n-2-k}\right) \\
&= \frac{1}{k(k+1)}\left((n-1)(2k-n+2) + (n-2)(n-k-1)\right)\binom{k+1}{n-k-1} \\
&= \frac{n}{k+1}\binom{k+1}{n-k-1} = f_k^{(n)}
\end{aligned}
$$

The first element of each row is $f_j^{(j+1)} \equiv 1$ by the definition of $f_k^{(n)}$. Further $f_{-1}^{(n)} = 0$ for $n \geq 1$ by the condition $m > \lfloor n/2 \rfloor$ (c.f. Lemma 4.5) and Equation (4.1). $\square$

Corollary 4.10. *The sum $\sum_{k=-1}^{\lfloor n/2 \rfloor} f_k^{(n)}$ equals the nth Lucas number L_n.*

Proof. Follows by the defining property of the (2,1)-Pascal triangle. $\square$

4.2 The Complete $MG^4_{1,n}$

In this section, the complete moduli space $MG^4_{1,n}$ is investigated. The f-vector $\boldsymbol{F_n}$ is derived by glueing the simplices $\langle\sigma\Sigma_n\rangle$ together, which first done by a group action. In the subsequent part an alternative derivation using complete graphs is presented.
It is useful to exploit the topology of the one-loop graph, and denote a matching by the external legs of the vertices it contains.

4.2.1 The f-Vector of $MG^4_{1,n}$

In the previous section, the f-vector $\boldsymbol{f_n}$ of a simplex generated by a facet of $MG^4_{1,n}$ has been derived. The upcoming theorem is about the f-vector of the whole moduli space $\boldsymbol{F_n}$. Therefore the previous result will be applied to all graphs in $\mathcal{S}_n$, the set of all permuted n-suns, see Definition 2.32. $\mathcal{S}_n$ is also the subset of $\mathcal{G}^3_n$ that only contains one-loop graphs. Now define a set of n-suns with m-matchings.

Definition 4.11. *Let $m, n \in \mathbb{N}$ and $m \leq \lfloor n/2 \rfloor$. Define the set of m-matched n-suns $\mathfrak{M}_m\mathcal{S}_n$ by*

$$\mathfrak{M}_m\mathcal{S}_n := \left\{(M,\gamma) \;\middle|\; \gamma \in \mathcal{S}_n, M \in \mathfrak{M}_m\gamma\right\}.$$

Remark. Since all graphs in $\mathfrak{M}_m\mathcal{S}_n$ have the same topology, they all have the same number of possible matchings. Consequently $|\mathfrak{M}_m\mathcal{S}_n| = |\mathcal{S}_n| \cdot |\overline{F}_{n,m}|$.

To calculate the f-vector of $MG^4_{1,n}$ it is essential to note that some elements of $\mathfrak{M}_m\mathcal{S}_n$ are identical. Therefore apply the group action of the set $\mathfrak{M}\mathcal{G}^3_n/\sim$ on $\mathfrak{M}_m\mathcal{S}_n$, see also Definition 2.44. Here two elements in $\mathfrak{M}_m\mathcal{S}_n$ which differ by a transposition of two external half-edges whose vertices are part of the same matching, need to be identified. Conclude that for one-loop graphs, the action of STU^m can be defined as follows.

Definition 4.12. *Let $(M, \sigma\Sigma_n) \in \mathfrak{M}_m\mathcal{S}_n$ and $M = \{\{h_1, h_2\}, \ldots, \{h_m, h_{m+1}\}\}$. Define a group action $\Psi : \mathbb{Z}_2^m \times \mathfrak{M}_m\mathcal{S}_n \to \mathfrak{M}_m\mathcal{S}_n$ by*

$$\Psi_\tau(M, \sigma\Sigma_n) := \left(M, ((h_1, h_2)^{t_1} \circ (h_3, h_4)^{t_2} \circ \cdots \circ (h_m, h_{m+1})^{t_m} \circ \sigma)\Sigma_n\right)$$

with $\tau = (t_1, \ldots, t_m) \in \mathbb{Z}_2^m$, $(h_i, h_{i+1})^0 := (1)$, and $(h_i, h_{i+1})^1 := (h_i, h_{i+1})$.

Remark. Remember that the n-suns are defined with a permutation σ (modulo symmetry) on their external legs.

Pictorially speaking the group action swaps the external legs, which are connected to the matched vertices:

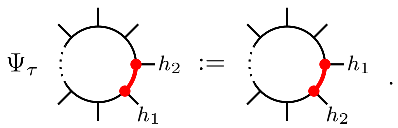

Lemma 4.13. *Let $n > 4$ and $(M,\gamma) \in \mathfrak{M}_m\mathcal{S}_n$ then $\mathrm{Stab}^{\Psi}_{(M,\gamma)} = \{e\}$, where e denotes the unit of $\mathbb{Z}_2^m$.*

Proof. First show that $\mathrm{Stab}^{\Psi}_{(\{h_1,h_2\},\gamma)} = \{0\}$, for all graphs $(\{h_1, h_2\}, \gamma) \in \mathfrak{M}_1\mathcal{S}_n$. Therefore Ψ has to map $(\{h_1, h_2\}, \gamma)$ into a different equivalence class in $\mathcal{S}_n$. Equivalently $(h_1, h_2) \notin R_n \ltimes \mathrm{Cyc}_n$. Assuming $n > 4$ it is evident that $(h_1, h_2) \notin R_n$ and $(h_1, h_2) \notin \mathrm{Cyc}_n$. Now show that $\nexists c \in \mathrm{Cyc}_n$ such that $r_n \circ c = (h_1, h_2)$. This is equivalent to $r_n \circ (h_1, h_2) \notin \mathrm{Cyc}_n$, which is true.

TABLE 4.1: The Euler-characteristic $\mathcal{X}_n$ of $MG^4_{1,n}$

n	5	6	7	8	9	10	11	12	13	14
$\mathcal{X}_n$	-3	0	45	-315	1260	0	-56700	623700	-3742200	0

For a general graph $(M,\gamma) \in \mathfrak{M}_m\mathcal{S}_n$ observe, that the matching M consists of pairwise disjoint edges and hence:

$$\Psi_\tau(M,\gamma) = (M,\gamma) \Leftrightarrow t_i = 0\,\forall i \in [m] \Leftrightarrow \tau = e\,. \qquad \square$$

Theorem 4.14. *Let $n > 4$ then the f-vector of $MG^4_{1,n}$ $\boldsymbol{F_n} = (F_{-1}, F_0, ..., F_{n-1})$ is given by*

$$F_k = \frac{(n-1)!}{2^{n-k}} f_k\,,$$

where f_k are the elements of the f-vector of $\langle\Sigma_n\rangle$, cf. Corollary 4.6.

Proof. $F_{n-1-m} = |\mathfrak{M}_m\mathcal{S}_n/\mathbb{Z}_2^m|$. Because of the Lemma 4.13 and the Orbit-Stabilizer Theorem 2.19 one has $|\operatorname{Orb}^\Psi_{(m,\gamma)}| = 2^m \quad \forall(m,\gamma) \in \mathfrak{M}_m\mathcal{S}_n$. Therefore the cardinality of the partition of $\mathfrak{M}_m\mathcal{S}_n$ by Ψ is given by

$$|\mathfrak{M}_m\mathcal{S}_n/\mathbb{Z}_2^m| = \frac{|\mathcal{S}_n||\overline{F}_{n,m}|}{|\operatorname{Orb}^\Psi_{(m,\gamma)}|} = \frac{(n-1)!}{2} f_{n-1-m}\frac{1}{2^m} \Leftrightarrow F_k = \frac{(n-1)!}{2^{n-k}} f_k\,. \qquad \square$$

Using the result for $\boldsymbol{F_n}$ the Euler-characteristic $\mathcal{X}_n$ is computed for some values of n, the outcome is displayed in Table 4.1. The first observation is that $\mathcal{X}_{4k+2} = 0\ \forall k \in \mathbb{N}$. A proof idea is given in the following corollary. Furthermore, by increasing n the absolute value of $\mathcal{X}_n$ increases and the sign alternates for the non-zero Euler-characteristics. These observations were all be made by a quick numerical calculation, whose extended results are displayed in the appendix in Table A.1.

Corollary 4.15. *The Euler-characteristic of $MG^4_{1,4k+2}$ is $\mathcal{X}_{4k+2} = 0 \quad \forall k \in \mathbb{N}$.*

Idea of proof. Let $\overline{\mathcal{X}}_{4k+2} := -\mathcal{X}_{4k+2}2^{(2k+1)}(2k+1)/(4k+2)!$. Then

$$\begin{aligned}\overline{\mathcal{X}}_{4k+2} &= \sum_{i=0}^{2k+1}(-1)^i\frac{2^{2k+1-i}(2k+1)}{4k+2-i}\binom{4k+2-i}{i}\\ &= \sum_{i=0}^{2k}(-1)^i\frac{2^{2k-i}(2k+1)}{2k+1-i}\binom{4k+1-i}{i} - 1 =: \sum_{i=0}^{2k}T(2k+1,i) - 1\,.\end{aligned}$$

The sequence $T(n,i)$ coincides with the integer sequence A204021 in OEIS [24]. There it is conjectured that $p(A_n,x) = \sum_{i=0}^{n-1}T(n,i)x^{n-i} - 1$, where $p(A_n,x)$ is the characteristic polynomial in x of the matrix A_n, defined by $(A_n)_{ij} := \min(2i-1, 2j-1)$ for $i,j \le n$. If true, then $\overline{\mathcal{X}}_{4k+2} = p(A_{2k+1},1) =: \det(B_{2k+1})$. Now show that $\det(B_{2k+1}) = 0$ by verifying that $\ker(B_{2k+1}) \neq 0$. Define a vector $v_{2k+1} \in \mathbb{R}^{2k+1}$ via $v_{2k+1} := (1,1,-1,-1,\ldots,\pm1,\pm1,\mp1)$ and demonstrate that

$$B_{2k+1}v_{2k+1} =: b = \begin{pmatrix} 0 & 1 & 1 & \cdots & 1\\ 1 & 2 & 3 & \cdots & 3\\ 1 & 3 & 4 & \cdots & 5\\ \vdots & \vdots & \vdots & \ddots & \vdots\\ 1 & 3 & 5 & \cdots & 4k\end{pmatrix}\begin{pmatrix}1\\1\\-1\\\vdots\\\mp1\end{pmatrix} = 0 \tag{4.2}$$

by explicit calculation row by row. Therefore it is useful to split the matrix B_{2k+1} into an upper diagonal matrix without the diagonal, denoted by $B^{\urcorner}_{2k+1}$ and a lower diagonal matrix denoted $B^{\llcorner}_{2k+1}$, such that $B^{\llcorner}_{2k+1} + B^{\urcorner}_{2k+1} = B_{2k+1}$.
Since each row of $B^{\urcorner}_{2k+1}$ consists of a repeated number, the alternating sum generated by multiplying with v_{2k+1} is zero for odd rows (then there are an even number of summands) and one element remains (with a sign) for even l. Conclude that $b^{\urcorner}_l = 0$ if l is odd and $b^{\urcorner}_l = (-1)^{l/2}(2l-1)$ for even l.
For the lower triangle write $b^{\llcorner}_l$ as the sum

$$b^{\llcorner}_l = \sum_{j=0}^{l-2}(-1)^{\lfloor j/2\rfloor}(2j+1) + (-1)^{\lfloor (l-1)/2\rfloor}(2l-2).$$

Observe that for odd l

$$\begin{aligned} b^{\llcorner}_{l+2} &= \sum_{j=0}^{l-2}(-1)^{\lfloor j/2\rfloor}(2j+1) + (-1)^{\lfloor (l-1)/2\rfloor}(2l-1) + (-1)^{\lfloor l/2\rfloor}(2l+1) \\ &\quad + (-1)^{\lfloor (l+1)/2\rfloor}(2l+2) \\ &= \sum_{j=0}^{l-2}(-1)^{\lfloor j/2\rfloor}(2j+1) + (-1)^{\lfloor (l-1)/2\rfloor}(2l-1+2l-1-2l+2) = b^{\llcorner}_l\,. \end{aligned}$$

The first line is just the definition with the two last summands written out explicitly. In the second line, the identities $\lfloor l/2\rfloor = \lfloor (l-1)/2\rfloor$ and $\lfloor (l+1)/2\rfloor = \lfloor (l-1)/2\rfloor + 1$ for odd $l \in \mathbb{N}$ were used. One can easily verify that $b^{\llcorner}_1 = b^{\llcorner}_3 = 0$ and therefore $b^{\llcorner}_l = 0$ for all odd l.
With similar arithmetic, one can show for even l that

$$b^{\llcorner}_l = b^{\llcorner}_{l-1} - (-1)^{(l/2)}(2l-1) = -(-1)^{(l/2)}(2l-1) = -b^{\urcorner}_l\,.$$

Conclude $B_{2k+1}v_{2k+1} = 0$. □

4.2.2 A Closer Look to $MG^4_{1,4}$

Theorem 4.14 does not cover the case $n = 4$, because the stabilizer of the group action Ψ is not the trivial group and there are isometries between some metric graphs in $MG^4_{1,4}$. To calculate $\boldsymbol{F_4}$ the groups $\mathrm{Stab}^{\Psi}_{(1,\gamma)}$ and $\mathrm{Stab}^{\Psi}_{(2,\gamma)}$, where $(1,\gamma)$ and $(2,\gamma)$ denote a 1- or 2-matching on the 4-sun γ respectively, are investigated. Here $\boldsymbol{F_4}$ is not the f-vector of $MG^4_{1,4}$, since it is no longer a relative simplex. However, $\boldsymbol{F_4}$ still counts the number of cells in each dimension, as long as the isometries are neglected.
When the matching consists of one edge $\{h_1, h_2\}$ the transposition (h_1, h_2) is not in the group $R_4 \ltimes \mathrm{Cyc}_4$, which can be verified by listing all elements. Therefore conclude $\mathrm{Stab}^{\Psi}_{(1,\gamma)} = \{0\}$ and $F^{(4)}_2 = |\mathcal{S}_4||F_{4,2}|/|\,\mathrm{Orb}^{\Psi}_{(1,\gamma)}\,| = 3 \cdot 4/2 = 6$.
For matchings that consist of two edges i.e. $|M| = 2$ the situation changes. Let $M = \{\{h_1, h_2\}, \{h_3, h_4\}\}$ then the permutation $(h_1, h_2)(h_3, h_4)$ can be written as $(h_1, h_3)c^3_+ \in R_4 \ltimes \mathrm{Cyc}_4$. It follows that $\Psi_{(1,1)}(M,\gamma) = (M,\gamma)$, so $(1,1)$ is an element of the stabilizer of Ψ. There is no other trivial action of $\mathbb{Z}^2_2$, since $\Psi_{(0,1)}$ or $\Psi_{(1,0)}$ act like before. In conclusion, $\mathrm{Stab}^{\Psi}_{(2,\gamma)} = \{e, (1,1)\}\ \forall (M,\gamma) \in \mathfrak{M}_2\mathcal{S}_4$ and therefore $F^{(4)}_1 = |\mathcal{S}_4||F_{4,1}|/|\,\mathrm{Orb}^{\Psi}_{(2,\gamma)}\,| = 3\cdot 2/2 = 3$.
Now it is important to note, that between the metric graphs in $MG^4_{1,4}$ with two internal legs exists an isometry.
As a consequence, the 1-dimensional faces of $MG^4_{1,4}$ are folded onto themselves and the space loses the structure of a relative simplicial complex. However, it is still possible to construct a

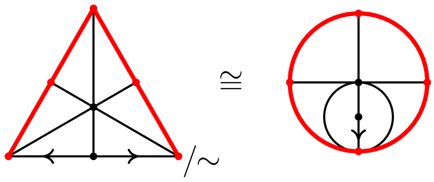

FIGURE 4.6: Barycentric subdivision of one 2-simplex in $MG^4_{1,4}$

Δ-complex. Theses are generalizations of complexes where the intersection of two simplices is not necessarily a simplex and the simplices are glued together using boundary maps. The barycentric subdivision of a 2-face of the moduli space complex is displayed in Figure 4.6. There the missing edges are depicted in red. The folding of the remaining edge emerging from the isometry is shown as an equivalence relation on the two edges marked with arrows. Now one can count the faces of each dimension, each of which is a generator for the free group C_k in the corresponding chain complex. Furthermore, the Euler characteristic of $MG^4_{1,4}$ is given by $\sum_k (-1)^k \dim C_k = \sum_k (-1)^k \dim H_k = \mathcal{X}$ [5].

Property 4.16. *The Euler characteristic of $MG^4_{1,4}$ is $\mathcal{X}_4 = 6$*

Proof. Count the number of faces after the barycentric subdivision and the identification in Figure 4.6 and conclude $\mathcal{X}_4 = 12 - 39 + 36 - 3 = 6$. □

In Figure 4.7 the subspace poset of $MG^4_{1,4}$ is shown. The subspace Γ_i is a space generated by one of the three 4-suns, γ_j is generated by a 1-matched 4-sun and lastly g_k is generated by a 2-matched 4-sun. Notice that the number of these spaces given by the vector $\boldsymbol{F_4}$.

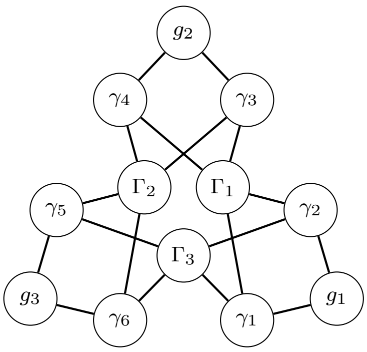

FIGURE 4.7: The subspace poset of $MG^4_{1,4}$.

4.3 The Complete Graph K_n

This section aims to explore a relation between matchings on the complete graph K_n and the f-vectors of the moduli spaces $MG^4_{1,n}$. A new derivation of the vector $\boldsymbol{F_n}$ is presented. First of all, complete graphs and cycles in graphs are defined.

Definition 4.17. *A complete graph K_n is the graph on n vertices where any two vertices share precisely one edge.*

Remark. In this definition, the complete graph does not have external legs, but they can always be added by giving each vertex one external leg. This is equivalent to naming the vertices and is done implicitly in the next considerations.

Definition 4.18. *A cycle c in a graph G is a subgraph that has precisely one loop and whose vertex set covers the vertex set of G.*

Combinatorially a n-cycle can be denoted here by a vector $c = (c_1, c_2, \dots, c_n)$, with $c_i \in [n]$ and $c_i \neq c_j \forall i \neq j$. Cycles that differ by a rotation or a reflection are considered to be the same since they will ultimately represent the one-loop Feynman graphs. Then the set of all (equivalence classes of) cycles in K_n is denoted by $\mathcal{C}_n$ and $|\mathcal{C}_n| = (n-1)!/2$. Note that this would be formalized completely analog to the previous considerations made to analyze the symmetry of the permuted n-suns in Section 2.3. Therefore also deduce $\mathcal{C}_n \cong \mathcal{S}_n$.

4.3.1 An Equivalent f-Vector of $MG^4_{1,n}$

In this segment, an alternative way to compute $\boldsymbol{F_n}$ is presented. This method will use complete graphs and cycles in these graphs. Therefore matchings on complete graphs and their cycles, that preserve a given matching (defined below) are investigated. These cycles correspond to the graphs $\sigma\Sigma_n$.

Some properties that relate the set of all permuted graphs $\mathcal{S}_n$ and the complete graph K_n are studied first. The upcoming property states that the union of all edges in $\mathcal{S}_n$ is the same as the edge set E_{K_n} of the complete graph K_n. An example of this relation for $n = 4$ can be seen in Figure 4.8.

Property 4.19. $\bigcup_{\gamma \in \mathcal{S}_n} E_\gamma = E_{K_n}$

Proof. Take any edge $e \in \bigcup_{\gamma \in \mathcal{S}_n} E_\gamma$, then $e \in E_{K_n}$, since $V_\gamma = V_{K_n}$ by definition for any $\gamma \in \mathcal{S}_n$. Therefore $\bigcup_{\gamma \in \mathcal{S}_n} E_\gamma \subseteq E_{K_n}$.
To proof $\bigcup_{\gamma \in \mathcal{S}_n} E_\gamma \supseteq E_{K_n}$ show that for any edge $e \in E_{K_n}$ which connects vertex v and w exists a permutation $\sigma \in S_n$ such that v and w are connected via one edge in $\sigma\Sigma_n$. Assume v and w are not connected in $\sigma'\Sigma_n$, but z and v are. Set $\sigma = (w, z) \circ \sigma'$, which connects v and w in $\sigma\Sigma_n$. (Notice that if $\sigma'\Sigma_n \sim \sigma\Sigma_n$ the vertices v and w share an edge in both graphs.) □

The second argument can be iterated such that one can deduce

Property 4.20. $\forall M \in \mathfrak{M}K_n\ \exists \sigma\Sigma_n \in \mathcal{S}_n$ *such that* $M \subset \sigma\Sigma_n$.

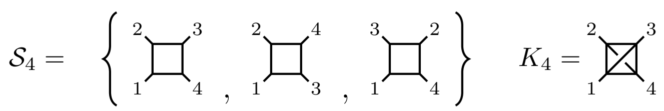

Figure 4.8: The set $\mathcal{S}_4$ and the complete graph K_4

Proof. Follows from $V_{K_n} = V_{\sigma\Sigma_n}$, $|M| = 0$ and the argument given in the proof of property 4.19. $\square$

Notice that for graphs $\Gamma \in \mathcal{G}^3_{l,n}$ the number of vertices is fixed $|V_\Gamma| = 2l - 2 + n$. The last property can be generalized to arbitrary graphs.

Property 4.21. *$\forall M \in \mathfrak{M}K_{2l-2+n}$ $\exists \Gamma \in \mathcal{G}^3_{l,n}$ such that $M \subset \Gamma$.*

Proof. Label the vertices of K_{2l-2+n} such that there are two types of vertices, of which $2l-2$ are called internal and n external.
Consider a graph $\gamma \in \mathcal{G}^3_{l,0}$ with the following topology

$\gamma \quad =$ 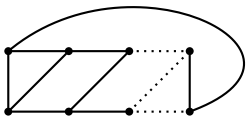 ,

where the dotted lines represent a repetition of the same structure until $|\gamma| = l$.
Let $\mu \in \mathfrak{M}K_{2l-2}$ be a maximal matching. Choose labels on the vertices of γ such that $\mu \subset \gamma$. For $\mu \in \mathfrak{M}K_{2l-2+n}$ add labeled external legs to γ, such that $\mu \subset \gamma$ stays true. It is ensured that μ is a valid matching since γ does not have any multi-edges. $\square$

Now return to the case of one-loop graphs and define set that will be proven to be isomorphic to the matchings in K_n.

Definition 4.22. *Let $\mathcal{M}_{n,i}$ be the union of all matchings on i edges over all graphs in $\mathcal{S}_n$.*

$$\mathcal{M}_{n,i} := \bigcup_{\gamma \in \mathcal{S}_n} \mathfrak{M}_i \gamma$$

The next property identifies $\mathcal{M}_{n,i}$ and $\mathfrak{M}_i K_n$ to be the same. Exemplary this is shown for $n = 4$ and $i = 2$ in Figure 4.9.

Property 4.23. $\mathfrak{M}_i K_n = \mathcal{M}_{n,i}$.

Proof. The inclusion $\mathcal{M}_{n,i} \subseteq \mathfrak{M}_i K_n$ is trivial, since $M \subseteq K_n$ $\forall M \in \mathcal{M}_{n,i}$, because M is just a disjoint union of edges and K_n has all possible edges by property 4.19 (also by the definition of K_n). The inverse inclusion is given by Property 4.20. $\square$

As before, the previous property can be generalized by the same means as before.

The observations above can be combined to count matched graphs by studying matchings on the complete graph (which captures the combinatorics of the matching process) and then count the subgraphs of a given type in K_n such that a given matching is preserved.

Definition 4.24. *A graph γ preserves a matching $M \subset K_n$ if M is a matching on γ.*

Therefore, to derive the f-vector $\boldsymbol{F_n}$, in the case of one-loop graphs, there are two more pieces of information needed, the number of matchings in $\mathfrak{M}_i K_n$ and how many cycles in $\mathcal{C}_n$ preserve a given matching. The following definition constructs a set, whose elements precisely coincide with the set of matched n-suns, but is built of matching preserving cycles.

$\mathcal{M}_{4,2} = \Bigg\{$ 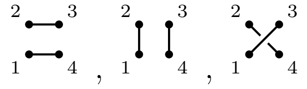

$\Bigg\} = \mathfrak{M}_2 K_4$

FIGURE 4.9: $\mathcal{M}_{4,2} = \mathfrak{M}_2 K_4$

Definition 4.25. *Define the set of matched cycles $\mathfrak{M}_m\mathcal{C}_n$ by*

$$\mathfrak{M}_m\mathcal{C}_n := \left\{(M,c) \;\middle|\; M \in \mathfrak{M}_m c, c \in \mathcal{C}_n\right\} .$$

Remark. From $\mathcal{C}_n \cong \mathcal{S}_n$ and property 4.23 follows $\mathfrak{M}_m\mathcal{C}_n \cong \mathfrak{M}_m\mathcal{S}_n$ and consequently $F_k = |\mathfrak{M}_{n-k-1}\mathcal{C}_n/\Psi|$.

Computing the size of $\mathfrak{M}_m\mathcal{C}_n$ is done next. Therefore write $|\mathfrak{M}_m\mathcal{C}_n| = |\mathfrak{M}_m K_n| q_{m,n}$, where $q_{m,n}$ is the number of cycles in the complete graph that preserve a given m-matching. This factorization can be done since $q_{m,n}$ is independent of the concrete m-matching. The two quantities $|\mathfrak{M}_m K_n|$ and $q_{m,n}$ are determined in the next lemmas.

Lemma 4.26. *The number of m-matchings in the complete graph K_n is given by*

$$|\mathfrak{M}_m K_n| = \frac{1}{m!}\prod_{i=0}^{m-1}\binom{n-2i}{2} .$$

Proof. A 1-matching in a complete graph is chosen by picking 2 of n indistinguishable vertices, hence there are $\binom{n}{2}$ 1-matchings in K_n. Repeat this process m times, since every time the remaining vertices are still indistinguishable one gets $\prod_{i=0}^{m-1}\binom{n-2i}{2}$. This establishes an order on the matched vertices, which is undone by dividing by $m!$. □

Lemma 4.27. *Let $q_{m,n}$ denote the number of cycles, that preserve a given m-matching in K_n. It is given by*

$$q_{m,n} = 2^m \frac{(n-m-1)!}{2} .$$

Proof. The matching consists of m pairs of vertices, which fixes m elements of the cycle. That means $|\mathcal{C}_{n-m}|$ possible cycles remain, but each matching is allowed to change the order of its vertices and therefore $q_{m,n} = 2^m|\mathcal{C}_{n-m}|$. □

Theorem 4.28. *Let $n > 4$ then the f-vector of $MG^4_{1,n}$ $\boldsymbol{F_n} = (F_{-1}, F_0, ..., F_{n-1})$ is given by*

$$F_k = \frac{k!}{2(n-1-k)!}\prod_{i=0}^{n-k-2}\binom{n-2i}{2} .$$

Proof.

$$\begin{aligned} F_k = |\mathfrak{M}_{n-k-1}\mathcal{C}_n/\mathbb{Z}_2^m| &= \frac{|\mathfrak{M}_{n-k-1}K_n| q_{n-k-1,n}}{2^{n-k-1}} \\ &= 2^{k+1-n}2^{n-k-1}\frac{k!}{2}\frac{1}{(n-k-1)!}\prod_{i=0}^{n-k-2}\binom{n-2i}{2} \\ &= \frac{k!}{2(n-k-1)!}\prod_{i=0}^{n-k-2}\binom{n-2i}{2} \end{aligned}$$

□

Note that the group action Ψ is not explicitly defined for the set $\mathfrak{M}_m\mathcal{C}_n$, but by the relation $\mathfrak{M}_m\mathcal{C}_n \cong \mathfrak{M}_m\mathcal{S}_n$ it is clear how to do that. Conclude that the orbits on $\mathfrak{M}_m\mathcal{C}_n/\mathbb{Z}_2^m$ are all of the same size as before (which has already been used in the proof above).
A quick calculation shows that the two representations of the f-vector of $MG^4_{1,n}$ indeed

coincide. First, rewrite the product in F_k of the Theorem 4.28:

$$\prod_{i=0}^{n-k-2} \binom{n-2i}{2} = 2^{1+k-n} \frac{n!}{(n-2)!} \frac{(n-2)!}{(n-4)!} \cdots \frac{(2k+4-n)!}{(2k+2-n)!}$$
$$= 2^{1+k-n} \frac{n!}{(2k+2-n)!} \,.$$

Bringing this back together with the expression of the theorem it amounts to

$$F_k = \frac{k!}{2(n-1-k)!} 2^{1+k-n} \frac{n!}{(2k+2-n)!} = \frac{n!}{2^{n-k}(k+1)} \binom{k+1}{n-1-k} \,,$$

which is the form of the f-vector in Theorem 4.14.

4.4 Generalizations

In this section, the previous result is slightly generalized by investigating colored and QCD one-loop graphs.

4.4.1 Colored Graphs

For the general, colored moduli space $MCG^v_{l,n,C}$ the size of the isomorphy classes can no longer be given explicitly since it depends on the coloring of the graph. Recall that a coloring of a graph G is a map $c : E_G \to [C]$, with $C \in \mathbb{N}$ the number of colors, assigning to each internal edge a color. A coloring from a physical viewpoint is just a place holder for different particle types. A colored graph is denoted by the pair (c, G).
Set $C = n$ for simplicity, but the general case can be retrieved most of the time. The study of $MCG^4_{1,n,n}$ is analogous to the prior investigation. First, the set of all permuted colored n-suns is defined. Secondly, matchings on these graphs are added.

Definition 4.29. *Define the set $\mathcal{CS}_n$ of all colored n-suns by*

$$\mathcal{CS}_n := \left\{(c, \sigma\Sigma_n) \,\middle|\, \sigma \in S_n,\, c : E_{\Sigma_n} \to [n]\right\} / \phi \,,$$

where ϕ is the group action from Definition 2.32. Denote an element by $[\gamma^c]$.

Remark. Technically one needs a further equivalence relation since two graphs $\gamma^c, \delta^{c'} \in \mathcal{CS}_n$ should be considered equal if an isomorphism $i : \gamma \to \delta$ exists, such that $c' = i \circ c$. To keep the notation simple let the equivalence classes $[\gamma^c] \in \mathcal{CS}_n$ include the previously described relation.

The main difference compared to the previous considerations is that the size $|\mathcal{CS}_n|$ is no longer known. That is because the size of the orbit $|\operatorname{Orb}^\phi_\gamma|$ is not the same for all permuted colored graphs $\gamma^c = (c, \sigma\Sigma_n)$.
The set of possible matchings on a graph $[\gamma^c] \in \mathcal{CS}_n$ is not changed and the previous result of Corollary 4.6 can be taken over. A set of matched colored n-suns $\mathfrak{M}_m\mathcal{CS}_n$ is constructed completely analogous to Definition 4.11. Moreover, it is still true that every graph has the same number of matchings, thus $|\mathfrak{M}_m\mathcal{CS}_n| = |\mathcal{CS}_n||\overline{F}_{n,m}|$. Note that here the matched graphs not only need to respect the equivalence relation of Definition 2.44, which takes permutations of the half-edges attached to the matched edge into account. However, a matched edge should no longer have a color, which means that graphs that differ only by colors on matched edges should be considered equal. As before this can be done by a group action.

Definition 4.30. *Define a group action $\Psi^c : \mathbb{Z}_2^m \times \mathbb{Z}_n^m \times \mathfrak{M}_m\mathcal{CS}_n \to \mathfrak{M}_m\mathcal{CS}_n$ for $\rho = (\tau, s) \in \mathbb{Z}_2^m \times \mathbb{Z}_n^m$ by*

$$\Psi^c_\rho(M, \gamma^c) := \left(M, (\Psi_\tau\gamma)^{\Psi^c_s c}\right) \text{ , where the colormap is given by}$$

$$\Psi^c_s c\,\big|_{E_\gamma \setminus M} := c\,\big|_{E_\gamma \setminus M} \text{ and } \Psi^c_s c\,\big|_M := c\,\big|_M + s\,.$$

The graph $\Psi_\tau\gamma$ is specified above in Defintion 4.12.

For the definition above, the colors are taken as elements in $\mathbb{Z}_n$, such that the action on the coloring orbits through every possible color for every edge in the matching. By this action, the color on these edges is effectively forgotten.
The result of the Lemma 4.13 stays true, since a change of color on a matching cannot result in a reflection or rotation. Therefore $\operatorname{Stab}^{\Psi^c}_{(M,\gamma^c)} = \{e\}$ $\forall (M, \gamma^c) \in \mathfrak{M}_m\mathcal{CS}_n$ and $|\operatorname{Orb}^{\Psi^c}| = |\mathbb{Z}_2^m \times \mathbb{Z}_n^m| = 2^m n^m$.

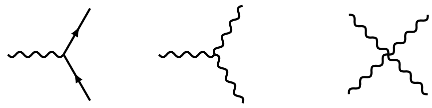

FIGURE 4.10: The vertices of QCD

Theorem 4.31. *The f-vector $\boldsymbol{F_n^c} = (F_{-1}^c, F_0^c, ..., F_{n-1}^c)$ of $MCG_{1,n,n}^4$ is given by*

$$F_{n-m-1}^c = \frac{|\mathcal{CS}_n||\overline{F}_{n,m}|}{|\operatorname{Orb}^{\Psi^c}|} = |\mathcal{CS}_n| \frac{n}{n-m}\binom{n-m}{m}\frac{1}{2^m n^m} \,.$$

Proof. By the above. □

Remark. Note that the number of colors in a graph can easily be promoted to an independent variable and allowing only one color restores the previous result.

The only unknown is the size of $\mathcal{CS}_n$, but it is finite (for a finite number of colors) and can in principle be calculated.

Consider the case, where the color map on the graph is required to be injective so that no color can appear twice. Denote the moduli space of these rainbow-colored graphs by $MRG_{1,n}^4$. Then deduce that

$$|\mathcal{CS}_n| = n!|\mathcal{S}_n|.$$

The orbit of the group action Ψ^c changes as well since not all colors are allowed on the matched edges. Instead, all colors, that are missing on the unmatched edges are allowed. Therefore here the orbit calculates as $|\operatorname{Orb}^{\Psi^c}| = |\mathbb{Z}_2^m \times S_m| = 2^m m!$. Combining these considerations leads to the following result for the f-vector of the moduli space of rainbow-colored graphs

Corollary 4.32. *The f-vector $\boldsymbol{F_n^r} = (F_{-1}^r, F_0^r, ..., F_{n-1}^r)$ of $MRG_{1,n}^4$ is given by*

$$F_{n-m-1}^r = \frac{|\mathcal{CS}_n||\overline{F}_{n,m}|}{|\operatorname{Orb}^{\Psi^c}|} = \frac{n}{n-m}\binom{n-m}{m}\frac{n!(n-1)!}{2^{m+1}m!} = \frac{n!}{m!}F_{n-m-1} \,.$$

The Euler characteristics for several n of the space $MRG_{1,n}^n$ are listed in the appendix in the Table A.2.

Rainbow-colored graphs are especially convenient since there are no isometries between them. In the one-loop case, the restriction on the color map could be loosened slightly by only requiring it to be injective on edges that are part of the same multi-edge, such that the colors of edges in a multi-edge are all different.

4.4.2 The One Loop Moduli Spaces of QCD: $MG_{l,n}^{\mathrm{QCD}}$

For moduli space of QCD, $MG_{l,n}^{\mathrm{QCD}}$, a new vertex type needs to be added, namely the interaction between fermions and gluons. In the full theory, the coupling to ghosts needs to be included as well, but here this does not add anything new and therefore ghosts are neglected in this section. The vertices under consideration are shown in Figure 4.10.

The first observation is that $MG_{l,n}^{\mathrm{QCD}}$ decomposes by the residue[2] of the graphs. Although the decomposition is true for any loop number, the following observations are again restricted

[2] The residue of a graph is given by its external half-edges. It distinguishes different edge types.

to one loop, write

$$MG^{\mathrm{QCD}}_{1,n} = \bigsqcup_{r \in \mathcal{R}_n} MG^{\mathrm{QCD}}_{1,\{r\}} \,.$$

Where $\mathcal{R}_n$ denotes the finite set of residues. A residue $\{r\} \in \mathcal{R}_n$ captures the external leg structure of a graph and can be written as $\{r\} = \{2f, g\}$, with $2f$ being the number of external fermions and g of external gluons. Consequently, $2f + g = n$.
In the following it is shown that $MG^{\mathrm{QCD}}_{1,\{r\}}$ is not connected and the f-vector $\boldsymbol{F}^{\mathrm{QCD}}$ of its connected components is derived. Therefore it is useful to look at the general form of the one-loop graph in QCD.

The 3-regular graphs of QCD are built of the following two tree subgraphs:

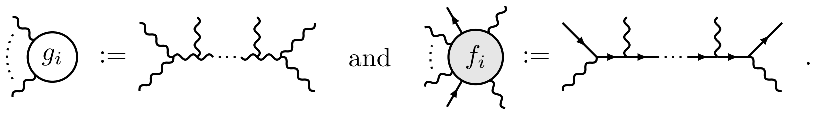

The index i is related to the total number of external gluons $|H^{ext}|$ by $i = |H^{ext}| - 2$.
First, consider the residues $r = \{0, n\}$, then there are two types of one-loop graphs: The loop could either be formed by fermions or by gluons. The first one is not very interesting regarding the moduli spaces of metric graphs since fermion edges can not be collapsed. The reason behind that is the absence of a four valent gluon fermion interaction. Consequently the graphs

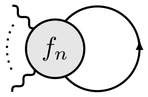

form a facet $\langle f_n \rangle \subseteq MG^{\mathrm{QCD}}_{1,\{0,n\}}$ without boundary (one for each permutation of the external legs). The other possibility is the one already treated in the previous section:

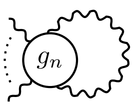

$$= \Sigma_n \,.$$

Note that $MG^{\mathrm{QCD}}_{1,\{0,n\}} = MG^4_{1,n} \sqcup \langle f_n \rangle^{\sqcup n!}$ is not connected.

Now lets consider the cases $f \neq 0$ and begin the classification of one-loop graphs by looking at the combination of two tree gluon graphs. Observe that

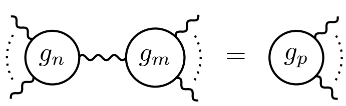

with $p = n + m$.
Now the most general 1-loop graph of QCD $\Sigma^{\mathrm{QCD}}_{\rho}$ can be constructed, where ρ is a multi-index given by $\rho := \{i_1, j_1, i_2, j_2, \dots i_f, j_f\}$. The graph $\Sigma^{\mathrm{QCD}}_{\rho}$ is made of f pairs g_i and f_j combined to a loop, where the graphs g_i are always glued in such that the whole graphs stays 1PI. It is shown in Figure 4.11.

Remark. The construction above ignores that fermion edges carry a direction. It would be possible to include that in the multi-index ρ, but for the following derivation, the direction does not matter.

$\Sigma_\rho^{\mathrm{QCD}} :=$ 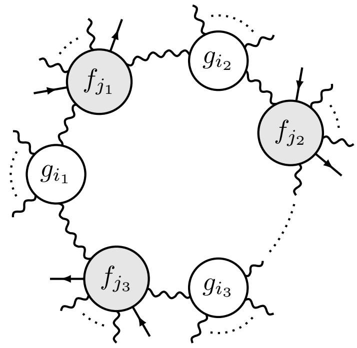

FIGURE 4.11: The general 1-loop graph of QCD: $\Sigma_\rho^{\mathrm{QCD}}$

For a residue r, the possible distributions of external gluon edges are given by the partition of $\sum_{k=1}^{f} i_k + j_k = g$, given by ρ. Call the set of all partitions $P_{g,2f}$. However, as before, two graphs $\Sigma_\rho^{\mathrm{QCD}}$ and $\Sigma_{\rho'}^{\mathrm{QCD}}$ might be isomorphic. This occurs when the two partitions ρ and ρ' are related by a permutation which is also an isomorphism of the graph. Denote the set of all partitions modulo the symmetry by $R_{g,2f}$.
Now fix a graph $\Sigma_\rho^{\mathrm{QCD}}$ and apply the same procedure as before. The first observation is that only the subgraphs $g_i \subseteq \Sigma_\rho^{\mathrm{QCD}}$ generate faces of the moduli spaces because only gluon edges can be collapsed. Consequently, only graphs that differ by a permutation of external legs of each g_i are connected in the moduli spaces:

Property 4.33. *The cells $\langle \sigma\Sigma_\rho^{QCD}\rangle$ and $\langle \Sigma_\rho^{QCD}\rangle$ are connected iff $\sigma = \sigma_1 \circ \cdots \circ \sigma_f$ and $\sigma_k : H^{ext}_{g_{i_k}} \to H^{ext}_{g_{i_k}}$.*

Denoting the space of all permuted graphs modulo symmetries as $\mathcal{S}_\rho^{\mathrm{QCD}}$, it follows the decomposition of $MG_{1,\{r\}}^{\mathrm{QCD}}$:

Property 4.34. *Let $f > 0$, then*

$$MG^{QCD}_{1,\{g,2f\}} = \bigsqcup_{\substack{\rho\in R_{g,2f}\\ \rho=\{i_1,j_1,\dots,i_f,j_f\}}} \left(MG^{QCD}_{1,\rho}\right)^{\sqcup\left(|\mathcal{S}^{QCD}_\rho| - i_1!\cdots i_f!\right)} .$$

Proof. If $\rho, \rho' \in R_{g,2f}$ and $\rho \neq \rho'$ clearly $MG_{1,\rho}^{\mathrm{QCD}} \bigcap MG_{1,\rho'}^{\mathrm{QCD}} = \emptyset$. Furthermore, any connected component of $MG_{1,\rho}^{\mathrm{QCD}}$ involves $i_1! \cdots i_f!$ facets by Property 4.33. There are $|\mathcal{S}_\rho^{\mathrm{QCD}}|$ facets in total and therefore each summand above contains $|\mathcal{S}_\rho^{\mathrm{QCD}}| - i_1! \cdots i_f!$ unconnected components. □

The f-vector $\boldsymbol{F}_\rho^{\mathrm{QCD}}$ of $MG_{1,\rho}^{\mathrm{QCD}}$ is now derived. Therefore the size of $\mathfrak{M}_m \Sigma_\rho^{\mathrm{QCD}}$, the set of all matchings on the graph, needs to be determined.

Lemma 4.35. *Let g_i be defined as above, $m \in \mathbb{N}$ and $m \leq \lceil (i-1)/2 \rceil$ then*

$$|\mathfrak{M}_m g_i| = \binom{i-m}{m} .$$

Proof. The number of $m-$matchings on g_i is equivalent to picking m non consecutive numbers in $[i-1]$. Place $i-m-1$ bars and fill the gaps with m stars. There are $\binom{i-m}{m}$ possibilities to place the stars. Number both from left to right, the numbers on the stars give a matching. □

$$\begin{array}{ccccc} | & \star & | & \star & | \\ 1 & 2 & 3 & 4 & 5 \end{array} \quad \longleftrightarrow$$

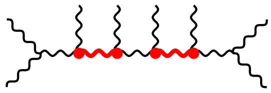

FIGURE 4.12: Example for the construction in the proof of Lemma 4.35 for $i = 6$ and $m = 2$.

An example for the construction of the proof above is given in Figure 4.12.

Remark. Note that for $m > \lceil (i-1)/2 \rceil$ one finds $|\mathfrak{M}_m g_i| = 0$.

Theorem 4.36. *Let $\rho = \{i_1, j_1 \dots i_f, j_f\} \in R_{g,2f}$.*
The f-vector $\boldsymbol{F}^{QCD}_\rho = (F^{QCD}_{-1}, F^{QCD}_0, ..., F^{QCD}_{n-1})$ of $MG^{QCD}_{1,\rho}$ is given by

$$F^{QCD}_{n-m-1} = \frac{i_1! \cdots i_f!}{2^m} \sum_{\substack{m_1+\cdots+m_f=m \\ 0 \le m_i \le m}} \prod_{k=1}^{f} \binom{i_k - m_k}{m_k} .$$

Proof. First, note that $i_1! \cdots i_f!$ is the number of facets of $MG^{\text{QCD}}_{1,\rho}$ by Property 4.33. The group action Ψ permuting the external half-edges attached to matchings acts like before, in particular $|\operatorname{Orb}^\psi| = 2^m$. Each composition of m into f integers gives rise to a m matching, where each g_{i_k} persists of a m_k-matching. Thus

$$|\mathfrak{M}_m \Sigma^{\text{QCD}}_\rho| = \sum_{\substack{m_1+\cdots+m_f=m \\ 0 \le m_i \le m}} \prod_{k=1}^{f} |\mathfrak{M}_{m_k} g_{i_k}| ,$$

with $F^{\text{QCD}}_{n-m-1} = \frac{i_1! \cdots i_f!}{2^m} |\mathfrak{M}_m \Sigma^{\text{QCD}}_\rho|$ the statement follows. $\square$

Chapter 5

Two Loop Moduli Space $MG^4_{2,n}$

This chapter mainly contains a section where the developed method in the previous chapter is applied to the moduli spaces $MG^4_{2,n}$ of rank two graphs with n external legs. The main result is a theorem about the number of two-loop gluon graphs with a given number of 4 valent vertices. This enables the calculation of the f-vector of the rainbow-colored moduli space $MRG^4_{2,n}$.

As before the starting point is the set of 3-regular graphs, with all possible permutations of labels on the external legs. Before the set is defined, observe that there is a unique topology for the admissible 2 loop graphs and it is defined below.

Definition 5.1. *Let $\sigma \in S_n$ and $n = \alpha + \beta + \gamma$, then define the two-loop graph $\sigma b_{\alpha,\beta,\gamma}$ by*

$\sigma b_{(\alpha,\beta,\gamma)}$:=

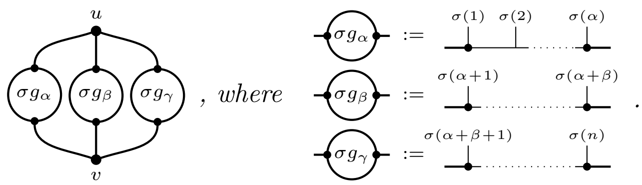

Remark. Throughout this chapter, the external legs of the subgraphs g_{α_i} are not displayed explicitly in their pictures.

Since all permutations of the external legs, modulo symmetry, give different graphs $\sigma b_{\alpha,\beta,\gamma}$, any $\sigma \in S_n$ is considered for the set of all two-loop graphs. Additionally, all partitions of n into three integers, representing the distribution of the external legs over the three tree subgraphs g_α, g_β and g_γ, are contemplated. These subgraphs are essentially the same graphs defined in the previous chapter as QCD tree subgraphs.

Definition 5.2. *Define the set of all partitions of n in 3 integers $P(n) \subset \mathbb{N}^3$ via*

$$P(n) := \left\{ (\alpha_1, \alpha_2, \alpha_3) \;\middle|\; \alpha_1 + \alpha_2 + \alpha_3 = n,\ \alpha_1 \geq \alpha_2 \geq \alpha_3 \geq 0 \right\} .$$

Now everything is set up to define the set of all permuted two-loop graphs $\mathcal{B}_n$.

Definition 5.3. *Write $\boldsymbol{\alpha} = (\alpha_1, \alpha_2, \alpha_3)$ and denote the set of admissible, 3-regular two-loop graphs by $\mathcal{B}_n \subset \mathcal{G}^3_n$, then define*

$$\mathcal{B}_n := \left\{ \sigma b_{\boldsymbol{\alpha}} \;\middle|\; \sigma \in S_n,\ \boldsymbol{\alpha} \in P(n) \right\} / \sim\ .$$

Where $\sigma b_{\boldsymbol{\alpha}} \sim \sigma' b_{\boldsymbol{\beta}}$ if they are isomorphic with fixed external legs.

5.1 Counting Matched Two Loop Graphs

Similar to Definition 4.11, a set of matched two loop graphs is defined. For the upcoming examination it will be useful to distinguish four different types of matchings, three of them are defined by how many internal vertices are matched. The last case, denoted by the letter τ, is needed to decide whether a matched graph corresponds to a tadpole graph or not. The distinction between the different matchings is defined as follows.

Definition 5.4. *Let $\sigma b_{\boldsymbol{\alpha}} \in \mathcal{B}_n$ then define admissible p-matchings $\mathfrak{M}^p_m(\sigma b_{\boldsymbol{\alpha}})$ with $p \in \{0,1,2,\tau\}$ by*

$$\begin{aligned}
\mathfrak{M}^0_m(\sigma b_{\boldsymbol{\alpha}}) &:= \left\{M \;\middle|\; M \in \mathfrak{M}_m(\sigma b_{\boldsymbol{\alpha}}), u, v \notin M\right\}, \\
\mathfrak{M}^1_m(\sigma b_{\boldsymbol{\alpha}}) &:= \left\{M \;\middle|\; M \in \mathfrak{M}_m(\sigma b_{\boldsymbol{\alpha}}), u \in M, v \notin M\right\}, \\
\mathfrak{M}^2_m(\sigma b_{\boldsymbol{\alpha}}) &:= \left\{M \;\middle|\; M \in \mathfrak{M}_m(\sigma b_{\boldsymbol{\alpha}}), u, v \in M, \{u,v\} \notin M\right\} \quad \textit{and} \\
\mathfrak{M}^\tau_m(\sigma b_{\boldsymbol{\alpha}}) &:= \begin{cases} \left\{M \;\middle|\; M \in \mathfrak{M}_m(\sigma b_{\boldsymbol{\alpha}}), \{u,v\} \in M\right\} & \textit{if } \alpha_2 \neq 0 \\ \emptyset & \textit{else} \end{cases}.
\end{aligned}$$

Remark. The set of all admissible matchings of a graph $\sigma b_{\boldsymbol{\alpha}} \in \mathcal{B}_n$, denoted by $\mathfrak{M}_m(\sigma b_{\boldsymbol{\alpha}})$, is given by the disjoint union of the sets defined above.

To clarify the definition of $\mathfrak{M}^\tau_m(\sigma b_{\boldsymbol{\alpha}})$ it is useful to look at an example.

Example 5.5. As before, denote a matched graph g by (M, g), where $M \subset E_g$ is a matching. Consider the matched graph $\big(\{u,v\}, \sigma b_{(1,1,0)}\big)$ which corresponds to the graph $g =$  $\in \mathcal{B}_2$, which is not a tadpole. However, matched graphs of the type $\big(\{u,v\}, \sigma b_{(\alpha,0,0)}\big)$ are tadpoles, for example for $\alpha = 2$ it corresponds to the graph  , which is clearly a tadpole and is therefore not in the set $\mathcal{B}_2$. This means that the matching $\{u,v\}$ is not admissible in graphs like $\sigma b_{(\alpha,0,0)}$ and is therefore excluded in the definition of admissible τ-type matchings above.

Now define sets of matched graphs corresponding to the types of matchings defined in Definition 5.4.

Definition 5.6. *The set of matched two-loop graphs $\mathfrak{M}_m\mathcal{B}_n$ is defined as*

$$\begin{aligned}
\mathfrak{M}_m\mathcal{B}_n &:= \bigsqcup_{p \in \{0,1,2,\tau\}} \mathfrak{M}^p_m\mathcal{B}_n, \textit{ with} \\
\mathfrak{M}^p_m\mathcal{B}_n &:= \left\{(M,\Gamma) \;\middle|\; \Gamma \in \mathcal{B}_n, M \in \mathfrak{M}^p_m(\Gamma)\right\}
\end{aligned}$$

As in the one loop case, there is a property linking all matchings of two-loop graphs and all matchings in a complete graph. Here the complete graph K_{n+2} is investigated since the two-loop graph has $n+2$ vertices. In the complete graph, n vertices are labeled from 1 to n representing the external legs and the remaining two vertices u and v. The vertices of K_{n+2} are indistinguishable, and hence, all possible labels are equivalent.

Property 5.7. *Let $p \in \{0,1,2,\tau\}$, then*

$$\mathfrak{M}^p_m K_{n+2} = \bigcup_{\gamma \in \mathcal{B}_n} \mathfrak{M}^p_m \gamma\,.$$

Proof. The proof is analogous to the proof of Property 4.23. ☐

The next property links the sets of all p-type matchings on the complete graph K_{n+2} to the sets of all matchings on a complete graph with fewer vertices. This enables the calculation of the size of $\mathfrak{M}^p_m K_{n+2}$ by the Lemma 4.26.

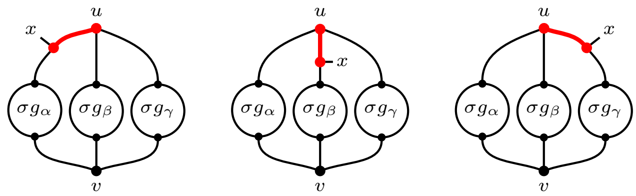

FIGURE 5.1: Graphs in Orb^{φ}

Property 5.8. *The p-type matchings on the complete graph K_{n+2} can be expressed as*

$$\begin{aligned}
\mathfrak{M}^0_m K_{n+2} &= \mathfrak{M}_m K_n,\\
\mathfrak{M}^1_m K_{n+2} &= \left(\mathfrak{M}_{m-1} K_{n-1}\right)^{\sqcup n},\\
\mathfrak{M}^2_m K_{n+2} &= \left(\mathfrak{M}_{m-2} K_{n-2}\right)^{\sqcup n(n-1)/2} \quad \text{and}\\
\mathfrak{M}^\tau_m K_{n+2} &= \mathfrak{M}_{m-1} K_n.
\end{aligned}$$

Proof. The case $p = 0$ simply excludes two vertices to be matched, so all m-matchings on K_n remain.
For $p = 1$ let $M \in \mathfrak{M}^1_m K_{n+2}$ and $M = M_0 \cup \{u, x\}$ for $x \neq v$, then M_0 is a $(m-1)$-matching on K_{n-1}, since by definition $v \notin M_0$. For any of the n choices to pick x there is a new set $\mathfrak{M}_{m-1} K_{n-1}$, where x takes a specific value. Use x to label the sets, which allows forming the disjoint union of the n copies.
Similarly for $p = 2$, but here are $n(n-1)/2$ disjoint copies, since the vertices u and v cannot be distinguished.
For τ-type matchings u and v are matched such that $m - 1$ matchings on the remaining n vertices remain. □

In the next step, the effect of the groupaction Φ from Definition 2.44, which ensures counting the 3-regular m-matched graphs is equivalent to counting graphs with m 4-valent vertices, is investigated. Note that if the matching does not include u or v, the equivalence relation is effectively the same as for the one loop case, cf. Definition 4.12.

Definition 5.9. *Let $(M, \Gamma) \in \mathfrak{M}^p_m \mathcal{B}_n$, $M_0 \subset M$, s.t., $u, v \notin M_0$, and $p \in \{0, 1, 2\}$. Write $(M, \Gamma) = ((M_0, \Gamma), (M \setminus M_0, \Gamma))$, $|M \setminus M_0| = p$ and define a groupaction $\Phi : S_2^{|M_0|} \times \mathrm{STU}^p \times \mathfrak{M}^p_m \mathcal{B}_n \to \mathfrak{M}^p_m \mathcal{B}_n$ for $(\tau, r) \in S_2^{|M_0|} \times \mathrm{STU}^p$ by*

$$\Phi_{(\tau,r)}(M, \Gamma) := (\Psi_\tau(M_0, \Gamma), \varphi_r(M \setminus M_0, \Gamma)) \;,$$

where Ψ_τ is from Definition 4.12 and $\varphi_r : \mathrm{STU}^p \times \mathfrak{M}^p_m \mathcal{B}_n \to \mathfrak{M}^p_m \mathcal{B}_n$ is a groupaction given in Figure 5.1.

This definition is equivalent to the groupaction defined in chapter two, since the the action of STU on a matching in M_0 reduces to an action of S_2, because else wise non 1PI graphs would be generated.

Remark. For $p = 2$ the definition of φ_r is not given explicitly, but straightforward.
The action of φ_r on τ-type matchings needs a more detailed treatment. In general, these matched graphs take the form

$$\left(\{u, v\} \cup M_0, b_{(\alpha,\beta,0)}\right) = \quad (5.1)$$
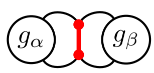

,

where the matching on the graphs g_α and g_β as well as their external legs are not pictured. The action of φ_r is now given by

$$\varphi_{(24)}\left(\{u,v\} \cup M_0, b_{(\alpha,\beta,0)}\right) = \quad (5.2)$$

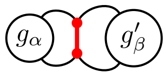

where g'_β is g_β with reversed order of the external legs. The remaining group element of $R_4 \ltimes \mathrm{Cyc}_4$ leads to a non 1PI graph. The two 4-valent graphs to which (5.1) and (5.2) correspond, are indeed the same, due to their symmetry.

Continue with the observation, that the group action Φ acts independently on the disjoint subsets of $\mathfrak{M}_m\mathcal{B}_n$ given in Definition 5.6 by the different types of matching. A matching is not altered by the action Φ and therefore it maps $\mathfrak{M}^p_m\mathcal{B}_n$ onto itself, hence the equation

$$\mathfrak{M}_m\mathcal{B}_n/\Phi = \bigsqcup_{p\in\{0,1,2,\tau\}} \mathfrak{M}^p_m\mathcal{B}_n/\Phi \tag{5.3}$$

is fulfilled.

Now the actual counting of graphs is done. Therefore define a set of all possible compositions of m. This is necessary since for a matched graph $(M, b_{\boldsymbol{\alpha}}) \in \mathfrak{M}_m\mathcal{B}_n$ the matching M_0 can be written as $M_0 = M_1 \sqcup M_2 \sqcup M_3$ with $u, v \notin M_0$, where M_i is a matching on g_{α_i} and $m = |M_1|+|M_2|+|M_3|+p$. To count all possible m-matchings on $b_{\boldsymbol{\alpha}}$ a sum over all possible values for the sizes of M_i is needed. Note that matched graphs in $\mathfrak{M}^\tau_m\mathcal{B}_n$ have $\alpha_3 = 0$ and therefore $M_3 = \emptyset$, and $p = 1$.

Definition 5.10. *Let $\boldsymbol{\alpha} \in P(n)$ and define the set of all compositions of a m-matching via*

$$C_{\boldsymbol{\alpha}}(m) := \left\{(m_1, m_2, m_3) \;\middle|\; \sum_{i=1}^{3} m_i = m,\, 0 \le m_i \le \left\lceil \frac{\alpha_i - 1}{2} \right\rceil,\, i = 1,2,3 \right\}.$$

In the definition above the restriction of m_i is precisely the same as in Lemma 4.35.
The symmetry of some graphs in $\mathfrak{M}_m\mathcal{B}_n$ leads to overcounting, i.e.,the corresponding graph gets counted multiple times. To take care of this overcounting, it is useful to introduce symmetry factors. The first factor $s(\boldsymbol{\alpha})$ origins in permutations of the subgraphs $g_{\alpha_1}, g_{\alpha_2}$ and g_{α_3}.

Definition 5.11. *Let $\boldsymbol{\alpha} \in P(n)$ and define a symmetry factor $s(\boldsymbol{\alpha})$ via*

$$s(\boldsymbol{\alpha}) := \prod_{j=1}^{n} a_j!\,,$$

where a_j is the number of α_i's for which $\alpha_i = j \neq 0$.

The cases $\alpha_i = 0$ are excluded in this definition because these subgraphs will not cause overcounting, since they do not possess external legs.
The second kind of symmetry factors takes care of the symmetry of exchanging the vertices u and v. This is only a symmetry of graphs in $\mathfrak{M}^0_m\mathcal{B}_n$ and $\mathfrak{M}^\tau_m\mathcal{B}_n$, since a matching on u or v (which is not the matching of u to v) brakes reflectional symmetry. They are denoted by $r_0(\boldsymbol{\alpha}, \boldsymbol{m})$ and $r_\tau(\boldsymbol{\alpha}, \boldsymbol{m})$.

Definition 5.12. *Let $\boldsymbol{\alpha} \in P(n)$, $\boldsymbol{m} \in C_{\boldsymbol{\alpha}}(m)$, and define a symmetry factor $r_0(\boldsymbol{\alpha}, \boldsymbol{m})$ via*

$$r_0(\boldsymbol{\alpha}, \boldsymbol{m}) := \begin{cases} 1 & \textit{if} \quad \alpha_i - m_i \le 1 \;\forall i = 1,2,3 \\ 2 & \textit{else} \end{cases}.$$

Notice that graphs $(M, \sigma b_{\boldsymbol{\alpha}}) \in \mathfrak{M}_m\mathcal{B}_n$ that correspond to the first case in the definition above have either zero, one or two to another matched vertices on each subgraph g_{α_i}. In these cases, the reversing the order of the external legs on each subgraph is trivial. (In the case of two vertices due to the group action Φ).
The factor r_τ prevents overcounting of the two graphs t and $\varphi_r t$ (cf. Equation (5.1) and (5.2)). This will include the factor of the definition above.

Definition 5.13. *Let $\boldsymbol{\alpha} \in P(n)$, $\boldsymbol{m} \in C_{\boldsymbol{\alpha}}(m)$, and define a symmetry factor $r_\tau(\boldsymbol{\alpha}, \boldsymbol{m})$ via*

$$r_\tau(\boldsymbol{\alpha}, \boldsymbol{m}) := r_0(\alpha_1, m_1) r_0(\alpha_2, m_2) \ ,$$

where $r_0(\alpha_i, m_i)$ is defined as

$$r_0(\alpha_i, m_i) := \begin{cases} 1 & \text{if} \quad \alpha_i - m_i \leq 1 \\ 2 & \text{else} \end{cases} .$$

The factor r_τ is built from two factors r_0, one for each subgraph g_{α_i}. They need to be treated independently, since reversing the order of the external legs on any of them is a symmetry of the graphs in $\mathfrak{M}^\tau_m\mathcal{B}_n$. The separation into the cases whether the reversing is trivial or not remains. This becomes important below when the graphs are counted.

Remember that a matching M is called *preserved* in $(M, b_{\boldsymbol{\alpha}}) \in \mathfrak{M}_m\mathcal{B}_n$ if $M \subset K_{n+2}$. Finally, a theorem about the size of $\mathfrak{M}_m\mathcal{B}_n/\Phi$ is formulated.

Theorem 5.14. *Let $n > 1$ then the number of two-loop graphs with m 4-valent vertices and n external legs is given by*

$$|\mathfrak{M}_m\mathcal{B}_n/\Phi| = \sum_{p \in \{0,1,2,\tau\}} |\,\mathfrak{M}^p_m K_{n+2}|\, q^p_{m,n} \ , \tag{5.4}$$

where $q^p_{m,n}$ is the number of graphs in $\mathfrak{M}_m\mathcal{B}_n/\Phi$ that preserve a given m-matching of K_{n+2} and is given by

$$\begin{aligned} q^0_{m,n} &= \sum_{\boldsymbol{\alpha} \in P(n)} \ \sum_{\boldsymbol{m} \in C_{\boldsymbol{\alpha}}(m)} \frac{A(\boldsymbol{\alpha}, \boldsymbol{m}, n, m)}{r_0(\boldsymbol{\alpha}, \boldsymbol{m}) s(\boldsymbol{\alpha})} \ , \\ q^p_{m,n} &= \sum_{\boldsymbol{\alpha} \in P(n-p)} \ \sum_{\boldsymbol{m} \in C_{\boldsymbol{\alpha}}(m-p)} \frac{A(\boldsymbol{\alpha}, \boldsymbol{m}, n-p, m-p)}{s(\boldsymbol{\alpha})} \ , \ \textit{for } p = 1, 2; m \geq p \textit{ and} \\ q^\tau_{m,n} &= \sum_{\substack{\boldsymbol{\alpha} \in P(n) \\ \alpha_2 \neq 0 = \alpha_3}} \ \sum_{\boldsymbol{m} \in C_{\boldsymbol{\alpha}}(m-1)} \frac{A(\boldsymbol{\alpha}, \boldsymbol{m}, n, m-1)}{r_\tau(\boldsymbol{\alpha}, \boldsymbol{m}) s(\boldsymbol{\alpha})} \ \textit{for } m \geq 1 \ , \ \textit{where} \end{aligned}$$

$$A(\boldsymbol{\alpha}, \boldsymbol{m}, n, m) := \binom{m}{m_1}\binom{n-2m}{\alpha_1 - 2m_1}\binom{m-m_1}{m_2}\binom{n-2m-\alpha_1+2m_1}{\alpha_2 - 2m_2}\prod_{i=1}^{3}(\alpha_i - m_i)! \, .$$

The quantity A is constructed such that it counts the number of matched graphs $(M, \sigma b_{\boldsymbol{\alpha}})$ for $|M| = m$ and a given composition of the matching. To account for symmetries A gets divided by the corresponding symmetry factors, which differ in between the different cases. Before the theorem is proven, look at an example to illustrate how this counting works.

Example 5.15. Consider the sets $\mathfrak{M}_m\mathcal{B}_3/\Phi$ for $m = 0, 1, 2$. The first set $\mathfrak{M}_0\mathcal{B}_3/\Phi = \mathcal{B}_3$ is given by

$$\mathcal{B}_3 = \left\{ \quad \right\} .$$

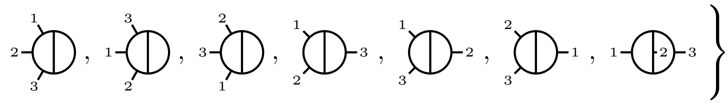

In the first partition of $3 = 3 + 0 + 0$, corresponding to the first three graphs, the factor $A((3, 0, 0), 0, 3, 0) = 3! = 6$, but since reflecting the pictured graphs along the horizontal axis is a symmetry, there are only three graphs. This is achieved by the factor $r_0((3, 0, 0), 0) = 2$. Furthermore, note that $s((3, 0, 0)) = 1$.
The next three graphs resemble the partition $3 = 2+1+0$, here we have $A((2, 1, 0), 0, 3, 0) = \binom{3}{2}2! = 6$. As for the previous graphs the reflectional symmetry needs to be taken into account, so there are only 3 graphs. Lastly, for the partition $3 = 1 + 1 + 1$ the factor $A((1, 1, 1)0, 3, 0) = \binom{3}{1}\binom{2}{1} = 6$, but the subgraphs g_1 can be permuted freely, so divide by $s((1, 1, 1)) = 3!$ and only one graph remains.
Now one edge of the graphs in $\mathcal{B}_3$ is matched. Consider the different cases as above. First, look at the set where the vertices u and v are not matched:

$$\mathfrak{M}^0_1\mathcal{B}_3/\Phi = \left\{ \quad \right\} .$$

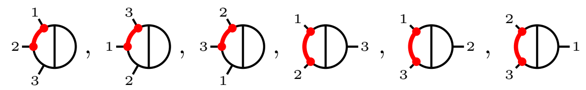

For the first partition, one gets the factor $A((3, 0, 0), (1, 0, 0), 3, 1) = 2!$, but as before it counts the reflected graph twice. For the remaining partition the factor $A((2, 1, 0), (1, 0, 0), 3, 1) = 1$, since the matching needs to be on the subgraph g_2. Note that no overcounting occurs. Now, there are 3 possible matchings on the graph K_3, so both partitions above correspond to 3 graphs in the set $\mathfrak{M}^0_1\mathcal{B}_3$.
Now consider the set $\mathfrak{M}^1_1\mathcal{B}_3$, where u is matched:

$$\mathfrak{M}^1_1\mathcal{B}_3/\Phi = \left\{ \quad \right\} .$$

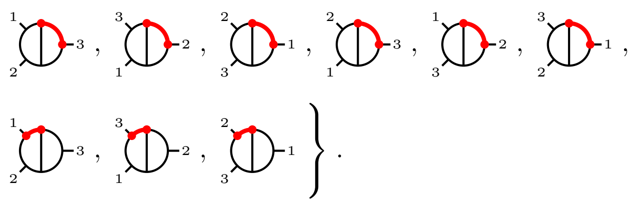

Most importantly notice that the matching on the vertex u breaks the reflectional symmetry. Therefore, e.g., the first and fourth graph in the set are not related by an isomorphism. Further observe that since one external leg (via its vertex) is matched to u, only the two remaining external legs need to be partitioned over the tree subgraphs g. There are two possible partitions: $(2, 0)$ and $(1, 1)$. The partition $(2, 0)$ corresponds to the first six and $(1, 1)$ to the remaining graphs.
The set of graphs, were u is matched to v is

$$\mathfrak{M}^\tau_1\mathcal{B}_3/\Phi = \left\{ \quad \right\} .$$

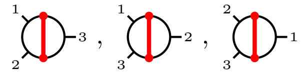

Finally the graphs with 2-matchings are given in the set

$$\mathfrak{M}_2\mathcal{B}_3/\Phi = \Bigg\{$$

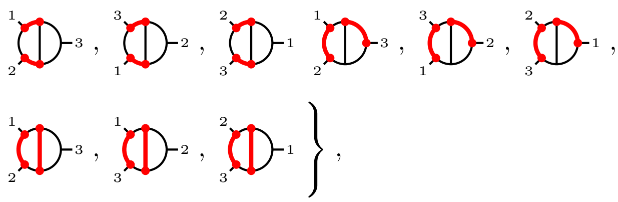

$$\Bigg\},$$

where again reflectional symmetry is broken in the first six graphs. The last three graphs are in the set $\mathfrak{M}_2^\tau\mathcal{B}_3$.

Proof. Let $\boldsymbol{\alpha} \in P(n)$, $\boldsymbol{m} \in C_{\boldsymbol{\alpha}}(m)$ and $M \in \mathfrak{M}_m K_{n+2}$. Due to Property 5.7 there exists a matched graph $(M, \sigma b_{\boldsymbol{\alpha}}) \in \mathfrak{M}_m\mathcal{B}_n/\Phi$. Denote its three matched subgraphs by $(M_i, \sigma_i g_{\alpha_i})$ for $i = 1, 2, 3$. The matching M is given by $M = M \setminus M_0 \sqcup M_0$, where $M_0 = \bigsqcup_{i=1,2,3} M_i$ contains all matchings that do not include the vertices u or v. Furthermore, the maps σ_i are a restriction of σ, namely $\sigma_i = \sigma|_{[\alpha_i]\setminus[\alpha_{i-1}]}$ for $i = 2, 3$ and $\sigma_1 = \sigma|_{[\alpha_1]}$. The map σ is a labeling of the external legs of the graph $(M, b_{\boldsymbol{\alpha}})$.
Further note that it is enough that σ labels only one of the matched vertices (more precisely the external edge connected to that vertex), because the matching fixes the other label. To clarify, one might write $\sigma \in S_{n-m}$, although this is technically not right. More importantly, note that different maps σ might result in labels that are considered equal by the group action Φ or by the symmetry of the graph. This overcounting needs to be properly treated in the derivation below.
Let $A(\boldsymbol{\alpha}, \boldsymbol{m}, n, m)$ be the number of possible labels σ on the matched graphs $(M_i, \sigma_i g_{\alpha_i})$, where the symmetry of the graphs is ignored. There are

$$\binom{m}{m_1}\binom{n-2m}{\alpha_1 - 2m_1}(\alpha_1 - m_1)!$$

maps σ_1, since m_1 matchings and $\alpha_1 - 2m_1$ vertices need to be chosen and can be arranged in any order. The number of possible maps σ_i for $i > 1$ is similar, but the already chosen vertices and matchings need to be taken into account, to ensure that σ is bijective. Then the given form of $A(\boldsymbol{\alpha}, \boldsymbol{m}, n, m)$ follows. Note that the order of two matched vertices is not incorporated, since the action of Φ renders them equal.
The number A needs to be altered due to the already mentioned overcounting. It happens because of the symmetries of the graphs, which can be divided into two cases. The first arises when $\alpha_i = \alpha_j$ for $i \neq j$, because the graphs $(M, \sigma b_{\boldsymbol{\alpha}})$ and $(M, \sigma' b_{\boldsymbol{\alpha}})$ are isomorphic if $\sigma_i' = \sigma_j \circ d_{j,i}$ and $\sigma_j' = \sigma_i \circ d_{i,j}$, where the map $d_{i,j} : \Omega_i \to \Omega_j$ is the unique order preserving bijection between the two domains of σ_i and σ_j. The order on these domains is given by the order of the vertices in the subgraphs $g_{\alpha_i} \subset b_{\boldsymbol{\alpha}}$. For two equal α_i's there are two maps in S_{n-m} that result in the same label and if all α_i's are identical there are 3! such maps, with the exception if $\alpha_2 = \alpha_3 = 0$, since then there are no maps σ_2, σ_3. The number of different maps $d_{i,j}$ is exactly the number of permutations of the subgraphs g_i which are a symmetry of the full graph. The factor $s(\boldsymbol{\alpha})^{-1}$ is defined such that it cancels the overcounting.
The second overcounting originates in the possible symmetry of exchanging the vertices u and v in $(M, \sigma b_{\boldsymbol{\alpha}})$, note that this is only a symmetry of graphs in $\mathfrak{M}_m^0\mathcal{B}_n/\Phi$ and $\mathfrak{M}_m^\tau\mathcal{B}_n/\Phi$. In terms of the maps σ_i it can be formulated as follows. A map σ is counted twice if $\exists \sigma_i' \neq \sigma_i$ such that $\sigma_i = \sigma_i' \circ r_{\alpha_i - m_i + 1}$ $\forall i = 1, 2, 3$, where $r_{\alpha_i - m_i + 1}$ is the map given in Definition 2.31, which reverses the order of the vertices on (M_i, g_{α_i}). Note that if $\alpha_i - m_i = 0$ then there is no map σ_i and if $\alpha_i - m_i = 1$ it follows that $r_{\alpha_i - m_i + 1} = (1)$. If one of these cases holds true for all $i = 1, 2, 3$, then these graphs are not counted twice. It is evident that for

$\alpha_i - m_i > 1$ one can always find such two maps σ_i and σ'_i [1]. This overcounting is precisely canceled by the factor $r_0(\boldsymbol{\alpha}, \boldsymbol{m})^{-1}$ for graphs in $\mathfrak{M}^0_m\mathcal{B}_n/\Phi$. The graphs in $\mathfrak{M}^\tau_m\mathcal{B}_n/\Phi$ need a related adjustment. Here the maps σ are also counted various times due to the group action φ, cf. Equation (5.2). Multiple counting of the same label occurs here whenever for one of the two maps σ_1 and σ_2 exists a different map σ'_i such that it is a reflection of σ_i in the sense of the above. The reflectional symmetry is included whenever for both maps σ_i exists such a reflection σ'_i. The factor $r_\tau(\boldsymbol{\alpha}, \boldsymbol{m})^{-1}$ precisely captures these cases.
To calculate $q^p_{m,n}$ for $p = 0, 1, 2$ sum the factor A together with the corresponding symmetry factors over $\boldsymbol{\alpha} \in P(n-p)$ and $\boldsymbol{m} \in C_{\boldsymbol{\alpha}}(m-p)$. Since $\boldsymbol{\alpha} \in P(n-p)$ it is given that $\alpha_1 \geq \alpha_2 \geq \alpha_3$, which ensures that permutations of the subgraphs g_{α_i} are only counted multiple times if $\alpha_i = \alpha_j$ for $i \neq j$, but these cases are treated by the symmetry factor $s(\boldsymbol{\alpha})$. Subtracting the number of matchings in $M \setminus M_0$ in the summation sets and in the factor $A(\boldsymbol{\alpha}, \boldsymbol{m}, n-p, m-p)$ ensures that any two labels that are equivalent by the group action φ (cf. Figure 5.1) are only counted once. In that cases the map σ does not label the external leg whose vertex is matched to u or v. Counting the different labels on that edges is done by the number of p-type matchings in K_{n+2}, cf. Property 5.8.
To calculate $q^\tau_{m,n}$ the sum runs over $\boldsymbol{\alpha} \in P(n)$, but $\alpha_2 \neq 0$, since else wise the graphs are tadpoles and further $\alpha_3 = 0$, because $\{u, v\} \in M$. The second sum runs over the set $C_{\boldsymbol{\alpha}}(m-1)$, since the matching of u to v is excluded. The summand then takes the form $A(\boldsymbol{\alpha}, \boldsymbol{m}, n, m-1)r_\tau(\boldsymbol{\alpha}, \boldsymbol{m})^{-1}s(\boldsymbol{\alpha})^{-1}$. Here the group action φ is already taken into account by the symmetry factor r_τ.
Conclude that $q^r_{m,n}$ counts the number of graphs in the corresponding subset of $\mathfrak{M}_m\mathcal{B}_n/\Phi$ that preserve a given matching $M \in \mathfrak{M}^r K_{n+2}$, for $r = 0, 1, 2, \tau$. It is clearly independent of the given matching and therefore the product $|\mathfrak{M}^r K_{n+2}|q^r_{m,n}$ is the number of graphs in the appropriate subset. By Equation (5.3) summing over the subsets gives the size of $\mathfrak{M}_m\mathcal{B}_n/\Phi$. □

Remark. The Theorem 5.14 above can be generalized to k-banana graphs, that are graphs where two vertices u and v are connected via k subgraphs of the form g_{α_i}. Therefore the sums need to run over partitions of n and compositions of m into k integers instead of three and the summand $A_k(\boldsymbol{\alpha}, \boldsymbol{m}, n, m)$ takes the form

$$A_k(\boldsymbol{\alpha}, \boldsymbol{m}, n, m) = \prod_{i=1}^{k} \binom{m - \sum_{j=1}^{i-1} m_j}{m_i} \binom{n - 2m + \sum_{j=1}^{i-1} 2m_j - \alpha_j}{\alpha_i - 2m_i} (\alpha_i - m_i)!\,.$$

The case of τ-type matchings is generalized by the following condition on $\boldsymbol{\alpha}$: $\alpha_n = 0$ and $\alpha_i \neq 0$ for $i \neq n$. The symmetry factors $r_0(\boldsymbol{\alpha}, \boldsymbol{m})$, $r_\tau(\boldsymbol{\alpha}, \boldsymbol{m})$ and $s(\boldsymbol{\alpha})$ can be adjusted easily.

5.1.1 Rainbow-Colored Two Loop Moduli Spaces $MRG^4_{2,n}$

Given Theorem 5.14 and therefore the number of two-loop graphs with n external legs and m 4-valent vertices one can deduce the f-vector of the rainbow-colored two loop moduli space $MRG^4_{2,n}$. Here each edge of a graph has a different color and since the 3-regular graph with n external legs has $n+3$ edges, there are a total of $n+3$ colors. The f-vector of the corresponding moduli space is easily deduced from the previous theorem. Denote the moduli space of rainbow graphs by $MRG^4_{2,n}$ and its f-vector by $\boldsymbol{F}^r$. Any graph $t \in (m, \mathcal{B}_n)/\Phi$ has exactly $n+3-m$ colored edges since as before the matched edges do not carry a color. So

[1] If such a pair σ_i, σ'_i exists, then there cannot be a third one σ''_i, since then $\sigma''_i \circ r_{\alpha_i - m_i + 1} = \sigma'_i \circ r_{\alpha_i - m_i + 1}$ $\Rightarrow \sigma''_i = \sigma'_i$.

there are $(n+3)!/m!$ different colorings of the edges of t. Therefore deduce the following corollary.

Corollary 5.16. *The f-vector $\boldsymbol{F}^r = \left(F^r_{-1}, F^r_0, \dots, F^r_{n+2}\right)$ of the moduli space of two-loop rainbow-colored graphs $MRG^4_{2,n}$ is given by*

$$F^r_{n-m-3} = \frac{(n+3)!}{m!} |\mathfrak{M}_m \mathcal{B}_n/\Phi|,$$

where $|\mathfrak{M}_m \mathcal{B}_n/\Phi|$ is given by Theorem 5.14.

The knowledge of the f-vector allows the calculation of the Euler characteristic $\mathcal{X}_n$. The results for the range $n = 2, \dots, 30$ is given in the appendix Table A.3. At first glance it does not show any interesting patterns, the modulus of $\mathcal{X}_n$ grows with growing n and it sign alternates almost everywhere, except for $n = 12, 13$ and $n = 25, 26$ where the Euler characteristic is negative. Up to $n = 90$ these irregularities were not found again.

To loosen the requirement of the color maps, such that they are no longer injective, one might alter the different cases in Theorem 5.14, to capture the number of possibilities to color a graph in $\mathfrak{M}_m \mathcal{B}_n/\Phi$. However, if any isometry between the graphs should still be avoided, it is not enough to require different colors on edges that are part of a multi-edge, as for one loop, but also take a different kind of isometries into account. These do not rely on the permutation of edges in a multi-edge, but on the exchange of the vertices u and v. This is best seen in an example.

Example 5.17. Let $t, t' \in MG^4_{2,2}$ and represent their metrics m_t and $m_{t'}$ as the actual length of the drawn edges. Next define

$t :=$ 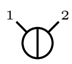 and $t' :=$ 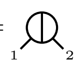 .

Then $t \sim t'$ as points in the moduli space, since the isomorphism i that maps t to t' as graphs, respects the metric, i.e. $m_{t'} \circ i = m_t$.

As a consequence, one might regard only colorings that make isometric graphs impossible. Note that the isometric graphs arising from the reflection, as in the example above, can also be excluded by requiring $n > 6$, since then no graphs have this reflectional symmetry. (Recall that the external legs are fixed.)

SUMMARY

In this master thesis, the f-vectors of some relative simplicial complexes of the moduli spaces of gluon graphs have been calculated. Points of these spaces are metric graphs with a maximal vertex valency of four. This restriction translates into missing faces of the complex.
Moduli spaces of graphs arise naturally in the representation of Feynman amplitudes in parametric variables. A better understanding of those might contribute to comprehending the complicated structure of Feynman integrals.
The f-vector of the one loop and the colored two loop moduli spaces for any number of external legs was calculated by analyzing the possible matchings of the graphs under consideration. Therefore the number of matchings on the complete graph with the same number of vertices was determined. Subsequently, the number of admissible graphs for which such a matching is also a matching was calculated. The knowledge of the f-vector further enables the computation of the Euler characteristic. An idea for a proof that $\mathcal{X}[MG^4_{1,4k+2}] = 0$ for $k \in \mathbb{N}$ is given. For a single cell, it was shown that the f-vector can be read of the $(2,1)$-Pascaltriangle and the Euler characteristic is related to Chebyshev polynomials.
For two loops, a formula for the number of graphs with m four valent vertices is given. It is related to the f-vector of the colored moduli space of two loop graphs. Furthermore, the counting can be generalized to any k-banana graphs.
Additionally, it is shown that the moduli spaces stay connected after removing the faces corresponding to graphs with vertices of higher valency then four.
Future work could investigate the algebraic properties of the complexes, for example, in [25]. A different possible approach for future work could follow the ideas in [8] to analyze the homology the moduli spaces. This would also be a starting point to investigate higher loop versions of these spaces. Lastly, it is desirable to establish a stronger connection to physical quantities.

Appendix

Tables

Table A.1: The Euler-characteristic $\mathcal{X}_n$ of $\mathcal{MG}^4_{1,n}$

n	$\mathcal{X}_n$
5	-3
6	0
7	45
8	-315
9	1260
10	0
11	-56700
12	623700
13	-3742200
14	0
15	340540200
16	-5108103000
17	40864824000
18	0
19	-6252318072000
20	118794043368000
21	$-118794043368 \cdot 10^4$
22	0
23	$27441424018008 \cdot 10^4$
24	$-631152752414184 \cdot 10^4$
25	$7573833028970208 \cdot 10^4$
26	0
27	$-24614957344153176 \cdot 10^6$
28	$664603848292135752 \cdot 10^6$
29	$-9304453876089900528 \cdot 10^6$
30	0

n	$\mathcal{X}_n$
31	$404743743609910672968 \cdot 10^7$
32	$-1254705605190723086200 8 \cdot 10^7$
33	$200752896830515693792128 \cdot 10^7$
34	0
35	$-112622375121919304217383808 \cdot 10^7$
36	$394178312926717564760843328 \cdot 10^8$
37	$-709520963268091616569517990 4 \cdot 10^8$
38	0
39	$4987932371774684064483711472512 \cdot 10^8$
40	$-194529362499212678514864747427968 \cdot 10^8$
41	$38905872499842535702972949485593 6 \cdot 10^9$
42	0
43	$-33497956222364423240259709507096089 6 \cdot 10^9$
44	$1440412117561670199331167508805131852 8 \cdot 10^9$
45	$-316890665863567443852856851937129007616 \cdot 10^9$
46	0
47	$327981839168792304387706841754928522882 56 \cdot 10^{10}$
48	$-154151464409332383062222215624816405754803 2 \cdot 10^{10}$
49	$369963514582397719349333317499559373811527 68 \cdot 10^{10}$
50	0
51	$-4532053053634372062029333139369602329191214 08 \cdot 10^{12}$
52	$231134705735352975163495990107849718788751918 08 \cdot 10^{12}$
53	$-600950234911917735425089574280409268850754987 008 \cdot 10^{12}$
54	0
55	$859959786158954279393303180795265663725430386408448 \cdot 10^{12}$
56	$-472977882387424853666316749437396115048986712524646 4 \cdot 10^{13}$

TABLE A.2: The Euler-characteristic $\mathcal{X}_n$ of $XR^4_{1,n}$

n	$\mathcal{X}_n$
5	-1260
6	39600
7	-1625400
8	84142800
9	-5315284800
10	396417369600
11	-33590885328000
12	3051847925280000
13	-260181757547712000
14	9325375067264256000
15	5545328982371418240000
16	$-297691683826842264960000$
17	12076656387588905688576000000
18	$-474519441227486534111232000000$
19	19213276487842765737589340160000
20	$-820064713683247755598150539264000$
21	372418585954768192757461848944640000000
22	$-180588785916532899378966889671475200000000$
23	935691427945232483280692331491570073600000
24	$-517589065092352512288176702250034552012800000$
25	3051129302880225313976262520440806780928000000000
26	$-1911955241034483597021666268623569502044160000000000$
27	126970197503513731822188871577325038830989312000000000
28	$-890278466619476928259877742460943521520325672960000000000$
29	65612711246870001814679007954167588418247885209600000000000000
30	$-50535382918646976107291887751678279086820966848462848000000000000$

Table A.3: The Euler-characteristic $\mathcal{X}_n$ of $XR^4_{2,n}$

n	$\mathcal{X}_n$
2	−180
3	4680
4	−194040
5	9172800
6	−596937600
7	46135656000
8	−4187422008000
9	431532541440000
10	−48324779350848000
11	5411407281344064000
12	−459264656566235520000
13	−40553651193525550080000
14	47809537645821454863360000
15	−24408232618492071456307200000
16	1110110330103046653508807680000
17	−502006926905537484470834995200000
18	23364729509385716642299026677760000000
19	−11318554291229419012408257142394880000000
20	57074100682568708315760577758985420800000
21	−29854993051659464179847356314091954176000000
22	15946835406148193345933109821699570196480000000
23	−844486112475596564411637563694481161314304000000000
24	413704618273591023315003519729408532740218880000000000
25	−1431269601049116397063188600929437967769305088000000000000
26	−50255251662631833023365748505576051628675581542400000000000
27	212210846891971252274620132691880703206052505198592000000000000
28	−377275686141843540245952345502981676356824048712925184000000000000
29	576104565757236035393201428333186102598575358026572890112000000000000
30	−845458308524698963981974339545999855896605523985814893887488000000000000

Bibliography

[1] Dirk Kreimer. Multi-valued Feynman Graphs and Scattering. preprint.

[2] Karen Vogtmann and Marc Culler. Automorphisms of free groups and outer space. *Geometriae Dedicata*, 94:1–31, 10 2002.

[3] Marko Berghoff. Feynman amplitudes on moduli spaces of graphs. *arXiv: 1709.00545*, 2017.

[4] Marko Berghoff and Max Mühlbauer. Moduli spaces of colored graphs. *arXiv: 1809.09954*, 2018. preprint.

[5] Allen Hatcher. *Algebraic Topology*. Cambridge University Press, 2001.

[6] J. Gallian. *Contemporary Abstract Algebra*. Cengage Learning, 2009.

[7] Michal Borinsky. Algebraic Lattices in QFT Renormalization. *Lett Math Phys*, 2016.

[8] James Conant, Allen Hatcher, Martin Kassabov, and Karen Vogtmann. Assembling homology classes in automorphism groups of free groups. *Commentarii Mathematici Helvetici*, 91, 2015.

[9] Mladen Bestvina and Mark Feighn. The topology at infinity of Out(Fn). *Inventiones mathematicae*, 140(3):651–692, Jun 2000.

[10] Predrag Cvitanović. *Field Theory*. Nordita Lecture Notes, 1983.

[11] Steven Weinberg. *The Quantum Theory of Fields*, volume 2. Cambridge University Press, 1996.

[12] Steven Weinberg. *The Quantum Theory of Fields*, volume 1. Cambridge University Press, 1995.

[13] Matthias Sars. *Parametric Representation of Feynman Amplitudes in Gauge Theories*. PhD thesis, HU Berlin, 2015.

[14] Erik Panzer. *Feynman integrals and Hyperlogarithms*. PhD thesis, HU Berlin, 2015.

[15] Stefan Weinzierl. The Art of Computing Loop Integrals. *arXiv:0604.068v1*, 2006.

[16] O. V. Tarasov. Connection between feynman integrals having different values of the space-time dimension. *Phys. Rev. D*, 54:6479–6490, Nov 1996.

[17] Dirk Kreimer, Matthias Sars, and Walter D. van Suijlekom. Quantization of gauge fields, graph polynomials and graph homology. *Annals of Physics*, 336:180 – 222, 2013.

[18] Seth Chaiken. A combinatorial proof of the all minors matrix tree theorem. *SIAM J. ALG. DISC. METH.*, 1982.

[19] J. W. Moon. Some determinant expansions and the matrix-tree theorem. *Discrete Mathematics*, 124:163–171, 1994.

[20] W. Zimmermann. Convergence of bogoliubov's method of renormalization in momentum space. *Communications in Mathematical Physics*, 15(3):208–234, Sep 1969.

[21] Francis Brown and Dirk Kreimer. Angles, scales and parametric renormalization. *Letters in Mathematical Physics*, 103(9):933–1007, Sep 2013.

[22] Christian Bogner. *Mathematical Aspects of Feynman Integrals.* PhD thesis, Johannes Gutenberg-Universität Mainz, 2009.

[23] J. C. Mason and D. C. Handscomb. *Chebyshev polynomials.* Chapman and Hall/CRC, 2003.

[24] OEIS Foundation Inc. (2019). The on-line encyclopedia of integer sequences. `http://oeis.org/A204021`.

[25] Richard P. Stanley. Cohen-macaulay complexes. In Martin Aigner, editor, *Higher Combinatorics*, pages 51–62. Springer Netherlands, 1977.

List of Figures

Selbstständigkeitserklärung

Ich erkläre hiermit, dass ich die vorliegende Arbeit selbstständig verfasst und noch nicht für andere Prüfungen eingereicht habe. Sämtliche Quellen einschließlich Internetquellen, die unverändert oder abgewandelt wiedergegeben werden, insbesondere Quellen für Texte, Grafiken, Tabellen und Bilder, sind als solche kenntlich gemacht. Mir ist bekannt, dass bei Verstößen gegen diese Grundsätze ein Verfahren wegen Täuschungsversuchs bzw. Täuschung eingeleitet wird.

Berlin, __________________